*Department*
*of*
# PHYSICS


## UNIVERSITY OF BERGEN

*Bergen, Norway*

# AN EXPERIMENTAL STUDY OF ODD MASS PROMETHIUM ISOTOPES USING PROTON STRIPPING AND PICKUP REACTIONS

Oddmund Straume

Thesis submitted to the University of Bergen

November 1979

CONTENTS: PAGE:

## Preface

The experiments that form the backbone of this thesis were performed at the Tandem Laboratory of the McMaster University, Ontario, Canada, and at Los Alamos Scientific Laboratory, New Mexico, U.S.A. during the period from 1975 to 1978 and the data analysis has been done partly at McMaster and partly at Universitetet i Bergen.

The present thesis consists of five papers (numbered I to V) with a general introduction. In the introduction the objective of this study is discussed and some of the more important results are pointed out along with a brief presentation of systematic features that can be obtained by combining the information contained in the five papers.

In paper I the results from the ($^3$He,d) and ($\alpha$,t) reaction study of the N=88 isotones ($^{149}$Pm, $^{151}$Eu, $^{153}$Tb) are presented. Paper II contains the results of the ($^3$He,d), ($\alpha$,t) and (t,$\alpha$) reactions into the N=86 isotones $^{147}$Pm and $^{149}$Eu and in paper III the ($^3$He,d) and ($\vec{t}$,$\alpha$) reactions were used to investigate the $^{151}$Pm nucleus. Paper IV gives the ($\vec{t}$,$\alpha$) data into $^{149}$Pm and summarizes the results from all the (t,$\alpha$) data, and finally in paper V the results from the ($^3$He,d) reaction investigating the $^{145,143}$Pm isotopes are presented.

I feel indebted to my friends and colleagues at McMaster, LASL and UiB for good working conditions, helpful comments and inspiring discussions during my work with this thesis. In particular I wish to express my thanks to Prof. D.G.Burke for his friendly hospitality and stimulating cooperation during my stay at McMaster University.

Financial support from Norges almenvitenskapelige forskningsråd is acknowledged.

## 1. Introduction

The nuclei in the mass 150 region have the peculiar feature that the deformation changes very rapidly as a function of neutron number, with the borderline between spherical and deformed nuclei being at neutron number N=89. This classification is however too coarse to describe the nuclear structure in this region, and there are now many examples of deformed structures on the "wrong" side of the N=89 borderline. The term transitional nuclei has been used to label these isotopes which seem to show both spherical and deformed features depending on the intrinsic structure of the valence nucleons.

In an effort to shed more light on these complicated systems a project has been undertaken to study in a systematic manner the energy levels and spectroscopic factors as obtained from single particle pick-up and stripping reactions. Since the deformation of the nuclei in this region seems mostly to be governed by the neutron number it would be of interest to study a chain of isotopes ranging from the closed shell at N=82 through the transitional region and to the well deformed nuclei at $N \gtrsim 90$. Furthermore it would be an advantage to be able to study the same set of states throughout this region independent of the increasing neutron fermi level.

One way to achieve this is to study the proton states in an isotope chain, and in the present investigation the odd promethium isotopes have been studied by the ($^3$He,d) and (t,$\alpha$) reactions on targets of even-even neodymium and samarium isotopes. This way one populates the spherical $g_{7/2}$, $d_{5/2}$, $h_{11/2}$, $s_{1/2}$ and $d_{3/2}$ shell model states and it is possible

to study the components which result from the fragmentation of these states.

This will yield information from an unbroken chain of isotopes ranging from the spherical case of $^{143}$Pm through the transitional region to the deformed nucleus $^{151}$Pm. It is of particular interest to study the behavior of the intruder state $h_{11/2}$ as a function of neutron number. A similar study [1] of the $h_{11/2}$ neutron state in this region showed that the deformed characteristics of this state stretched far into the transitional region and that the full shell model transfer strength was never observed when experiments were carried out in the spherical regime.

In order to reduce the uncertainties in the measured cross sections from one nucleus to the other, the present series of ($^3$He,d) experiments have all been performed in the same laboratory using the same equipment and under similar conditions, and thereby improving the accuracy of the measured spectroscopic factors. As an additional check on the relative cross sections, separate ($^3$He,d) experiments were done with a target of natural neodymium.

Systematics from the stripping reactions

For a stripping reaction on an even-even target the spectroscopic factor $S_{lj}$ is related to the experimental cross-section through the formula

$$d\sigma/d\Omega = S_{lj}\ (2j+1)\ N\sigma_{lj}\ (\theta)_{DW}$$

Thus the spectroscopic factors can simply be obtained by dividing the experimentally observed cross-sections with the normalized cross-sections obtained from a distorted wave calculation.

A normalization of N=6 for the ($^3$He,d) reaction has been used throughout this thesis. By summing the strengths $S_{lj}$ (2j+1) one should get the number of holes in the Z=50→82 shell for the Nd target nuclei used in this investigation. Theoretically this number is 32-10=22.

By summing the spectroscopic factors $S_{lj}$ for all fragments of a shell model state "lj" one gets a measure of the partial filling of that state. According to pairing theory on has to a first approximation $U^2_{lj} = \Sigma S_{lj}$ where $U^2_{lj}$ is the emptiness of the orbital "lj". Following the method outlined in paper III energy centroids and single particle energies are computed along with summed spectroscopic strengths for the shell model states $g_{7/2}$, $d_{5/2}$, $h_{11/2}$, $s_{1/2}$ and $d_{3/2}$ in the promethium isotopes using an energy gap parameter $\Delta$=1100 keV.

With the completion of the present experiments it is now possible to display in a systematic manner the trends of the spectroscopic strengths in promethium isotopes ranging in mass number from 143 to 151 as obtained by the ($^3$He,d) reaction. Furthermore the use of a natural neodymium target provides an internal check on experimental cross sections to states in the various isotopes. Thereby the problems with the absolute normalization in each experiment are bypassed and it is possible to present experimental cross-sections and spectroscopic factors with relative accuracy better than 10%.

At first it is interesting to compare the summed strength to each isotope. These figures represent the number of holes in the neodymium targets and should thus be 22 for all the isotopes provided all the fragments have been identified in the spectra. The resulting numbers as obtained

from paper I,II,III and V yield 20.4 ($^{143}$Pm), 20.0 ($^{145}$Pm), 20.7 ($^{147}$Pm), 17.7 ($^{149}$Pm) and 13.3 ($^{151}$Pm). In view of the rather dramatic changes in the fragmentation of the shell model states observed in the three lightest isotopes the total strength is remarkably constant. Furthermore the reduction in strength that occurs in going to $^{149}$Pm can be traced to the $h_{11/2}$ orbital which in $^{147}$Pm accounts for a strength of 9.7 while in $^{149}$Pm it is only 7.0. The further reduction in strength observed in going to $^{151}$Pm is brought about by the static deformation of the $^{151}$Pm nucleus which scatters some of the fragments outside the range of our spectra. In particular the $h_{11/2}$ strength is further reduced to 4.6. The reaction data [2] on $^{151}$Pm are adequately described in terms of the Nilsson model. At this point the evidence from the reaction data seems to indicate that the nuclei $^{143,145,147}$Pm are all spherical and $^{151}$Pm is deformed while $^{149}$Pm is slightly deformed when the odd proton occupies the $h_{11/2}$ state, otherwise spherical.

A comparison to pairing theory is given in Figure 1 where the curved line represents the emptiness factor $U^2_{lj}$ as a function of single particle energy. The horizontal bars represent the shell model states and are plotted at energies $(\varepsilon-\lambda)$ obtained from the energy centroids $\bar{E}$, assuming the fermi level $\lambda$ to be at the ground state energy $\varepsilon_o$. The lengths of the bars represent spectroscopic strengths. In Figure 1 both stripping and pick-up data [3,4,5] for $^{143-149}$Pm are presented in the same plot, where stripping data are represented by horizontal bars plotted from the left and pick-up data are plotted from the right. Agreement between experiment and theory would thus be obtained if the horizontal bars were just long enough to reach to the $U^2_{lj}$ curve.

The agreement is quite satisfactory for the lightest nuclei, and it is gratifying to notice how all the fragments in the $^{145}$Pm spectrum add up to the same general shell model scheme as in $^{143}$Pm. Figure 1 also shows quite clearly the energy gap in the middle of the Z=50 - 82 shell, supporting the idea of a subshell closure at Z=64 after the filling of the $d_{5/2}$ and $g_{7/2}$ orbitals [2]. It is seen that the complementary pick-up data [3]for $^{143}$Pm are in excellent agreement with the pairing model. However, the breakdown of this simpled-minded description is starting already in the $^{147}$Pm nucleus. Here only the $h_{11/2}$ and $s_{1/2}$ states are in reasonable agreement with the model while the $g_{7/2}$ and $d_{5/2}$ states located closer to the fermi surface deviate from the model. Note that the $d_{5/2}$ orbital is more than half full and in paper II it was placed below the fermi surface. In Figure 1, however, the level ordering of the $g_{7/2}$ and $d_{5/2}$ orbitals in $^{147}$Pm is chosen to be consistent with that found in $^{143,145}$Pm. In $^{149}$Pm it appears that all orbitals have approximately the same filling and the resemblance with pairing theory is rather poor.

In Figure 2 the trends of the spectroscopic factors for the $s_{1/2}$, $d_{3/2}$, $h_{11/2}$ and $d_{5/2}$ states are summarized and the complexity in the fragmentation of the $s_{1/2}$ and $d_{3/2}$ states demonstrates that also the $^{145}$Pm and $^{147}$Pm isotopes ought to be classified as transitional nuclei. The main component of the $s_{1/2}$ state can, however, be traced through the three lightest isotopes; only in $^{145}$Pm is the strength split between the two strongly populated levels at 728 and 1059 keV. This can possibly be attributed to the coupling of a $2^+$ phonon to the $5/2^+$ ground state of $^{145}$Pm which would create a $1/2^+$ vibrational state in the vicinity of the $s_{1/2}$ state.

A similar coupling scheme based on the $7/2^+$ ground state might be used to explain the splitting of the $d_{3/2}$ strength into the two levels at 416 and 751 keV in $^{149}$Pm, while a more involved scheme will have to be introduced to account for the apparent chaotic fragmentation of the $d_{3/2}$ state in $^{147}$Pm.

The $d_{5/2}$ state seems to be much more resistant against fragmentation and contains its full strength in one prominent peak throughout the transitional region and splits up according to the Nilsson model in the deformed $^{151}$Pm isotope. This splitting is visualised in Figure 3 where the energies of the most prominent peaks from the $d_{5/2}$ and from the $g_{7/2}$ orbitals are plotted versus isotope number. In the deformed regime the Nilsson labelling is given. The $7/2^+$ [404] assignment in $^{153}$Pm is a new tentative assignment based on the data from ref. 4.

Contrary to what was found for the $h_{11/2}$ neutron hole state in this region, the $h_{11/2}$ proton particle state appears with the full strength expected from the shell model in the three lightest isotopes. In $^{149}$Pm it breaks into a pattern resembling that expected for a slightly deformed, strongly Coriolis coupled nucleus. Indeed the results from a recent (p, 2nγ) study [5] revealed a strongly perturbed rotational band based on the lowest lying $11/2^-$ state.

## Systematics from the pick-up reactions

The differential cross section for a pick-up reaction on an even-even target is given by

$$\frac{d\sigma}{d\Omega} = S_{\ell j} \, N\sigma_{\ell j}(\theta)_{DW}$$

A value of N=23 has been used for all polarized (t,α)

experiments included in this thesis.

Measures of the spectroscopic strengths, $S_{\ell j}$, can thus be obtained simply by dividing the experimentally observed cross sections by the quantity $N\sigma_{\ell j}(\theta)_{DW}$. As was pointed out in ref. 4, however, the values of $\sigma_{\ell j}(\theta)_{DW}$ are quite sensitive to the choice of optical model parameters for the (t,α)reaction. Therefore the extracted spectroscopic strengths will also depend on these parameters.

In a shell-model basis one may consider the samarium targets as systems with 12 protons outside a Z=50 closed shell core. By summing the strengths $S_{\ell j}$ from the (t,α) reaction, one should get the average number of particles in the Z=50-82 shell for the samarium target nuclei.

By summing the experimental strengths $S_{\ell j}$ of all fragments of a shell model state "ℓj" one gets the average number of particles in that orbit and thus one gets a measure of the distribution of the valence protons among the shell model states forming the Z=50-82 shell.

With the completion of the present study it is now possible to compare the (t,α) strength to fragments of the $h_{11/2}$, $g_{7/2}$, $d_{5/2}$ and $d_{3/2}$ states in promethium nuclei with mass number ranging from A=147 to A=153 (data for $^{153}$Pm are taken from ref.4). This comparison is shown in Figure 4 where the number associated with each level is the spectroscopic strength extracted as discussed above. It should be noted that the nucleus $^{147}$Pm has only been studied by an incomplete angular distribution of unpolarized (t,α), thus larger uncertainties should be associated with these spectroscopic factors. The numbers in brackets correspond to levels for which the spins have not been measured and only ℓ=values

are known. For the deformed nuclei the Nilsson orbitals assigned to the various levels are also shown. To illustrate the general flow of the spectroscopic strength some levels are connected with dotted lines.

For the strongly populated $g_{7/2}$ hole state it is seen that the major part of its strength is connected to one level in $^{147}$Pm and $^{149}$Pm, and that a dramatic change occurs in going to the deformed nuclei $^{151}$Pm and $^{153}$Pm where the $g_{7/2}$ strength is observed to be distributed over many Nilsson orbitals.

For the $h_{11/2}$ particle state the situation is somewhat different in that the deformed regime seems to penetrate into the $^{149}$Pm nucleus, and only in $^{147}$Pm is the strength gathered into one state. Also the particle nature of this state is well displayed, in the spherical nucleus $^{147}$Pm the $h_{11/2}$ state is far above the fermi surface and is almost empty, while in the deformed case some of the fragments are found to be below the fermi surface and thus give larger spectroscopic factors in the pick-up reaction.

Only with the technique of the polarized (t,α) reaction has it become possible to distinguish fragments of the $d_{5/2}$ state from those of the $d_{3/2}$ state observed in transfer reactions. Examining the top half of Figure 4 it appears that for both $d_{5/2}$ and $d_{3/2}$ some strong coupling effects in $^{147}$Pm distribute the strengths over many levels. Then in $^{149}$Pm the $d_{5/2}$ strength is again concentrated in mainly one strong peak, while de $d_{3/2}$ is still split almost evenly into two peaks. Finally in the deformed nuclei the strength is distributed over the Nilsson orbitals, but still some peculiar coupling distributes the strength to the $5/2^+$ [402] orbital over several fragments. By summing the pick-up strengths to all known fragments of the four states $d_{3/2}$, $d_{5/2}$, $g_{7/2}$ and $h_{11/2}$ one obtains the numbers:

10.1 ($^{153}$Pm), 9,9 ($^{151}$Pm), 11,9 ($^{149}$Pm). This shows that although a quite marked redistribution of pick-up strengths occurs passing through this chain of Pm isotopes, the total strength of all assigned peaks remains quite stable with a variation of less than 15%. This is in contrast to the result obtained by Maher et al. (6) where it was reported that for the $^{152}$Sm (d,$^{3}$He) $^{151}$Pm reaction only 10% of the total strength in the other Pm isotopes was observed.

## Summary and Conclusion

In the present thesis odd Pm isotopes have been studied by one proton pick-up and stripping reactions. Spin assignment and spectroscopic factors have been obtained for a number of energy levels. In the stripping reactions, the relative cross-sections have been measured with an unusually high precision by the use of a target of natural neodymium. The spectroscopic strengths have been extracted using standard distorted wave methods.

The nuclear structures of these promethium isotopes fall into three categories. The spherical approach seems valid for $^{143,145}$Pm and the deformed regime covers $^{151,153}$Pm, while $^{147,149}$Pm remain as transitional nuclei.

In a very recent report [5] the Pm-isotopes were studied by in-beam gamma and electron spectroscopy and a variety of different model calculations were performed in order to reproduce the experimental data on the transitional Pm isotopes. Both vibrational (intermediate-coupling and cluster-vibration) and rotational (axial and triaxial) models were tried with the conclusion that both rotational and vibrational models are compatible in this region. Indeed, from the transfer-reaction studies of odd Ho isotopes [7] and Tm isotopes [8] the gamma vibration

is seen to couple strongly to the single particle orbitals causing a fragmentation of the single particle strength in these rotational nuclei. Similar effects are observed in odd Tb isotopes [9] and Eu isotopes [10] where fragmentation of the single particle transfer strength is believed to be due to particle-vibration couplings. This suggests that any model trying to give a unified description of the odd Pm isotopes will have to incorporate both rotational and vibrational degrees of freedom.

One such model called the dynamical deformation theory (DDT) [11] has shown some success in describing even-even rotational, transitional and vibrational nuclei. Recently a project has been started [12] to develop a program that will calculate the single particle transfer cross sections based on DDT wave functions. The present data will then serve as a critical test of those calculations.

## References


1) G.Løvhøiden, J.R.Lien, S.El-Kazzaz, J.B.Rekstad, C.Ellegaard, J.Bjerregaard, P.Knudsen and P.Kleinheinz, to be published.

J.Rekstad, G.Løvhøiden, J.R.Lien, S.El-Kazzaz, C.Ellegaard, J.Bjerregaard, P.Knudsen and P.Kleinheinz, to be published.

2) P.Kleinheinz, S.Lunardi, M.Ogawa and M.R. Maier, Z.Phys. A284 (1978) 351.
P.Kleinheinz, M.Ogawa, R.Broda, P.J.Daly, D.Haenni, H.Beuscher and A.Kleinrahm, Z.Phys. A286 (1978) 27.

3) Nuclear Data Sheets 25 (1978) 603.

4) D.G.Burke, G.Løvhøiden, E.R.Flynn and J.W.Sunier, Phys. Rev. C18 (1978) 693.

5) M.Kortelahti, A.Pakkanen, M.Piiparinen, E.Hammaren, T.Komppa and R.Komu, Annual Report (1978) 85, Dept. of Physics, University of Jyväskylä, Finland.

6) J.V.Maher, R.Kamermans, J.W.Smith and R.H.Siemssen, Annual Report KVI Groningen, (1975) 28.

7) J.D.Panar, O.Straume and D.G.Burke, Can.J.Phys. 55 (1977) 1657.

8) H.C.Cheung, D.G. Burke and G.Løvhøiden, Can.J.Phys. 52 (1974) 2108.

9) J.C.Tippet and D.G.Burke, Can. J.Phys. 50 (1972) 3152.

10) D.G.Burke, G.Løvhøiden, O.Straume, E.R.Flynn and J.W. Sunier, Can.J.Phys. 57 (1979) 271.

11) K.Kumar, B.Remaud, P.Aguer, J.S.Vaagen, A.C.Rester, R.Foucher and J.H.Hamilton, Phys. Rev. C16 (1977) 1235.

12) J.S.Vaagen, private communication.

## Figure Captions

Fig. 1 The summed spectroscopic strengths for the various shell model states represented by horizontal bars and plotted at the appropriate single particle energies are compared to the pairing prediction represented by the $U^2$ curve. Bars plotted from the right stem from the pick-up reactions.

Fig. 2 Energy levels for fragments of the $s_{1/2}$, $d_{3/2}$, $d_{5/2}$ and $h_{11/2}$ states populated in the ($^3$He,d) reaction. The numbers associated with each level are the spectroscopic strengths $(2j+1)\ S_{lj}$ found from the ($^3$He,d) reaction.

Fig. 3 Bandhead energies for Nilsson orbitals originating in the $d_{5/2}$ and $g_{7/2}$ states are plotted for some Pm isotopes. Negative energies correspond to hole states. In $^{147,149}$Pm the strongest $5/2^+$ and $7/2^+$ states are plotted for comparison.

Fig. 4 Energy levels for fragments of the $d_{3/2}$, $d_{5/2}$, $g_{7/2}$ and $h_{11/2}$ states populated in the (t,α) reaction. The numbers associated with each level are the spectroscopic strengths $S_{lj}$ found from the (t,α) reaction.

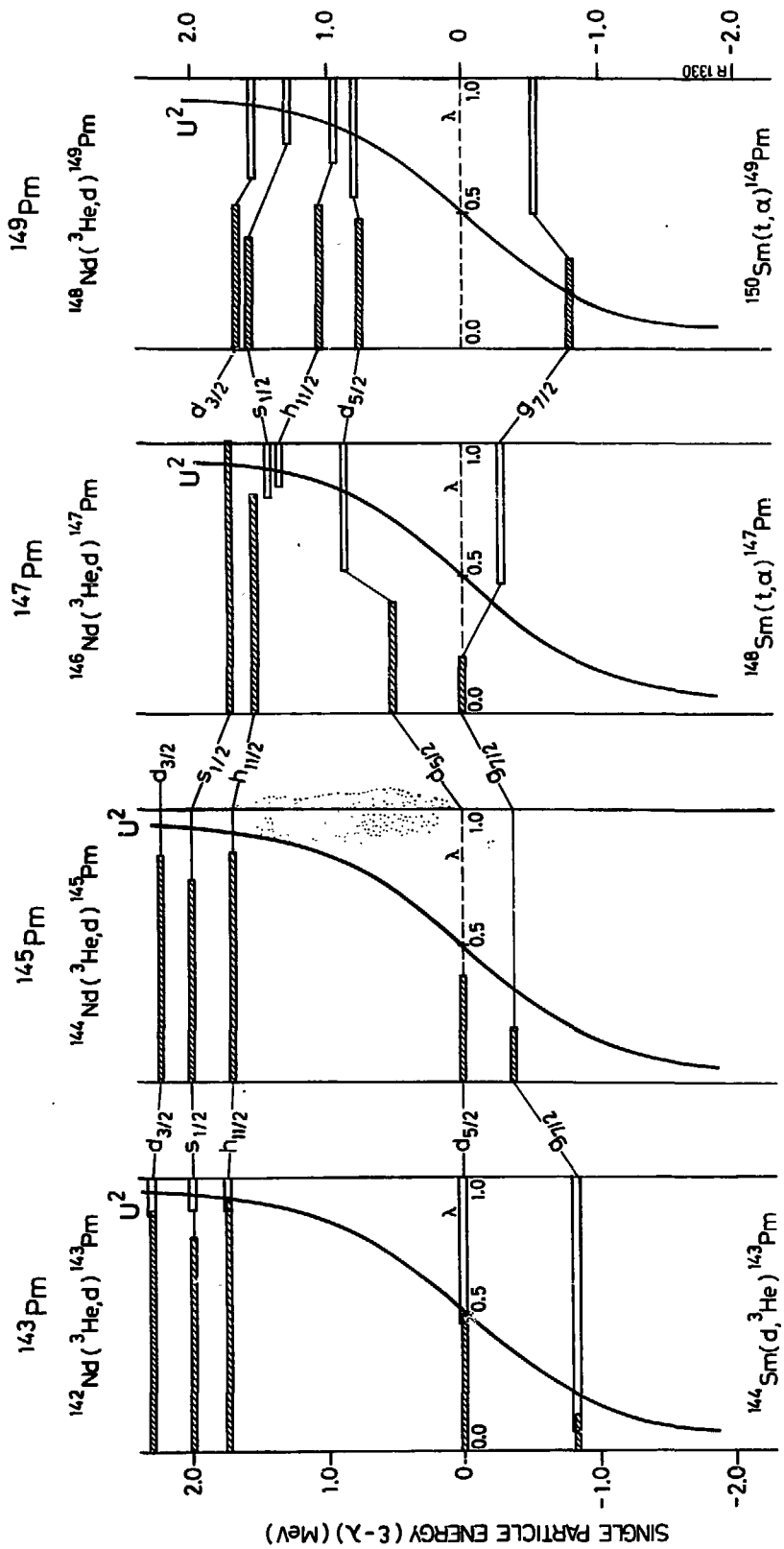
149Pm
147Pm
145Pm
143Pm
148Nd(3He,d)149Pm
146Nd(3He,d)147Pm
144Nd(3He,d)145Pm
142Nd(3He,d)143Pm
150Sm(t,α)149Pm
148Sm(t,α)147Pm
144Sm(d,3He)143Pm
U2
λ
d3/2
s1/2
h11/2
d5/2
g7/2
SINGLE PARTICLE ENERGY (ε-λ) (MeV)
2.0
1.0
0
-1.0
-2.0
0.0
0.5
1.0

FIGURE 1.

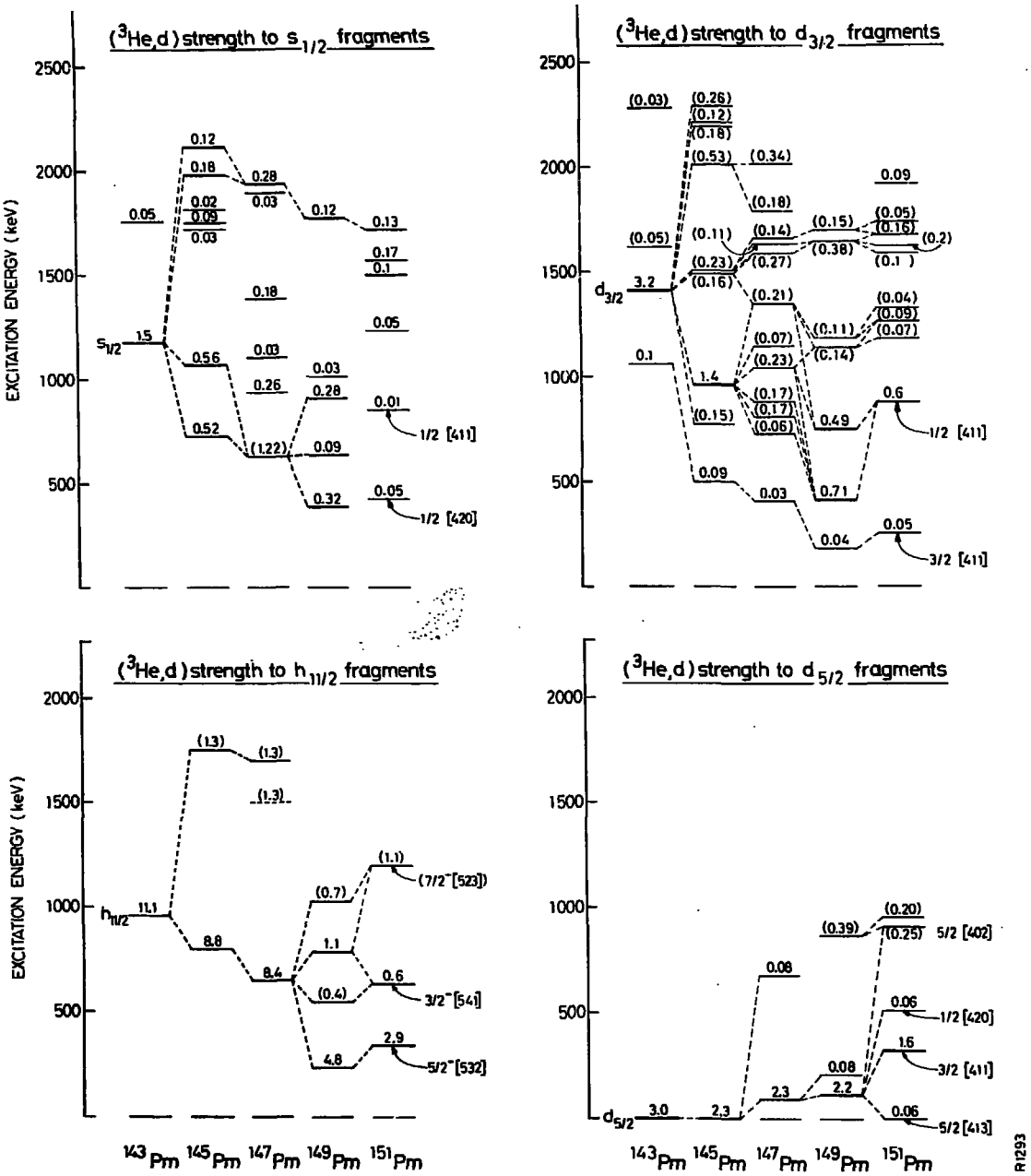
(3He,d) strength to s1/2 fragments
(3He,d) strength to d3/2 fragments
(3He,d) strength to h11/2 fragments
(3He,d) strength to d5/2 fragments
EXCITATION ENERGY (keV)
2500
2000
1500
1000
500
s1/2
d3/2
h11/2
d5/2
1/2 [411]
1/2 [420]
3/2 [411]
(7/2⁻[523])
3/2⁻[541]
5/2⁻[532]
5/2 [402]
1/2 [420]
3/2 [411]
5/2 [413]
143Pm 145Pm 147Pm 149Pm 151Pm
R1293

FIGURE 2

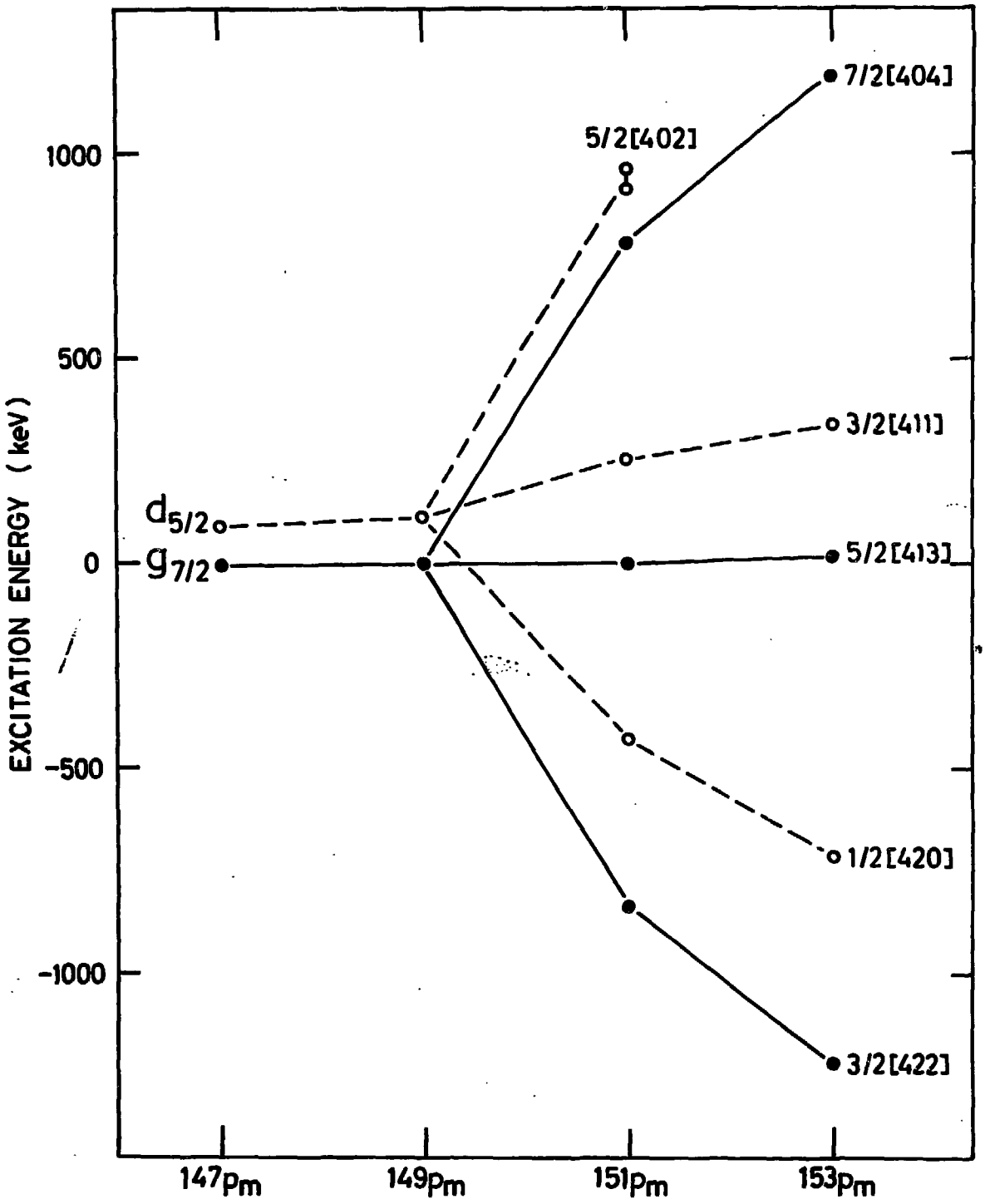
EXCITATION ENERGY ( keV )
1000
500
0
-500
-1000
147Pm
149Pm
151Pm
153Pm
7/2[404]
5/2[402]
3/2[411]
d5/2
g7/2
5/2[413]
1/2[420]
3/2[422]

FIGURE 3

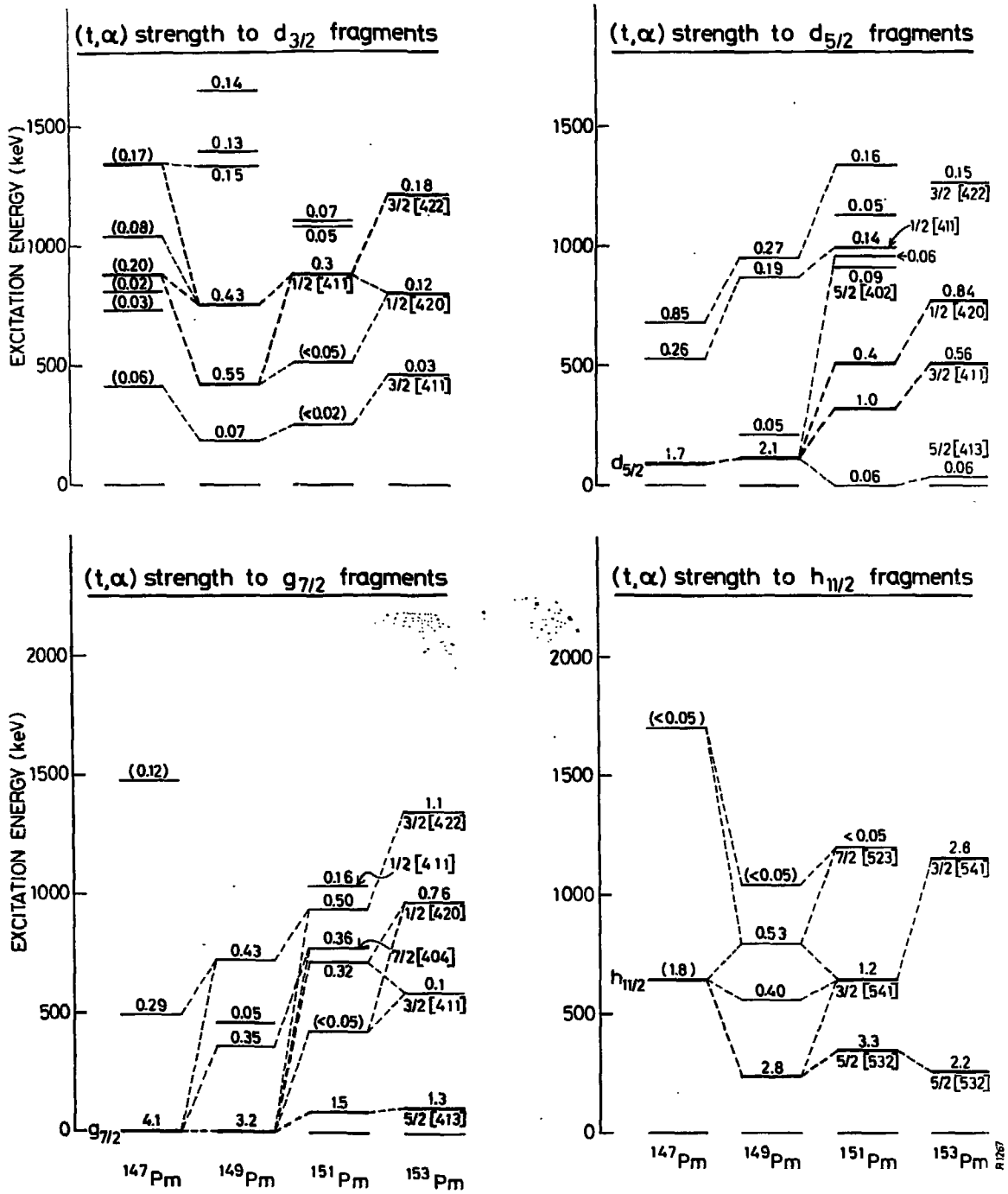
(t,α) strength to d3/2 fragments
(t,α) strength to d5/2 fragments
(t,α) strength to g7/2 fragments
(t,α) strength to h11/2 fragments
EXCITATION ENERGY (keV)
147Pm
149Pm
151Pm
153Pm
3/2 [422]
1/2 [411]
1/2 [420]
3/2 [411]
5/2 [402]
5/2 [413]
7/2 [404]
7/2 [523]
3/2 [541]
5/2 [532]

FIGURE 4

# P A P E R I

## PROTON STATES IN THE N = 88 NUCLEI

## $^{149}Pm$, $^{151}Eu$ AND $^{153}Tb$

## POPULATED IN THE($\tau$,d) AND($\alpha$,t) REACTIONS

1.E.1:2.G *Nuclear Physics* A266 (1976) 390–412; 

# PROTON STATES IN THE $N = 88$ NUCLEI $^{149}$Pm, $^{151}$Eu AND $^{153}$Tb POPULATED IN THE (τ, d) AND (α, t) REACTIONS

O. STRAUME, G. LØVHØIDEN† and D. G. BURKE
*McMaster University, Hamilton, Ontario*

Received 23 March 1976

**Abstract:** The (τ, d) and (α, t) reaction on targets of $^{148}$Nd, $^{150}$Sm and $^{152}$Gd have been studied, using beams of 24 MeV $^3$He and 27 MeV $^4$He from the McMaster University FN tandem Van de Graaff accelerator. The reaction products were analyzed with a magnetic spectrograph and detected with photographic emulsions. The (α, t) spectra were measured at two angles for each target, and the (τ, d) reactions were studied at 8 or 9 angles. The $l$-values for a number of low-spin states were determined from the (τ, d) angular distributions, and ratios of the (α, t) and (τ, d) cross sections were used to obtain $l$-values for several other states. There are some striking similarities in the observed structures of the three final nuclei, $^{149}$Pm, $^{151}$Eu and $^{153}$Tb. In each case there are low-lying strongly populated $\frac{11}{2}^-$ states and a higher lying $l = 5$ level somewhat below 1 MeV of excitation energy. Several states (10 in $^{149}$Pm, 17 in $^{151}$Eu and 8 in $^{153}$Tb) appear to be populated via $l = 2$ transitions, and there are strongly excited $\frac{1}{2}^+$ levels at $\geq$ 1 MeV of excitation energy in each case. Of particular interest is a $\frac{7}{2}^-$ state located $\leq$ 50 keV above the lowest $\frac{11}{2}^-$ state in each nuclide. The relatively strong populations of these $\frac{7}{2}^-$ levels in the present experiments are contrary to expectations based on the simple shell model as there are no $f_{\frac{7}{2}}$ states in the $50 < Z < 82$ shell.

E NUCLEAR REACTIONS $^{148}$Nd, $^{150}$Sm, $^{152}$Gd(τ, d), $E = 24$ MeV; measured $\sigma(\theta, E_d)$. $^{148}$Nd, $^{150}$Sm, $^{152}$Gd(α, t), $E = 27$ MeV; measured $\sigma(E_t)$. $^{149}$Pm, $^{151}$Eu and $^{153}$Tb deduced levels, $J$, π, $l$S. $^{153}$Tb deduced proton separation energy. Enriched targets.

## 1. Introduction

The nuclei $^{149}$Pm, $^{151}$Eu and $^{153}$Tb, with 88 neutrons, are situated in a region where the deformation changes rapidly with neutron number. They are all believed to be predominantly spherical with $d_{\frac{5}{2}}$ ($^{151}$Eu and $^{153}$Tb) and $g_{\frac{7}{2}}$ ($^{149}$Pm) ground states, while the neighbouring heavier $^{151}$Pm, $^{153}$Eu and $^{155}$Tb isotopes show rotational behaviour with many features explained by the Nillsson model. However, in the $86 < N < 90$ region one may expect to find both rotational and spherical states coexisting as low-lying excitations. This was found to be the case [1–4]) in $^{149}$Sm and $^{151}$Gd with $N = 87$ and therefore the level structures of $^{149}$Pm, $^{151}$Eu and $^{153}$Tb may show similar features. Such rotational behaviour appears in $^{153}$Eu(p, t)$^{151}$Eu measurements [5, 6]) where a $\frac{5}{2}^+$[413] rotational band was indicated to be strongly populated.

† Now at the University of Bergen, Norway.

The nuclear structure of $^{149}$Pm has been investigated [7]) by the decay of $^{149}$Nd. Levels in $^{151}$Eu have previously been studied [8, 9]) by the radioactive decay from $^{151}$Gd, Coulomb excitation [10]) and the previously mentioned (p, t) experiments [5, 6]). States in $^{153}$Tb have been studied [11, 12]) by the decay of $^{153}$Dy.

The aim of the present work was to complement these earlier works by measurements of (α, t) spectra and (τ, d) angular distributions. Both the (α, t) and (τ, d) reactions were measured because the ratio of their cross sections is a useful indicator of $l$-values, and because high spin states are only weakly populated in the (τ, d) re-

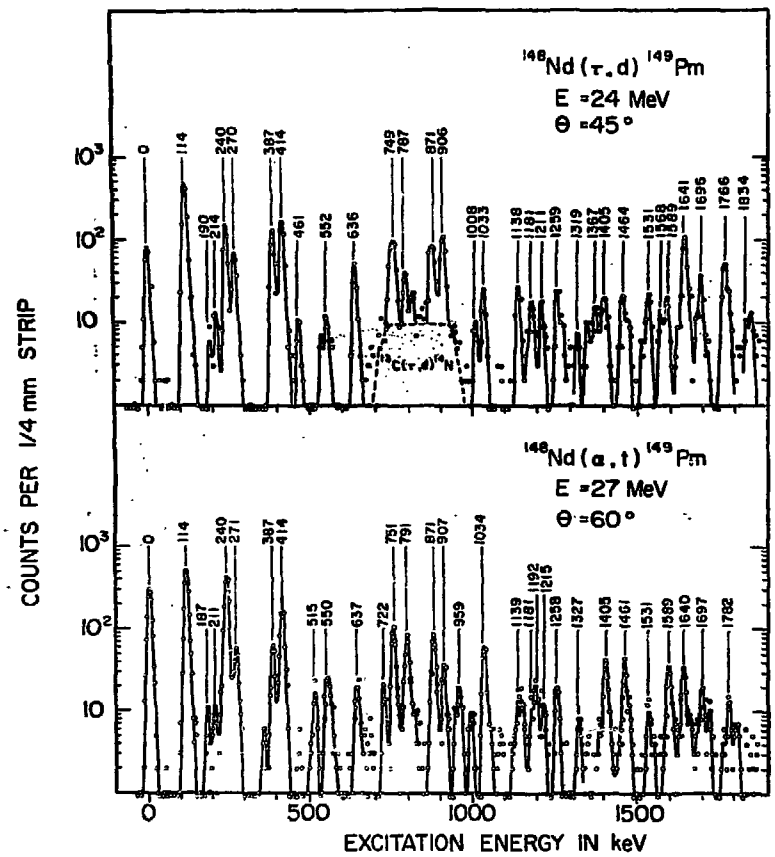


Fig. 1. The $^{148}$Nd(τ, d)$^{149}$Pm spectrum at 45° and the $^{148}$Nd(α, t)$^{149}$Pm spectrum at 60°. The numbers associated with the peaks are the excitation energies in keV.

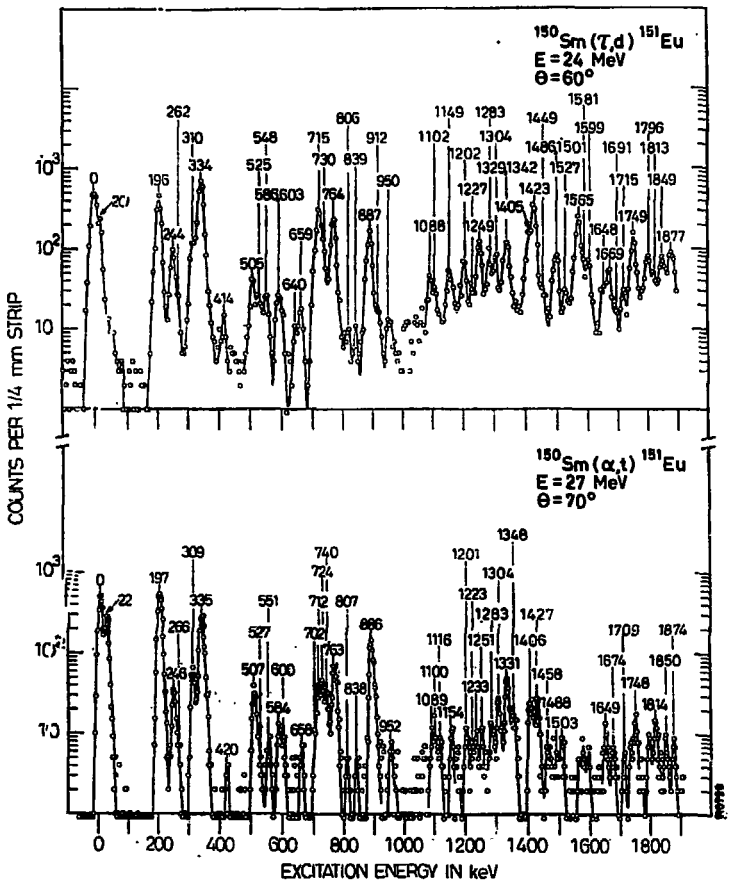


Fig. 2. The $^{150}$Sm(τ, d)$^{151}$Eu spectrum at 60° and the $^{150}$Sm(α, t)$^{151}$Eu spectrum at 70°. The numbers associated with the peaks are the excitation energies in keV.

action. Spectroscopic factors have been determined from the observed cross sections, and these are compared with shell-model predictions in sect. 3.

## 2. Experimental details and results

The experiments were performed with 24 MeV $^{3}$He and 27 MeV $^{4}$He beams from the McMaster University Tandem Van de Graaff accelerator. The reaction products were analyzed with an Enge split-pole magnetic spectrograph and detected with nuclear emulsions. The $^{152}$Gd target was prepared in an isotope separator by direct

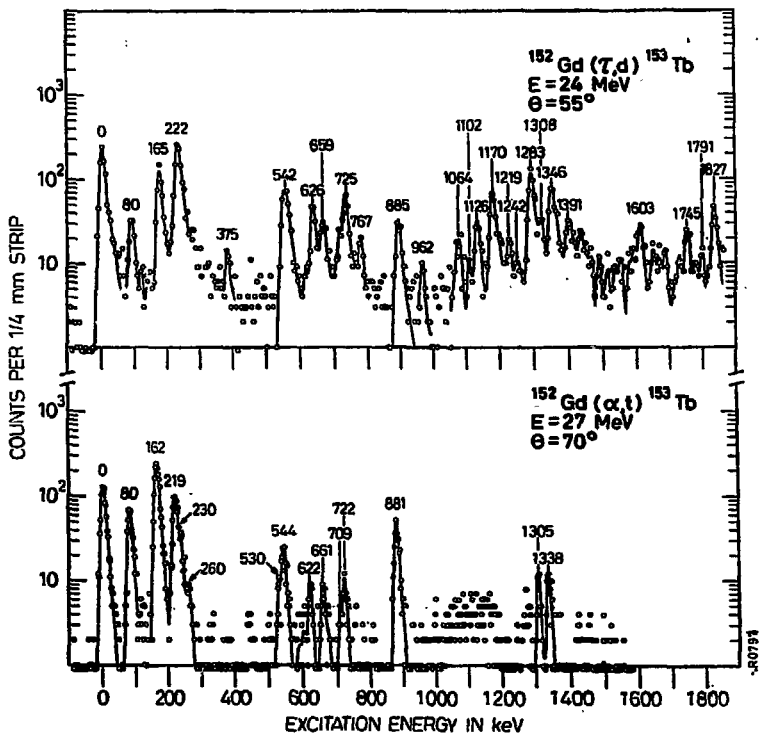


Fig. 3. The $^{152}$Gd(τ, d)$^{153}$Tb spectrum at 55° and the $^{152}$Gd(α, t)$^{153}$Tb spectrum at 70°. The numbers associated with the peaks are the excitation energies in keV.

deposition of the separated isotope on a carbon foil. It is expected that the isotopic enrichment would be > 99 %. The $^{148}$Nd and $^{150}$Sm targets were made from samples of $Nd_2O_3$ and $Sm_2O_3$ isotopically enriched ot 95.4 % and 99.9 % in $^{148}$Nd and $^{150}$Sm, respectively. The oxides were reduced by heating in vacuum with thorium metal and the enriched isotopes were vacuum evaporated onto carbon foils. The target thicknesses were ≈30 μg/cm². The exposures were normalized by using a Si(Li) monitor detector at $\theta = 30°$ in the target chamber and also by making short exposures on photographic emulsions in the spectrograph, recording elastically scattered particles at $\theta = 30°$. The cross sections for elastic scattering were determined from the distorted wave born approximation (DWBA) calculations described below.

Exposures were recorded at two angles for each target with the (α, t) reaction. Experience has shown that there is no advantage in measuring (α, t) angular distributions as there is essentially no diffraction structure or distinction between the curves for different $l$-values in this mass region with the beam energy used here. Spectra from

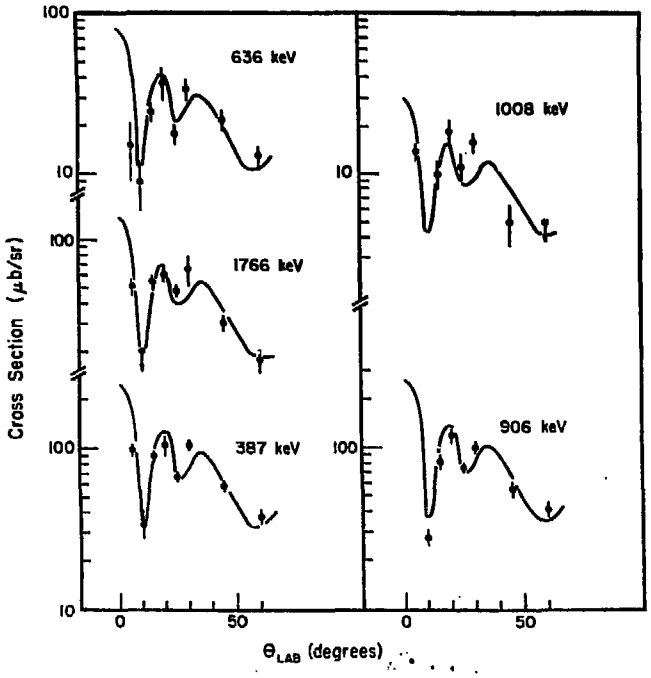


Fig. 4a. Angular distributions for $l = 0$ transitions in the $^{148}$Nd(τ, d)$^{149}$Pm reaction. The solid curves result from DWBA calculations and the points represent the experimental data.

the (τ, d) reactions were measured at 8 or 9 angles getween 6° and 60° for each target. Sample spectra from each of the six reactions studied are shown in figs. 1–3 and (τ, d) angular distributions for a number of states in $^{149}$Pm, $^{151}$Eu and $^{153}$Tb are presented in figs. 4–6. Cross sections for two typical angles are given in tables 1–3. Excitation energies determined from the (τ, d) and (α, t) reactions, as well as a set of adopted energies, are also given in tables 1–3. The energies shown in figs. 1–6 are values obtained from the reaction indicated. Those shown in subsequent figures and in the text are the adopted energies from tables 1–3. The uncertainties for the energy measurements are estimated to be less than 4 keV for both the (τ, d) and (α, t) reactions. The main uncertainties in the cross-section measurements result from the normalization procedure. It is expected that the relative cross sections at different angles should be accurate within 15 %, but the absolute values may be in error by as much as 30 %.

The proton separation energies for $^{149}$Pm and $^{151}$Eu are kown quite precisely [13]) but the mass of $^{153}$Tb has been estimated on the basis of systematics only. In the present study the difference in $Q$-values for the $^{152}$Gd(τ d)$^{153}$Tb and $^{150}$Sm(τ,

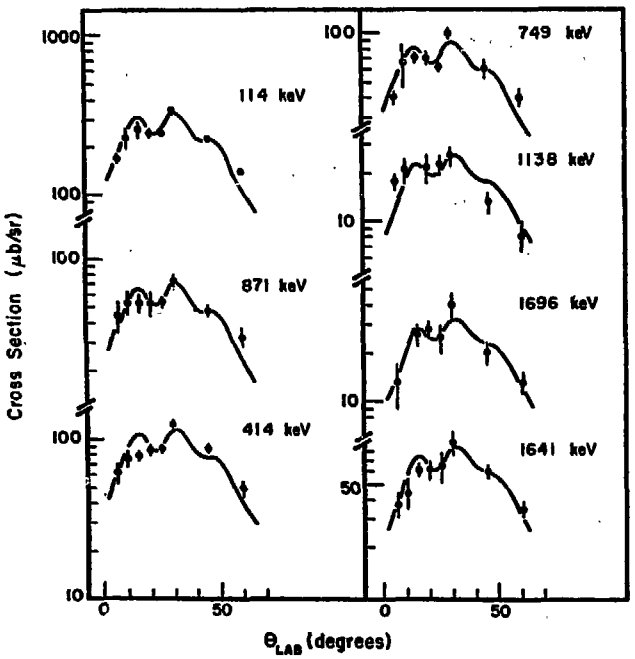


Fig. 4b. Angular distributions for $l = 2$ transitions in the $^{148}$Nd(τ, d)$^{149}$Pm reactions. See caption to fig. 4a.

d)$^{151}$Eu reactions was obtained by comparing the excitation energies at which peaks from the $^{13}$C(τ, d)$^{14}$N reaction occurred in the spectra. Assuming a proton separation energy [13]) $S_p = 4890.2 \pm 2.3$ keV for $^{151}$Eu, a value of $S_p = 3860 \pm 30$ keV was obtained for $^{153}$Tb.

It has been shown that the ratio of (α, t) and (τ, d) cross sections is a useful indicator of $l$-values, since this ratio varies by about an order of magnitude as the $l$-value changes from 0 to 5. Figs. 7–9 show plots of this ratio as a function of excitation energy in $^{149}$Pm, $^{151}$Eu and $^{153}$Tb. The solid curves result from DWBA calculations, and the data points represent the experimental results of the present work. The numbers associated with the data points are the excitation energies in keV.

The DWBA calculations were done using the computer code DWUCK [14]). The optical model parameters for the (τ, d) and (α, t) reactions are the same as those used in a study of the heavier odd terbium isotopes [15]), but with no spin-orbit term. It is customary to use a normalization factor $N = 4.42$ for the (τ, d) reactions. However, in a number of previous studies [15–19]) it was found that the spectroscopic strengths obtained from experimental cross sections using this normalization constant were

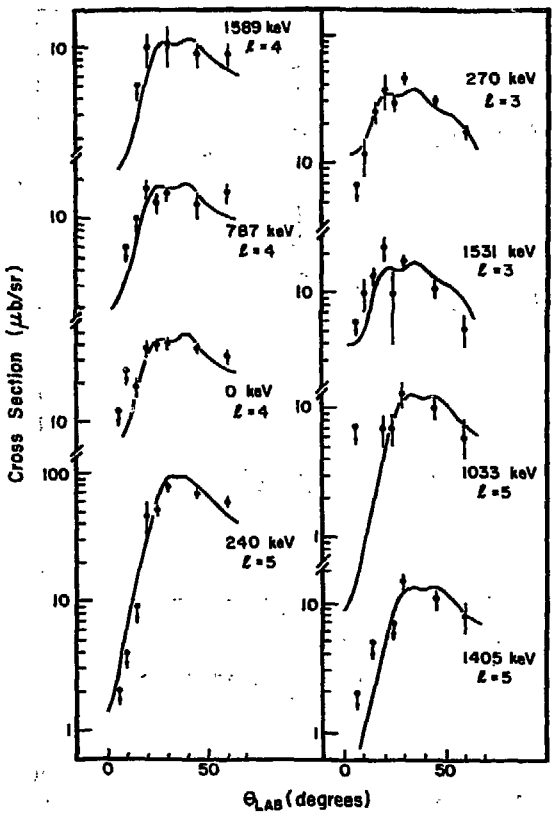


Fig. 4c. Angular distributions for $l = 3, 4$ and $5$ transitions in the $^{148}$Nd(τ, d)$^{149}$Pm reaction. See caption to fig. 4a.

30–40 % larger than the value predicted theoretically. This descrepancy has been ascribed to shortcomings of the DWBA calculations. In the present study a normalization constant $N = 6.0$ has therefore been adopted for the (τ, d) reaction. The magnitude of $N$ for the (α, t) reaction is not well known, and a value of $N = 111$ has been used in order that the experimental spectroscopic factors for the two stripping reactions have similar values for the best understood states in the three nuclides.

## 3. Interpretation of the results

The assignments of spins and parities for levels in $^{149}$Pm, $^{151}$Eu and $^{153}$Tb are discussed in subsects. 3.1, 3.2 and 3.3 respectively. These interpretations are based on

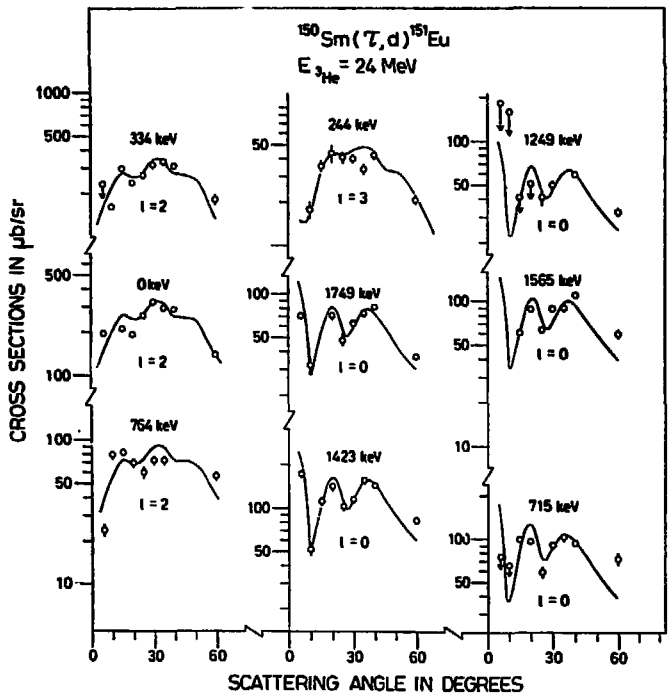


Fig. 5. Angular distributions for the $^{150}$Sm(τ, d)$^{151}$Eu reaction. See caption to fig. 4a.

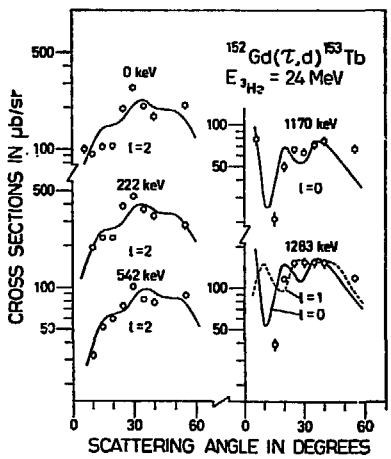


Fig. 6. Angular distributions for the $^{152}$Gd(τ, d)$^{153}$Tb reaction. See caption to fig. 4a.

TABLE 1

Levels populated in $^{149}Pm$

| Energy (keV) | | | | $d\sigma/d\Omega$ ($\mu$b/sr) | | | | Assignment | | | $(d\sigma/d\Omega)/N\,\sigma_t^{DW}(\theta)$ | | |
|---|---|---|---|---|---|---|---|---|---|---|---|---|---|
| (τ, d) | (α, t) | adopted | previous | (τ, d) | | (α, t) | | present exp | previous [a] | adopted | (τ, d) [b] | (α, t) [c] | adopted |
| | | | | 45° | 60° | 40° | 60° | | | | | | |
| 0 | 0 | 0 | 0 | 40 | 33 | 146 | 108 | $l = 4, 5$ | $\frac{7}{2}^+$ | $\frac{7}{2}^+$ | 1.8 | 2.6 | 2.2 |
| 114 | 114 | 114 | 114 | 236 | 146 | 209 | 171 | $l = 2$ | $\frac{5}{2}^+$ | $\frac{5}{2}^+$ | 2.2 | 2.5 | 2.4 |
| 190 | 187 | 189 | 189 | ≈2 | 3 | ≈3 | 2 | $l = 2, 3, 4$ | $\frac{3}{2}^+$ | $\frac{3}{2}^+$ | 0.043 | 0.033 | 0.039 |
| 214 | 211 | 211 | 211 | 6 | 6 | ≈3 | 2 | | $\frac{5}{2}^+$ | $\frac{5}{2}^+$ | 0.084 | 0.033 | 0.058 |
| 240 | 240 | 240 | 240 | 74 | 62 | 281 | 147 | $l = 5$ | $\frac{11}{2}^-$ | $\frac{11}{2}^-$ | 4.8 | 3.9 | 4.3 |
| 270 | 271 | 270 | 270 | 33 | 19 | 20 | 20 | $l = 2, 3$ | $\frac{7}{2}^-$ | $\frac{7}{2}^-$ | 0.34 | 0.18 | 0.26 |
| 387 | 387 | 387 | 388 | 61 | 38 | 12 | 19 | $l = 0$ | $(\frac{1}{2}^+)$ | $\frac{1}{2}^+$ | 0.32 | 0.23 | 0.28 |
| 414 | 414 | 414 | | 91 | 50 | 62 | 56 | $l = 2$ | | $l = 2$ | 0.71 | 0.85 | 0.78 |
| 461 | | 461 | | 5 | 3 | | | | | | | | |
| 514 | 515 | 515 | | | 4 | 7 | 6 | | | | | | |
| 552 | 550 | 550 | | 5 | 5 | 7 | 12 | $(l = 5)$ | | $l = 5$ | 0.39 | 0.21 | 0.30 |
| 636 | 637 | 636 | | 23 | 14 | ≈4 | 8 | $l = 0$ | | $\frac{1}{2}^+$ | 0.090 | 0.11 | 0.10 |
| 721 | 722 | 722 | | | 5 | ≈4 | 6 | | | | | | |
| 749 | 751 | 750 | | 63 | 42 | 33 | 33 | $l = 2$ | | $l = 2$ | 0.49 | 0.55 | 0.52 |
| 787 | 791 | 789 | | 14 | 17 | 46 | 29 | $l = 4, 5$ | | $l = 4$ | 0.60 | 0.89 | 0.74 |
| 871 | 871 | 871 | | 49 | 34 | 26 | 27 | $l = 2$ | | $l = 2$ | 0.39 | 0.48 | 0.44 |
| 906 | 907 | 906 | | 58 | 43 | ≈4 | 12 | $l = 0$ | | $\frac{1}{2}^+$ | 0.28 | 0.15 | 0.28 |
| | 959 | 959 | | | | ≈3 | 6 | | | | | | |

| | | | | | | | | | | | |
|---|---|---|---|---|---|---|---|---|---|---|---|
| 1008 | | 1008 | 5 | ≈5 | | | $l = 0$ | $\frac{1}{2}^+$ | 0.033 | | 0.033 |
| 1033 | 1034 | 1034 | 11 | 6 | 38 | 22 | $(l = 5)$ | $l = 5$ | 0.65 | 0.73 | 0.69 |
| 1138 | 1139 | 1138 | 14 | 8 | 5 | 4 | $l = 2$ | $l = 2$ | 0.14 | 0.12 | 0.13 |
| 1181 | 1181 | 1181 | 13 | 4 | 6 | 4 | $l = 2$ | $l = 2$ | 0.11 | 0.14 | 0.12 |
| | 1192 | 1192 | | ≈3 | 6 | 7 | | | | | |
| 1211 | 1215 | 1212 | 8 | ≈4 | | ≈4 | | | | | |
| 1259 | 1258 | 1259 | 15 | 9 | 8 | 6 | $l = 2, 3$ | | | | |
| 1319 | | 1319 | 4 | | | | | | | | |
| | 1327 | 1327 | | | 4 | 3 | | | | | |
| 1367 | | 1367 | 11 | ≈5 | | | | | | | |
| 1405 | 1405 | 1405 | 12 | 8 | 23 | 14 | $l = 5$ | $l = 5$ | 0.67 | 0.51 | 0.59 |
| 1464 | 1461 | 1462 | 14 | ≈7 | 19 | 12 | $l = 4, 5$ | | | | |
| 1531 | 1531 | 1531 | 12 | 6 | 7 | 4 | $l = 3$ | $l = 3$ | 0.12 | 0.11 | 0.11 |
| 1568 | | 1568 | 6 | ≈3 | | | | | | | |
| 1589 | 1589 | 1589 | 9 | 9 | ≈13 | 12 | $l = 4$ | $l = 4$ | 0.32 | 0.50 | 0.41 |
| 1641 | 1640 | 1641 | 63 | 37 | | 11 | $l = 2$ | $l = 2$ | 0.38 | 0.33 | 0.38 |
| 1696 | 1697 | 1696 | 21 | 14 | | 6 | $l = 2, 3$ | $l = 2$ | 0.15 | 0.20 | 0.15 |
| 1766 | 1764 | 1766 | 33 | 19 | | <2 | $l = 0$ | $\frac{1}{2}^+$ | 0.12 | | 0.12 |
| | 1782 | 1782 | | ≈4 | | 4 | | | | | |
| 1834 | | 1834 | 5 | 5 | | | | | | | |

[a]) Ref. [7]).
[b]) Normalization factor $N$ for the (τ, d) reaction taken to be 6.0.
[c]) Normalization factor $N$ for the (α, t) reaction taken to be 111.

TABLE 2

Levels populated in $^{151}$Eu

| Energy (keV) | | | | dσ/dΩ(μb/sr) | | | | Assignment | | | (dσ/dΩ)/N σ$_l^{DW}$(θ) | | |
|---|---|---|---|---|---|---|---|---|---|---|---|---|---|
| (τ, d) | (α, t) | adopted | previous | (τ, d) | | (α, t) | | present | previous | adopted | (τ, d) [a] | (α, t) [b] | adopted |
| | | | | 30° | 60° | 60° | 70° | | | | | | |
| 0 | 0 | 0 | 0 | 325 | 141 | 106 | 124 | $l = 2$ | $\frac{5}{2}^+$ [c] | $\frac{5}{2}^+$ | 2.1 | 2.7 | 2.4 |
| ≈20 | 22 | 22 | 21.5 | ≈53 | 57 | 68 | 71 | $l = 4$ | $\frac{7}{2}^+$ [c] | $\frac{7}{2}^+$ | 2.5 | 2.9 | 2.7 |
| 196 | 197 | 197 | 196.2 | 109 | 116 | 165 | 139 | $l = 5$ | $\frac{11}{2}^-$ [d] | $\frac{11}{2}^-$ | 7.6 | 5.3 | 6.4 |
| 244 | 246 | 245 | 243.2 | 40 | 21 | 9 | 9 | $l = 3(2)$ | $\frac{7}{2}^-$ [d,c] | $\frac{7}{2}^-$ | 0.35 | 0.16 | 0.26 |
| 262 | ≈266 | 262 | 261 | ≈4 | ≈4 | ≈1 | ≈1 | $l = 0, 1, 2$ | $\frac{5}{2}^+$ [c] | $\frac{5}{2}^+$ | 0.037 | 0.028 | 0.033 |
| 310 | 309 | 309 | 307 | 80 | 33 | 11 | 15 | $l = 1, 2$ | $\frac{3}{2}^+$ [c] | $\frac{3}{2}^+$ | 0.47 | 0.37 | 0.47 |
| 334 | 335 | 335 | | 321 | 183 | 69 | 74 | $l = 2$ | | $l = 2$ | 2.2 | 2.1 | 2.2 |
| ≈414 | ≈420 | 417 | 415 | 1 | 3 | | 1 | | $(\frac{9}{2}^+)$ [c] | | | | |
| 505 | 507 | 506 | 503.5 | ≈8 | 10 | 7 | 9 | $l = 4, 5$ | $\frac{9}{2}^+$ [c] | $\frac{9}{2}^+$ | 0.35 | 0.36 | 0.36 |
| 525 | 527 | 525 | | 11 | 6 | | 1 | $l = 0, 1$ | | $\frac{1}{2}^+$ | 0.041 | | 0.041 |
| 548 | 551 | 549 | | 11 | 6 | 2 | 2 | $l = 2$ | | $l = 2$ | 0.073 | | 0.073 |
| 586 | 584 | 585 | 587 | 10 | 5 | 3 | 3 | $l = 2, 3$ | $\frac{5}{2}^+$ [c] | $\frac{5}{2}^+$ | 0.059 | | 0.059 |
| ≈603 | 600 | 600 | 600 | 2 | 4 | | 1 | | $(\frac{3}{2}^+)$ [c] | $\frac{3}{2}^+$ | 0.13 | 0.13 | 0.13 |
| ≈640 | | 640 | | ≈3 | ≈2 | | | | | | | | |
| 659 | 658 | 659 | 653 | 8 | 4 | | 1 | $l = 2$ | $\frac{3}{2}^+$ [c] | $\frac{3}{2}^+$ | 0.046 | | 0.046 |
| ≈701 | ≈702 | 702 | 696 | ≈17 | ≈11 | 2 | 2 | $(l = 2)$ | $\frac{5}{2}^+$ [c] | $\frac{5}{2}^+$ | 0.11 | | 0.11 |
| 715 | ≈712 | 714 | | 91 | 76 | 3 | 8 | $l = 0, 1$ | | $\frac{1}{2}^+$ | 0.43 | 0.49 | 0.43 |
| ≈730 | ≈724 | 727 | | ≈23 | ≈19 | 10 | 8 | | | | | | |
| | ≈740 | 740 | | | | 3 | 5 | | | | | | |
| 764 | 763 | 763 | | ≈72 | 57 | 14 | 18 | $l = 2$ | | $l = 2$ | 0.53 | 0.58 | 0.56 |
| 806 | 807 | 807 | | ≈3 | ≈4 | 1 | 1 | $l = 1, 2, 3$ | | | | | |
| 839 | 838 | 838 | | ≈1 | 2 | ≈1 | 1 | $l = 3, 4$ | | | | | |
| 887 | 886 | 886 | | ≈21 | 41 | 35 | 36 | $l = 5$ | | $l = 5$ | 2.8 | 1.9 | 2.4 |
| 912 | | 912 | 911 [c] | ≈14 | 4 | | | | | | | | |
| 950 | 952 | 952 | | ≈6 | ≈4 | 2 | 2 | $l = 3, 4$ | | | | | |
| ≈1088 | ≈1089 | 1089 | | 14 | 15 | 2 | 2 | | | | | | |
| 1102 | 1100 | 1100 | | | | | 2 | | | | | | |
| | 1116 | 1116 | 1117 [c] | | | 1 | 2 | | | | | | |
| 1149 | 1154 | 1151 | 1154 [c] | ≈6 | ≈11 | 3 | 2 | | | | | | |
| 1202 | 1201 | 1202 | 1200 [c] | 26 | 16 | 2 | 3 | $l = 2$ | | $l = 2$ | 0.15 | | 0.15 |
| 1227 | 1223 | 1225 | | ≈11 | ≈8 | ≈1 | ≈1 | | | | | | |
| | 1233 | 1233 | | | | ≈2 | ≈2 | | | | | | |

TABLE 2 (continued)

| Energy (keV) | | | | dσ/dΩ(μb/sr) | | | | Assignment | | | (dσ/dΩ)/N σ_t^DW(0) | | |
|---|---|---|---|---|---|---|---|---|---|---|---|---|---|
| (τ, d) | (α, t) | adopted | previous | (τ, d) | | (α, t) | | present exp | previous | adopted | (τ, d) [a] | (α, t) [b] | adopted |
| | | | | 30° | 60° | 60° | 70° | | | | | | |
| 1249 | 1251 | 1249 | 1247 [c] | 50 | 33 | 2 | 2 | $l = 0, 1$ | | $\frac{1}{2}^+$ | 0.13 | | 0.13 |
| 1283 | 1283 | 1283 | | 25 | 18 | 1 | 1 | $l = 0, 1$ | | $\frac{1}{2}^+$ | 0.082 | | 0.082 |
| 1304 | 1304 | 1304 | | 16 | 19 | 7 | 6 | $(l = 4)$ | | $l = 4$ | 0.61 | 0.46 | 0.54 |
| ≈1329 | 1331 | 1331 | | ≈13 | ≈9 | 11 | 11 | $l = 5$ | | $l = 5$ | 0.64 | 0.77 | 0.71 |
| 1342 | ≈1348 | 1342 | | 26 | 29 | 4 | 4 | | | | | | |
| ≈1405 | 1406 | 1406 | 1406 [c] | ≈51 | ≈33 | 7 | 7 | $l = 2, 3$ | | $l = 2$ | 0.27 | 0.49 | 0.27 |
| 1423 | 1427 | 1425 | | 115 | 83 | 6 | 5 | $l = 0$ | | $\frac{1}{2}^+$ | 0.29 | 0.41 | 0.29 |
| ≈1449 | | 1449 | | ≈3 | ≈6 | | | | | | | | |
| | 1458 | 1458 | | | | 3 | ≈2 | | | | | | |
| ≈1486 | 1488 | 1488 | | ≈21 | 6 | | ≈1 | $l = 0, 1, 2$ | | | | | |
| ≈1501 | 1503 | 1503 | | ≈25 | ≈21 | 3 | 2 | $(l = 2)$ | | $l = 2$ | 0.15 | | 0.15 |
| 1527 | | 1527 | | 11 | 8 | | | | | | | | |
| 1565 | 1566 | 1565 | | 90 | 60 | ≈2 | ≈1 | $l = 0$ | | $\frac{1}{2}^+$ | 0.22 | | 0.22 |
| ≈1581 | 1576 | 1579 | | ≈26 | ≈13 | ≈2 | ≈1 | $(l = 2)$ | | $l = 2$ | 0.11 | | 0.11 |
| 1599 | 1593 | 1599 | | ≈24 | ≈16 | 2 | 1 | | | | | | |
| ≈1648 | 1649 | 1649 | | 21 | 9 | 4 | 3 | $(l = 3)$ | | | | | |
| 1669 | 1674 | 1672 | | 18 | 14 | ≦1 | 2 | $l = 2, 3$ | | $l = 2$ | 0.10 | | 0.10 |
| 1691 | | 1691 | | ≈5 | ≈5 | | | | | | | | |
| | 1709 | 1709 | | | | ≦1 | 1 | | | | | | |
| 1715 | | 1715 | | 15 | 8 | | | | | | | | |
| 1749 | 1748 | 1749 | | 62 | 37 | 2 | 3 | $l = 0$ | | $\frac{1}{2}^+$ | 0.14 | | 0.14 |
| 1796 | 1793 | 1796 | | 30 | 27 | 1 | 2 | $l = 2, 3$ | | $l = 2$ | 0.18 | | 0.18 |
| ≈1813 | 1814 | 1814 | | ≈13 | ≈13 | 3 | 3 | $(l = 4)$ | | $l = 4$ | 0.40 | | 0.40 |
| 1849 | 1850 | 1850 | | 33 | 21 | 1 | 2 | $l = 2, 3$ | | $l = 2$ | 0.15 | | 0.15 |
| 1877 | 1874 | 1877 | | 54 | 23 | 2 | 2 | $l = 2$ | | $l = 2$ | 0.20 | | 0.20 |

[a] Normalization factor $N$ for the (τ, d) reaction taken to be 6.0.
[b] Normalization factor $N$ for the (α, d) reaction taken to be 111.
[c] Ref. [5]).
[d] Ref. [9]).
[e] Ref. [10]).

TABLE 3

Levels populated in $^{153}$Tb

| Energy (keV) | | | | dσ(dΩ(μb/sr) | | | | Assignment | | | (dσ/dΩ)/$N\sigma_l^{DW}$(θ) | | |
|---|---|---|---|---|---|---|---|---|---|---|---|---|---|
| (τ, d) | (α, t) | adopted | previous [a]) | (τ, d) | | (α, t) | | present exp | previous [a]) | adopted | (τ, d) [b]) | (α, t) [c]) | adopted |
| | | | | 30° | 55° | 40° | 70° | | | | | | |
| 0 | 0 | 0 | 0 | 279 | 209 | ≈24 | 40 | $l = 2$ | $\frac{5}{2}^+$ | $\frac{5}{2}^+$ | 1.8 | 1.9 | 1.9 |
| 80 | 80 | 80 | 80.8 | 41 | 31 | ≈17 | 20 | $l = 4$ | $\frac{7}{2}^+$ | $\frac{7}{2}^+$ | 1.4 | 1.3 | 1.4 |
| 165 | 162 | 163 | 163.3 | 84 | 119 | 98 | 74 | $l = 4, 5$ | $\frac{11}{2}^-$ | $\frac{11}{2}^-$ | 6.9 | 5.4 | 6.2 |
| 222 | 219 | 219 | 218.5 | 457 | 285 | 10 | 31 | $l = 2$ | $\frac{5}{2}(\frac{3}{2})^+$ | $l = 2$ | 2.6 | 2.0 | 2.6 |
| | ≈230 | 230 | | | | ≈5 | ≈5 | $(l = 5)$ | | $\frac{11}{2}^-$ | | 0.34 | 0.34 |
| | 260 | 260 | 263.0 | | | ≈1 | ≈2 | $l > 3$ | $\frac{9}{2}^-$ | | | | |
| 375 | | 375 | 371.6 | 19 | 9 | | | $l < 3$ | $(\frac{5}{2}, \frac{7}{2}, \frac{9}{2})^+$ | | | | |
| | 530 | 520 | 529.5 | | | ≈2 | ≈2 | $l > 3$ | $\frac{9}{2}(\frac{7}{2}, \frac{9}{2})^+$ | | | | |
| 542 | 544 | 543 | 543.5 | 104 | 88 | ≈6 | 6 | $l = 2$ | $(\frac{5}{2}, \frac{7}{2})$ | $\frac{5}{2}^+$ | 0.63 | 0.49 | 0.63 |
| 626 | 622 | 625 | | 65 | 43 | <1 | 2 | $l = 1, 2$ | | $l = 2$ | 0.38 | | 0.38 |
| 659 | 661 | 660 | 660.1 | 22 | 27 | 2 | 2 | $l = 2$ | $\frac{5}{2}(\frac{5}{2}, \frac{7}{2})^+$ | $\frac{5}{2}^+$ | 0.16 | | 0.16 |
| ≈710 | ≈709 | 710 | | ≈43 | ≈19 | <1 | ≈1 | $l = 1, 2$ | | $l = 2$ | 0.18 | | 0.18 |
| ≈725 | ≈722 | 725 | 726.9 | ≈44 | ≈47 | <1 | ≈2 | $l = 1, 2$ | $\frac{5}{2}(\frac{7}{2}, \frac{9}{2})^+$ | $\frac{5}{2}^+$ | 0.29 | | 0.29 |
| 767 | | 767 | | 25 | 15 | | | $l < 2$ | | | | | |
| 885 | 881 | 883 | | 25 | 31 | 17 | 13 | $(l = 5)$ | | $l = 5$ | 1.8 | 1.4 | 1.6 |
| 962 | | 962 | 960 | 8 | 7 | | | $l \leqq 3$ | $\pi = +$ | | | | |
| 1064 | | 1064 | | 33 | 22 | | <2 | $l < 3$ | | | | | |
| 1102 | | 1102 | | 13 | 9 | | 3 | $l \leqq 3$ | | | | | |
| 1126 | | 1126 | | 46 | 30 | | <2 | $l \leqq 3$ | | | | | |
| 1170 | | 1170 | | 63 | 67 | | <2 | $l = 0$ | | $\frac{1}{2}^+$ | 0.21 | | 0.21 |
| 1187 | | 1187 | | 23 | 19 | | <2 | $l < 3$ | | | | | |
| 1219 | | 1219 | | 24 | 19 | | <1 | $l < 3$ | | | | | |
| 1242 | | 1242 | 1240.5 | 11 | ≈7 | | <1 | $l \leqq 3$ | | | | | |
| 1283 | | 1283 | | 155 | 119 | | <2 | $(l = 0)$ | $\frac{1}{2}^+$ | 0.41 | | | 0.41 |
| ≈1308 | 1305 | 1307 | | ≈39 | ≈20 | 2 | 2 | $l < 4$ | | | | | |
| 1346 | 1338 | 1342 | 1341.4 | 80 | 86 | 3 | 2 | $l = 2$ | | $l = 2$ | 0.42 | | 0.42 |
| 1391 | | 1391 | | 38 | 24 | | 2 | $l \leqq 2$ | | | | | |
| 1603 | | 1603 | | ≈20 | 25 | | | | | | | | |
| 1745 | | 1745 | | 40 | 23 | | | | | | | | |
| 1791 | | 1791 | | 21 | 10 | | | | | | | | |
| 1827 | | 1827 | | 55 | 51 | | | | | | | | |

[a]) Ref. [12]). [b]) Normalization factor $N$ for the (τ, d) reaction taken to be 6.0.
[c]) Normalization factor $N$ for the (α, t) reaction taken to be 111.

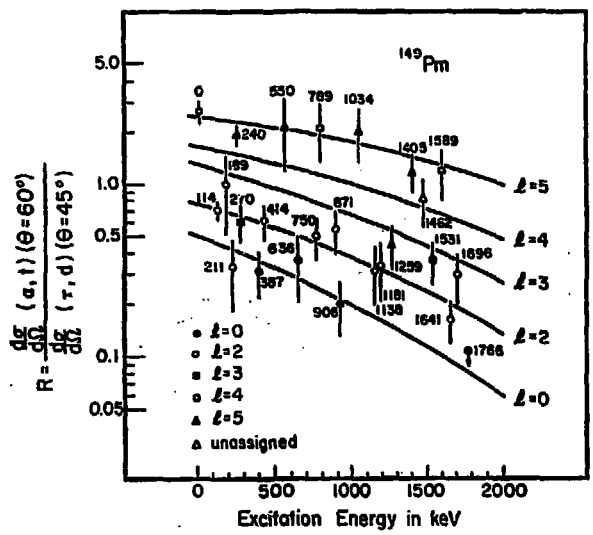


Fig. 7. Ratios of the (α, t) cross sections at 60° to the (τ, d) cross sections at 45° for $^{149}$Pm. The solid curves result from DWBA calculations, and the points represent experimental ratios for the levels indicated. Points with arrows indicate upper (or lower) limits.

previously available data as well as the (τ, d) and (α, t) results from the present work. In subsect. 3.4, the spectroscopic strengths deduced from the experimental cross sections are discussed.

### 3.1. THE NUCLEUS $^{149}$Pm

*3.1.1. States populated by $l = 0$ transitions.* The angular distributions displayed in fig. 4a show that the levels at 387, 636, 906, 1008 and 1766 keV are populated by $l = 0$ transitions. All these levels, except for the weakly populated ones at 1008 and 1766 keV, were also observed in the (α, t) reaction and the cross-section ratios (shown in fig. 7) confirm the $l = 0$ assignments. These five levels are therefore $\frac{1}{2}^+$ states which must each contain a fragment of the $s_{\frac{1}{2}}$ strength.

*3.1.2. States populated by $l = 2$ transitions.* Several of the observed levels have (τ, d) angular distributions and ratios of (α, t) and (τ, d) cross sections which indicate $l = 2$ transfers. This is to be expected since fragments of the $d_{\frac{3}{2}}$ and $d_{\frac{5}{2}}$ shell-model states will be populated in the present experiment. The 114 and 211 keV levels were previously known [7] to be $\frac{5}{2}^+$. It is not possible at the present time to make strong arguments for the spins of the remaining $l = 2$ states. However, some tentative comments based mainly on systematics among the $^{149}$Pm, $^{151}$Eu and $^{153}$Tb levels, and on model dependent arguments, are postponed to subsect. 3.4.

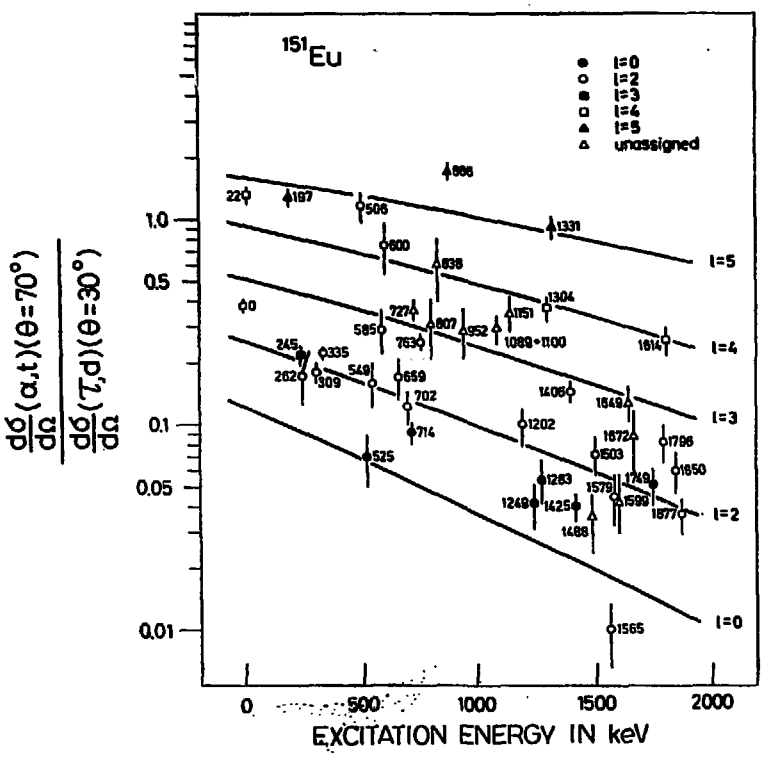


Fig. 8. Ratios of the (α, t) cross sections at 70° to the (τ, d) cross sections at 30° for $^{151}$Eu. See caption to fig. 7.

*3.1.3. States with higher spin.* The ground state of this nucleus is known [7]) to have spin and parity $\frac{5}{2}^+$. This assignment is supported by the angular distribution shown in fig. 4c. However the cross-section ratio for this state is close to the value expected for an $l = 5$ transfer. The state at 240 keV has been assigned [7]) as $\frac{11}{2}^-$ and both the angular distribution and the cross-section ratio confirm this assignment. It is thus seen that the cross-section ratio alone cannot distinguish between $l = 4$ and $l = 5$ transfers. However, in the angular distributions the rapid decrease at forward angles for the $l = 5$ transfer may, in favourable cases, be used to distinguish between $l = 4$ and $l = 5$. In this way the states at 789 and 1589 keV are tentatively assigned as $l = 4$ and those at 550, 1034 and 1405 keV as $l = 5$.

On the basis of the shell model the only negative parity states expected at low excitation energies would be fragments of the $h_{\frac{11}{2}}$ state. However, a $\frac{7}{2}^-$ assignment was previously given [7]) to a state at 270 keV and in the present experiment a level at this

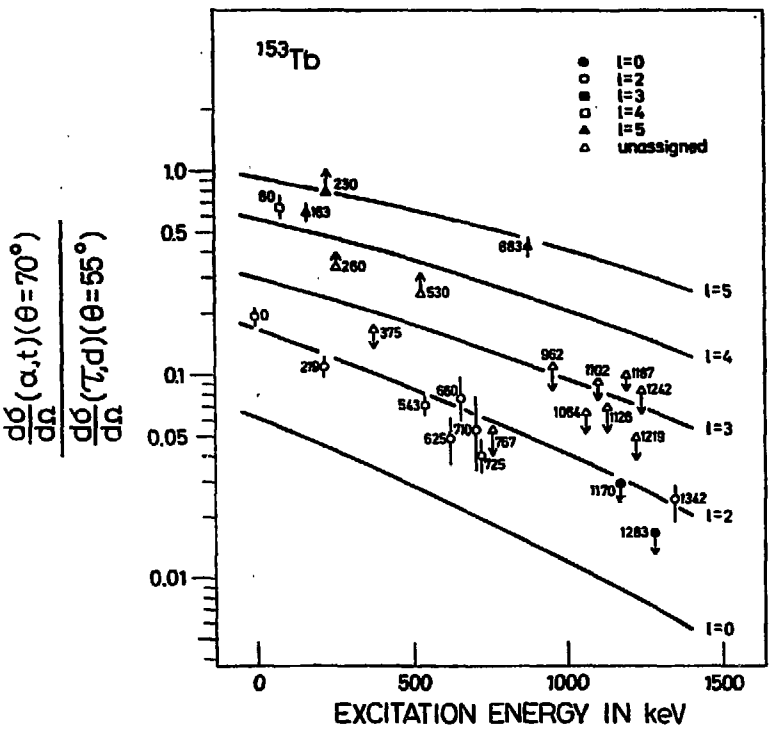


Fig. 9. Ratios of the (α, t) cross sections at 70° to the (τ, d) cross sections at 55° for $^{153}$Tb. See caption to fig. 7.

energy is populated quite strongly with a (τ, d) angular distribution consistent with $l = 3$ (fig. 4c). The state at 1531 keV shows a similar angular dependence and is also given a tentative $l = 3$ assignment.

### 3.2. THE NUCLEUS $^{151}$Eu

*3.2.1. States populated by $l = 0$ transitions.* The angular distributions displayed in fig. 5 show that the levels at 1425 and 1749 keV are populated by $l = 0$ transitions. There is less conclusive evidence from the angular distributions on the 525, 714, 1249, 1283 and 1565 keV levels that have also been assigned $l = 0$. The particle groups associated with these levels were obscured by impurity peaks at forward angles. However, the ratios of (α, t) and (τ, d) cross sections are consistent with low spin ($l = 0, 1$) for these states. The $l = 0$ assignment is favoured because no $l = 1$ strength is available in the $Z = 50$–82 shell. Thus each of the above mentioned states is assigned spin and parity $\frac{1}{2}^+$.

*3.2.2. States populated by $l = 2$ transitions.* There are several levels excited in the present experiments which have been assigned $l = 2$. As in $^{149}$Pm fragments of both the $d_{\frac{5}{2}}$ and $d_{\frac{3}{2}}$ states should be populated. In the (p, t) experiments [5, 6]) $\frac{5}{2}^+$ levels were excited at energies of 0, 261, 307, 587, 653 and 696 keV. The present experiments indicates $l = 2$ transitions to all these levels if the weak peak labelled $\approx$ 702 keV on the edge of the much larger 714 keV peak is assumed to correspond to the previously known 696 keV level. In addition there are also $l = 2$ transitions to levels at 335, 549, 763, 1202, 1406, 1503, 1579, 1672, 1796, 1850 and 1877 keV.

*3.2.3. States with higher spins.* A few levels with high spins were previously located [5, 6, 8–10]) in $^{151}$Eu, namely the 22 keV ($\frac{7}{2}^+$), 196 keV ($\frac{11}{2}^-$), 504 keV ($\frac{9}{2}^+$) and 600 keV ($\frac{9}{2}^+$) levels. The ratios of ($\alpha$, t) and ($\tau$, d) cross sections are consistent with high spin assignments for these levels. The 600 keV level could not be reliably resolved from the 585 keV state which has spin and parity $\frac{5}{2}^+$ but the experimental value of the cross-section ratio for the doublet (fig. 7) is near the value for $l = 4$ thereby suggesting high spin for the 600 keV level. On the basis of the extreme single particle shell model one would not expect to find strongly populated $\frac{9}{2}^+$ states in the present work as the $g_{\frac{9}{2}}$ shell is filled. The spectroscopic strengths to the previously assigned $\frac{9}{2}^+$ states at 504 and 600 keV are in fact very small.

The previously known [9]) $\frac{7}{2}^-$ level at 243.2 keV is populated with appreciable strength in the present experiment in spite of the fact that no spherical $l = 3$ strength is expected in these nuclei. The angular distribution shown in fig. 5 is consistent with $l = 3$ although the cross-section ratio is closer to the value expected for $l = 2$.

In addition to the previously known high spin states, there are levels at 838, 952, 1304, 1649 and 1814 keV for which the ratios of ($\alpha$, t) and ($\tau$, d) cross sections indicate $l$-values of 3 or 4. These states were all weakly populated so the assignments are rather tentative. The 1304 and 1814 keV levels have cross-section ratios giving a stronger $l = 4$ indication than exists for the other levels, so they have been tentatively assigned $l = 4$.

The levels at 886 keV and 1331 keV have cross-section ratios indicating $l = 5$. These may be fragments of the $h_{\frac{11}{2}}$ shell-model state, the main component of which is found at 197 keV, although the possibility that they result from the $h_{\frac{9}{2}}$ shell cannot be excluded.

*3.2.3. Other states.* In the $^{153}$Eu(p, t)$^{151}$Eu experiments levels were observed [5, 6]) at 261, 415 and 600 keV which were interpreted as the $\frac{5}{2}$, $\frac{7}{2}$, and $\frac{9}{2}$ members of a $\frac{5}{2}^+$ [413] band. In the present work weakly populated levels were located at similar excitation energies of 262, 417 and 600 keV. However the levels are populated so weakly that a meaningful comparison of the predicted "fingerprint" pattern for the $\frac{5}{2}^+$ [413] band with the experimental intensities cannot be made. The largest observed cross section for any of these states is of the order of 1 % of the largest peaks in the spectra, and thus there is little assurance that the observed populations result from direct, single-step processes.

### 3.3. THE NUCLEUS $^{153}$Tb

*3.3.1. States populated by $l = 0$ transitions.* The (τ, d) angular distributions and ratios of (α, t) and (τ, d) cross sections shown in figs. 6 and 9 indicate that the 1170 and 1283 keV levels are populated by $l = 0$ transitions. Thus each of these levels is assigned spin and parity $\frac{1}{2}^+$.

*3.3.2. States populated by $l = 2$ transitions.* Several of the observed levels have (τ, d) angular distributions and ratios of (α, t) and (τ, d) cross sections consistent with $l = 2$. Of the presently observed levels only the ground state was definitely known to be $\frac{5}{2}^+$. In previous decay studies [11, 12]) tentative $\frac{3}{2}^+$ and $\frac{5}{2}^+$ assignments have been made for many states in $^{153}$Tb, only but a few of these levels appear to be populated appreciably in the present work. By combining the results from the decay work [12]) with the present data one can assign $I^\pi = \frac{3}{2}^+$ to the level at 660 keV and $\frac{5}{2}^+$ to the levels at 534 and 725 keV. The 219 keV level, which is strongly populated in the present work, probably corresponds to the 218.6 keV $\frac{5}{2}^+$ (or $\frac{3}{2}^+$) state found in decay studies [12]). Also the levels at 625, 710 and 1342 keV are tentatively given $l = 2$ assignments although the possibility of $l = 1$ can not be ruled out for the 625 and 710 keV levels.

*3.2.3. States with higher spins.* The levels at 80 and 163 keV were previously assigned $\frac{7}{2}^+$ and $\frac{11}{2}^-$, respectively [11, 12]). These assignments are in agreement with the present study where the ratios of (α, t) and (τ, d) cross sections are consistent with high spins for these levels (fig. 9). The states at 230 and 883 keV are also populated via high angular momentum transfers which are most likely $l = 5$. Also in $^{153}$Tb a low-lying $\frac{7}{2}^-$ level is located [12]) at an excitation energy of 213.8 keV. A spectroscopic factor for this $\frac{7}{2}^-$ level cannot be deduced as the particle group associated with it is obscured by the heavily populated 219 keV level.

### 3.4. SPECTROSCOPIC STRENGTHS

The theoretical differential cross section for a direct single particle stripping reaction on a doubly even target is given by

$$\frac{d\sigma}{d\Omega} = S_{lj}(2j+1)N\sigma_l(\theta)_{\mathrm{DWBA}}. \qquad (1)$$

In the present work $N$ is taken to be 6.0 and 111.0 for the (τ, d) and (α, t) reactions respectively, as discussed in sect. 2. Thus, by dividing the experimentally observed cross sections by the quantity $N\sigma_l(\theta)_{\mathrm{DWBA}}$, one can obtain a measure of the spectroscopic strengths $(2j+1)S_{lj}$.

In a shell-model basis one may consider the target nuclei $^{148}_{60}$Nd, $^{150}_{62}$Sm and $^{152}_{64}$Gd to be systems with 10, 12 and 14 "active" protons outside a $Z = 50$ "inert core". The $g_{\frac{7}{2}}$, $d_{\frac{5}{2}}$, $h_{\frac{11}{2}}$, $d_{\frac{3}{2}}$ and $s_{\frac{1}{2}}$ shells should yield the lowest lying states in $^{149}$Pm, $^{151}$Eu and $^{153}$Tb. The particle states, such as $h_{\frac{11}{2}}$, $d_{\frac{3}{2}}$ and $s_{\frac{1}{2}}$, would be expected to have large spectroscopic factors in the stripping reaction, whereas the $g_{\frac{7}{2}}$ and $d_{\frac{5}{2}}$ states should be already partly filled.

By summing the strengths $S_{lj}(2j+1)$ obtained from the $(\tau, d)$ and $(\alpha, t)$ processes for all these final states one should get the average number of holes in the $Z = 50$–82 shell. Theoretically this number is 32–10 = 22 for $^{148}$Nd, 32–12 = 20 for $^{150}$Sm and 32–14 = 18 for $^{152}$Gd. The spectroscopic strengths for most of the strongly populated states are listed in tables 1–3. As no spin-orbit term was used in the optical model potentials, these quantities could be obtained using the $l$-value assignments from the previous section without having to know the $j$-values. The assigned levels account for 85 %, 91 % and 82 % of the observed $(\tau, d)$ cross section at 30° up to an excitation energy of ≈1.85 MeV in $^{149}$Pm, $^{151}$Eu and $^{153}$Tb, respectively. For these levels the sums $S_{lj}(2j+1)$ are ≈ 15, ≈ 22 and ≈ 16 for $^{149}$Pm, $^{151}$Eu and $^{153}$Tb respectively, which are equal to the expected numbers within the experimental uncertainties for the two heaviest nuclei. For $^{149}$Pm it appears as though some of the expected strength was not found. It is noted however, that in $^{149}$Pm only 38 levels are found below 1.85 MeV while in $^{151}$Eu there were 56 levels. This may indicate that the missing strength in $^{149}$Pm could occur at higher excitation energies and was therefore not included.

It would be desirable to compare the observed spectroscopic factors with theoretical values for each shell-model state and also to determine whether the proton holes were distributed amongst these states in accordance with pairing theory. However the lack of information on $j$-values, particularly for the $l = 2$ states, makes a detailed comparison impossible. The observed strengths to the various states are summarized in table 4, where it has been assumed as before that the $s_{\frac{1}{2}}$, $g_{\frac{7}{2}}$ and $h_{\frac{11}{2}}$ shell-model states are responsible for the $l = 0$, 4 and 5 transitions, respectively. The levels known to be $I^\pi = \frac{1}{2}^+$ are categorized as $d_{\frac{3}{2}}$ and other $l = 2$ transitions are labelled as "d". The latter group may contain some $d_{\frac{5}{2}}$ states but one might expect that those at higher excitation energies are more likely to be $d_{\frac{3}{2}}$ fragments.

The total strengths $\sum(2j+1)S_{lj}$ in these categories appear to be in reasonable agreement with the values calculated by Kumar [20]) for the $^{150}$Sm target. The last column of table 4 shows values of $(2j+1)U_{jl}^2$ which were obtained from the $(2j+1)V_{jl}^2$ values of Kumar, and which can be compared directly with the experimental $\sum(2j+1)S_{lj}$ quantities. The amount of observed $l = 0$ strength is lower than expected, perhaps because part of it could have occurred at higher excitation energies and was thus not included. Considerable uncertainty arises in the case of the $l = 2$ states because in each nuclide there is a strongly populated state of unknown $j$ at a fairly low excitation energy. These states occur at 414 keV in $^{149}$Pm, 335 keV in $^{151}$Eu and 219 keV in $^{153}$Tb. It is seen from table 4 that the states in $^{151}$Eu and $^{153}$Tb already known to be $I = \frac{1}{2}$ have total strengths comparable to the predicted $d_{\frac{3}{2}}$ value. If the 335 keV level in $^{151}$Eu and the 219 keV level in $^{153}$Tb were $I = \frac{1}{2}$ the observed $d_{\frac{3}{2}}$ strengths would be ≈ 50 % greater than those predicted. On the other hand, these levels could have $I = \frac{3}{2}$ without creating such a discrepancy, as the total strength for all $l = 2$ levels which could possibly be $I = \frac{3}{2}$ is equal, within experimental error, to the predicted $d_{\frac{3}{2}}$ value for $^{151}$Eu and $^{153}$Tb. As stated earlier, the total observed strength in $^{149}$Pm is somewhat smaller than expected so there is no particular preference for the 414 keV

TABLE 4

Spectroscopic information on states populated in $^{149}$Pm, $^{151}$Eu and $^{153}$Tb

| Shell-model state | Excitation energy (keV) | | | $(2j+1)S_{jl}$ | | | $\Sigma(2j+1)S_{jl}$ | | | Calculated [a] $\Sigma(2j+1)U^2_j$ for $^{151}$Eu | |
|---|---|---|---|---|---|---|---|---|---|---|---|
| | $^{149}$Pm | $^{151}$Eu | $^{153}$Tb | $^{149}$Pm | $^{151}$Eu | $^{153}$Tb | $^{149}$Pm | $^{151}$Eu | $^{153}$Tb | spher. | def. [b] |
| $g_{\frac{7}{2}}$ | 0 | 22 | 80 | 2.2 | 2.7 | 1.4 | | | | | |
| | 789 | 1304 | | 0.74 | 0.54 | | 3.4 | 3.6 | 1.4 | 3.29 | 3.57 |
| | 1589 | 1814 | | 0.41 | 0.40 | | | | | | |
| $d_{\frac{5}{2}}$ | 114 | 0 | 0 | 2.4 | 2.4 | 1.9 | | | | | |
| | 211 | 262 | | 0.058 | 0.033 | | | | | | |
| | | 309 | 543 | | 0.47 | 0.63 | 2.5 | 3.1 | 2.8 | 2.94 | 3.13 |
| | | 585 | | | 0.059 | | | | | | |
| | | 659 | | | 0.046 | | | | | | |
| | | 702 | 725 | | 0.11 | 0.29 | | | | | |
| $h_{\frac{11}{2}}$ | 240 | 197 | 163 | 4.3 | 6.4 | 6.2 | | | | | |
| | 550 | | | 0.30 | | | 5.3 | 9.5 | 7.8 | 8.68 | 8.48 |
| | 1043 | 886 | 883 | 0.69 | 2.4 | 1.6 | | | | | |
| | | 1331 | | | 0.71 | | | | | | |
| "d" | 189 | | | 0.039 | | | | | | | |
| | 414 | 335 | 219 | 0.78 | 2.2 | 2.6 | | | | | |
| | 750 | 549 | 625 | 0.52 | 0.073 | 0.38 | | | | | |
| | 871 | 763 | 660 | 0.44 | 0.56 | 0.16 | | | | | |
| | 1138 | 1202 | 710 | 0.13 | 0.15 | 0.18 | 2.6 | 4.1 | 3.7 | 3.49 | 3.29 |
| | 1181 | 1406 | 1342 | 0.12 | 0.27 | 0.42 | | | | | |
| | 1641 | 1503 | | 0.38 | 0.15 | | | | | ($d_{\frac{5}{2}}$) | ($d_{\frac{5}{2}}$) |
| | *1696* | *1579* | | *0.15* | *0.11* | | | | | | |
| | | 1672 | | | 0.10 | | | | | | |
| | | 1796 | | | 0.18 | | | | | | |
| | | 1850 | | | 0.15 | | | | | | |
| | | 1877 | | | 0.20 | | | | | | |
| $s_{\frac{1}{2}}$ | | 525 | 1170 | | 0.041 | 0.21 | | | | | |
| | 387 | 714 | 1283 | 0.28 | 0.43 | 0.41 | | | | | |
| | 636 | 1249 | | 0.10 | 0.13 | | | | | | |
| | | 1283 | | | 0.082 | | 0.81 | 1.3 | 0.62 | 1.76 | 1.64 |
| | 906 | 1425 | | 0.28 | 0.29 | | | | | | |
| | 1008 | 1565 | | 0.033 | 0.22 | | | | | | |
| | 1766 | 1749 | | 0.12 | 0.14 | | | | | | |

[a]) Ref. [20]).
[b]) The deformation corresponds to the rms values $\beta = 0.138$ and $\gamma = 22°$ in the ground state of $^{150}$Sm.

level being $I = \frac{3}{2}$ or $I = \frac{5}{2}$ on this basis. In view of the marked similarity in the low-lying level structure of these three nuclides however, it is quite likely that these three $I = 2$ states of unknown $j$ are of similar nature. It is interesting to note that in the odd-neutron Ru and Pd nuclei, for which the neutron numbers are the same as the proton numbers of the nuclides studied here, there are also two $l = 2$ states strongly populated in the neutron stripping reaction leading to each final nucleus [21]). The lower of these levels is $\frac{5}{2}^+$ (as in the present case) and the other is $\frac{3}{2}^+$. Thus there is some indirect evidence favouring $I = \frac{3}{2}$ assignments for the second strong $l = 2$ transitions observed in the present experiments, although decay studies [12]) suggest an $I = \frac{5}{2}$ preference for the 219 keV level in $^{153}$Tb.

The results presented in table 4 show that the total observed strengths for $l$-values of 0, 2, 4 and 5 can be accounted for assuming the nuclei are spherical, even though severe fragmentation of the shell-model states must occur. However, one interesting feature of this work is that the levels at 270 keV in $^{149}$Pm and 245 keV in $^{151}$Eu, previously known to have $I^\pi = \frac{7}{2}^-$, are populated with appreciable intensity. A similar state [12]) at 213.8 keV in $^{153}$Tb may have been populated but the peak would have been obscured by the larger peak due to the 219 keV level. It is noticed that in each of the three nuclides the lowest $\frac{7}{2}^-$ state is found to be 30–50 keV above the first $\frac{11}{2}^-$ state. As no $f_{\frac{7}{2}}$ strength is expected in this region on the basis of the simple shell model, the presence of these states may provide evidence that a slightly deformed model would be more applicable to these $N = 88$ nuclides. It is seen from table 4 that Kumar's calculations for a deformed $^{150}$Sm target result in spectroscopic strengths for $l$-values of 0, 2, 4 and 5 which are similar to those for the spherical case. Hence the present data for these $l$-values are equally consistent with either a spherical or a weakly deformed description. A "typical" Coriolis calculation was performed for the Nilsson orbitals originating from the $h_{\frac{11}{2}}$ shell. Using "reasonable" parameters one could readily reproduce the energy spacing of the lowest $\frac{7}{2}^-$ and $\frac{11}{2}^-$ states and the spectroscopic strength of the lowest $\frac{11}{2}^-$ state. The strength to the $\frac{7}{2}^-$ level obtained from this calculation was only about 30 % of the value observed in $^{149}$Pm and $^{151}$Eu. The similarity of the energy spacing between the lowest $\frac{7}{2}^-$ and $\frac{11}{2}^-$ states in the three nuclides is easily reproduced by such a description.

In a similar approach, some success has been obtained [12]) in applying the rotational alignment model to the negative parity states of $^{153}$Tb. In addition to explaining the high spin rotational levels for which this model was originally intended, their calculation also predicts the existence of some low spin states at fairly small excitation energies. At least some of the negative parity levels which have been tentatively ascribed to this type of behaviour [12]), such as the 263 keV ($I^\pi = \frac{9}{2}^-$) and 537.5 keV ($I^\pi = \frac{5}{2}^-$ or $\frac{7}{2}^-$) states in $^{153}$Tb, could correspond to states weakly populated in the present work.

In view of the observed strengths to the $\frac{7}{2}^-$ states, which are not expected in the $Z = 50$ to $Z = 82$ shell, it is not safe to assume the $l = 4$ and $l = 5$ transitions correspond to $g_{\frac{7}{2}}$ and $h_{\frac{11}{2}}$ strengths respectively. It is possible that some of the $l = 5$

transitions could populate $\frac{9}{2}^-$ states since the neighbouring (deformed) terbium isotopes exhibit considerable $h_{\frac{1}{2}}$ strength below 1 MeV excitation in the form of the $\frac{1}{2}^-$ [541] bands [15]). The $l = 4$ and $l = 5$ transitions were categorized as $g_{\frac{7}{2}}$ and $h_{\frac{9}{2}}$ for the purposes of comparing strengths with shell-model predictions in table 4, but these should not be construed as assignments of spin.

## 4. Summary and conclusions

In the present work single-proton stripping reactions have been used to determine $l$-values and spectroscopic strengths for states in $^{149}$Pm, $^{151}$Eu and $^{153}$Tb. These nuclei have been traditionally regarded as "spherical" and in the present study no well-developed fingerprint patterns of rotational bands were observed. However, most of the Nilsson states which would be expected in this region, such as the $\frac{5}{2}^+$ [402] and $\frac{7}{2}^+$ [404] orbitals, have their strength concentrated in one $j$-value so that only one spin member would be strongly populated and the bands are difficult to identify. Furthermore, Nilsson orbitals originating from the $h_{\frac{11}{2}}$ shell-model state would be strongly Coriolis coupled, resulting in a larger spectroscopic factor for the lowest $\frac{11}{2}^-$ level than would be expected for any single orbital by itself. The net result is that it can be difficult to distinguish between spherical states and Coriolis-coupled states of small deformation on the basis of cross sections to the strongly populated levels. However, there is increasing evidence that the spherical shell model is inadequate to explain the observed levels. The apparent rotational band in $^{151}$Eu found in the (p, t) studies [5, 6]) and the observed strength to low-lying $\frac{7}{2}^-$ states in the present work are not consistent with the simple shell model.

The present results could equally well have been interpreted in terms of the Nilsson model with a relatively small deformation. In this case the lowest $d_{\frac{5}{2}}$ and $g_{\frac{7}{2}}$ levels would be called the $\frac{5}{2}^+$ [402] and $\frac{7}{2}^+$ [404] bandheads as these states contain large amounts of $d_{\frac{5}{2}}$ and $g_{\frac{7}{2}}$ strength. Also the systematics show that these orbitals are dropping to very low excitation energy with decreasing neutron number in the neighbouring deformed isotopes. In a deformed picture the lowest $\frac{11}{2}^-$ state in each nucleus could have been interpreted as the lowest nember of a Coriolis mixed band made up of orbitals from the $h_{\frac{11}{2}}$ shell. This approach has not been taken in the present report as there is no good basis for the assignment of additional rotational band members and thus it gives no better insight in the interpretation of the other levels observed.

It has been found that the amount of $l = 2$, 4 and 5 strengths observed can be explained by the basic shell model, although considerable fragmentation is evident in each case. The amount of $l = 0$ strength found was less than predicted for a pure $s_{\frac{1}{2}}$ state but some of it may exist at higher excitation energies. The introduction of a deformed potential is one means of producing fragmentation of the shell-model states but there is not yet enough information to see whether this provides a unique explanation. It is hoped that his problem will encourage more experiments, such as (HI,

$xn\gamma$) studies, which should help to identify some of the rotational bands and provide values of the parameters needed for a deformed-well interpretation.

The authors are very thankful to John Huizenga of the University of Rochester Nuclear Structure Research Laboratory for the loan of the $^{152}$Gd target. Financial support for this work was provided by the National Research Council of Canada and in part by Norges Almenvitenskaplige Forskningsråd and is gratefully acknowledged. One of us (G. L.) wants to thank Meltzers Høyskolefond for a travel grant.

## References

1) H. J. Smith, D. G. Burke, M. W. Johns, G. Løvhøiden and J. C. Waddington, Phys. Rev. Lett. 31 (1973) 944
2) P. Kleinheinz, R. K. Sheline, M. R. Maier, R. M. Diamond and F. S. Stephens, Phys. Rev. Lett. 32 (1974) 68
3) J. Kownacki, Z. Sujkowski, Z. Haratym and H. Ryde, Proc. Int. Conf. on reactions between complex nuclei, Nashville, Tenn. (1974) vol. 1, p. 174
4) G. Løvhøiden and D. G. Burke, Can. J. Phys. 53 (1974) 1182
5) D. G. Burke, G. Løvhøiden and J. C. Waddington, Phys. Lett. 43B (1973) 470
6) H. Taketani, H. L. Sharma and N. M. Hintz, Phys. Rev. C12 (1975) 108
7) T. Seo and T. Hayashi, Nucl. Phys. A159 (1970) 494
8) Å. Höglund and S. G. Malmskog, Nucl. Phys. A138 (1969) 470
9) J. W. Ford, A. V. Ramayya and F. F. Pinajian, Nucl. Phys. A146 (1970) 397
10) J. E. Thun and T. R. Miller, Nucl. Phys. A193 (1972) 337
11) B. Harmatz and T. H. Handley, Nucl. Phys. A191 (1972) 497
12) M. D. Devous, Sr. and T. T. Sugihara, to be published
13) J. O. Meredith and R. C. Barber, Can J. Phys. 50 (1972) 1195
14) P. D. Kunz, Computer code DWUCK, University of Colorado, unpublished, 1969
15) J. C. Tippett and D. G. Burke, Can J. Phys. 50 (1972) 3152
16) D. G. Burke and J. C. Waddington, Nucl. Phys. A193 (1972) 271
17) H. C. Cheung, D. G. Burke and G. Løvhøiden, Can J. Phys. 52 (1974) 2108
18) D. A. Lewis, A. S. Broad and W. S. Gray, Phys. Rev. C10 (1974) 2286
19) L. K. Wagner, D. G. Burke, H. C. Cheung, P. Kleinheinz and R. K. Sheline, Nucl. Phys. A246 (1975) 43
20) K. Kumar, Nucl. Phys. A231 (1974) 189
21) J. Rekstad, Nucl. Phys. A247 (1975) 7

# P A P E R II

## PROTON STATES IN THE N=86 NUCLEI $^{147}$Pm AND $^{149}$Eu POPULATED IN THE ($^{3}$He,d),(α,t) AND (t,α) REACTIONS

Z. Physik 290, 67–80 (1979)

Zeitschrift für Physik A


# Proton States in the $N=86$ Nuclei $^{147}$Pm and $^{149}$Eu Populated in the ($^3$He, $d$), ($\alpha$, $t$) and ($t$, $\alpha$) Reactions

O. Straume and G. Løvhøiden
University of Bergen, Bergen, Norway

D.G. Burke
McMaster University, Hamilton, Ontario, Canada

Received September 11, Revised Version October 27, 1978

The ($^3$He, $d$) and ($\alpha$, $t$) reactions on targets of $^{146}$Nd and $^{148}$Sm have been studied, using beams of 24 MeV $^3$He and 27 MeV $^4$He from the McMaster University tandem van de Graaff accelerator. Also the ($t$, $\alpha$) reaction on a target of $^{148}$Sm has been studied, using 17 MeV tritons from the Los Alamos Scientific Laboratory tandem accelerator. The reaction products were analyzed with magnetic spectrographs. Information on the $l$-values was obtained from ($^3$He, $d$) angular distributions and from ratios of ($\alpha$, $t$) and ($^3$He, $d$) cross sections. In each nucleus a severe fragmentation of the shell-model strength is found. In particular a total of 13(7) $l=2$ transitions and 6(6) $l=0$ transitions have been identified in $^{147}$Pm($^{149}$Eu). The results are analyzed in terms of the spherical shell model, which accounts fairly well for the summed spectroscopic strengths. However, with the existence of the ($t$, $\alpha$) data a more detailed investigation of the emptiness of individual levels observed in $^{147}$Pm gives some indication that a deformed scheme might be more successful in describing these nuclei.

## 1. Introduction

The shape transitional region near $A=150$ has been the subject of a great many papers over the last few years. The present study is part of a survey intended to investigate the fragmentation of single proton strength in this region. The $N=86$ isotones $^{147}$Pm and $^{149}$Eu are believed to be predominantly spherical with $g_{7/2}$ and $d_{5/2}$ ground states, respectively. However, recent ($HI, xn\gamma$) experiments [1] have revealed a band structure based on the $h_{11/2}$ state at 496 keV in $^{149}$Eu. The present study extends the knowledge about these nuclei by presenting results of ($^3$He, $d$), ($\alpha$, $t$) and ($t$, $\alpha$) reactions with $^{147}$Pm and $^{149}$Eu as final nuclei. Spectroscopic strengths from single proton transfer reactions can be obtained for all promethium isotopes from the closed shell nucleus $^{143}$Pm to the well deformed $^{153}$Pm, and in a subsequent paper the fragmentation of the single proton strength will be discussed in a systematic manner. The nucleus $^{147}$Pm has recently been investigated [2] by $\gamma$-ray spectroscopy and $^{149}$Eu has previously been studied by the ($p$, $t$) reaction [3] and by $\gamma$-ray spectroscopy (Ref. 4).

## 2. Experimental Details and Results

The experiments were performed with 24 MeV $^3$He and 27 MeV $^4$He beams from the McMaster University Tandem Van de Graaff accelerator giving typical beam currents of 1.5 μA. The reaction products were analyzed with an Enge type splitpole magnetic spectrograph and detected with Kodak NTB50 nuclear emulsions. Appropriate aluminium absorbers were placed in front of the photographic emulsions to stop unwanted reaction products. The resolution was typically ~14 keV FWHM (full width at half maximum). The ($t$, $\alpha$) experiments were performed with beams of 17 MeV tritons from the Los Alamos Scientific Laboratory Tandem Van de Graaff accelerator. The emerging $\alpha$-particles were analyzed in a

0340-2193/79/0290/0067/$02.80

**Table 1.** Isotopic composition of the targets (%)

| | 142 | 143 | 144 | 145 | 146 | 147 | 148 | 149 | 150 | 152 | 154 |
|---|---|---|---|---|---|---|---|---|---|---|---|
| $^{146}$Nd | 0.43 | 0.20 | 0.70 | 0.69 | 97.46 | – | 0.32 | – | 0.13 | | |
| $^{148}$Sm | – | – | 0.1 | – | – | 1.1 | 95.37 | 1.45 | 0.45 | 0.92 | 0.62 |

Q3D magnetic spectrograph and detected by a helical delay line proportional counter. The resolution was ~20 keV (FWHM).

Targets of $^{146}$Nd and $^{148}$Sm were made from samples of $Nd_2O_3$ and $Sm_2O_3$ enriched to 97.46% and 95.37% respectively. The detailed isotopic compositions as stated by the supplier, the Stable Isotopes Division of the Oak Ridge National Laboratory, are listed in Table 1. The oxides were reduced with thorium metal and the enriched isotopes were vacuum evaporated onto 30 μg/cm$^2$ carbon foils. The resulting neodymium thickness was 25 μg/cm$^2$ while the samarium thickness was 50 μg/cm$^2$.

Absolute cross sections were determined by comparing the numbers of tracks in the peaks of the spectra with the numbers of elastically scattered particles detected by a semiconductor monitor detector placed at $\theta=30°$ in the scattering chamber. The cross sections for elastic scattering were determined from the distorted wave Born approximation (DWBA) calculations described below. As a separate check on the normalizations for the ($^3$He, $d$) and ($\alpha, t$) measurements, short exposures of elastically scattered particles were recorded with the spectrograph, on another photographic plate, before and after each regular exposure. For these, the monitor counter was used only to determine the ratio of "exposure times" for the long and short runs. The absolute cross sections obtained in this manner agreed, within ±10%, with those determined using only the monitor counter and the known solid angles.

The ($^3$He, $d$) reactions were studied at 8 or 9 angles for each target, and the ($\alpha, t$) and ($t, \alpha$) reactions were recorded at two angles. Figures 1–2 show representative spectra for these reactions plotted on a common energy scale. The solid line represents a fit to the data, generated by the peak finding program SPECTR on the McMaster CDC 6400 computer. In Tables 2–3 are listed energies, cross sections and assignments for the observed peaks. The uncertainties for the energy measurements are estimated to be less than 4 keV. The relative cross sections for large well resolved peaks have probable errors of ±10%, whereas the absolute cross sections may have uncertainties of ~25%. Angular distributions for transitions which can be given definite $l$-values are shown in Figs. 3–4.

Additional information on the $l$-values is obtained from the ratios of the ($\alpha, t$) and ($^3$He, $d$) cross sections. This ratio varies by more than one order of magnitude as the $l$-value changes from 0 to 5, and is particularly useful in locating high angular momentum states because these have prominent peaks in the ($\alpha, t$) spectra but weak ones in the ($^3$He, $d$) reaction. In Figs. 5–6 this ratio is plotted as a function of excitation energy. The solid lines result from DWBA calculations, and the data points represent experimental results of the present work. The numbers associated with the data points are excitation energies in keV.

The DWBA calculations were performed with the code DWUCK [5]. The optical model parameters are the same as those used in a recent study of $N=88$ nuclei [6].

## 3. Interpretation of the Results

The assignments of spins and parities for levels in $^{147}$Pm and $^{149}$Eu are discussed in Sects. 3.1 and 3.2. These interpretations are based on previously available data as well as the ($^3$He, $d$), ($\alpha, t$) and ($t, \alpha$) results from the present study. A discussion of the deduced experimental cross sections in terms of the shell model is presented in Sect. 3.3.

### *3.1. The Nucleus $^{147}$Pm*

#### 3.1.1. States Populated by $l=0$ Transitions

From the angular distributions shown in Fig. 3 it is seen that the five levels at 633, 931, 1,100, 1,378 and 1,930 keV all exhibit the characteristic shape of an $l=0$ transitions. These levels therefore have spin and parity $1/2^+$ and must each contain a fragment of the $s_{1/2}$ strength. The cross section ratios (Fig. 5) support these assignments and suggest also that the weakly populated level at 1,892 keV may be an $l=0$ transition.

#### 3.1.2. States Populated by $l=2$ Transitions

Fragments of the $d_{3/2}$ and $d_{5/2}$ states are expected to be found at low excitation energies, and will both be

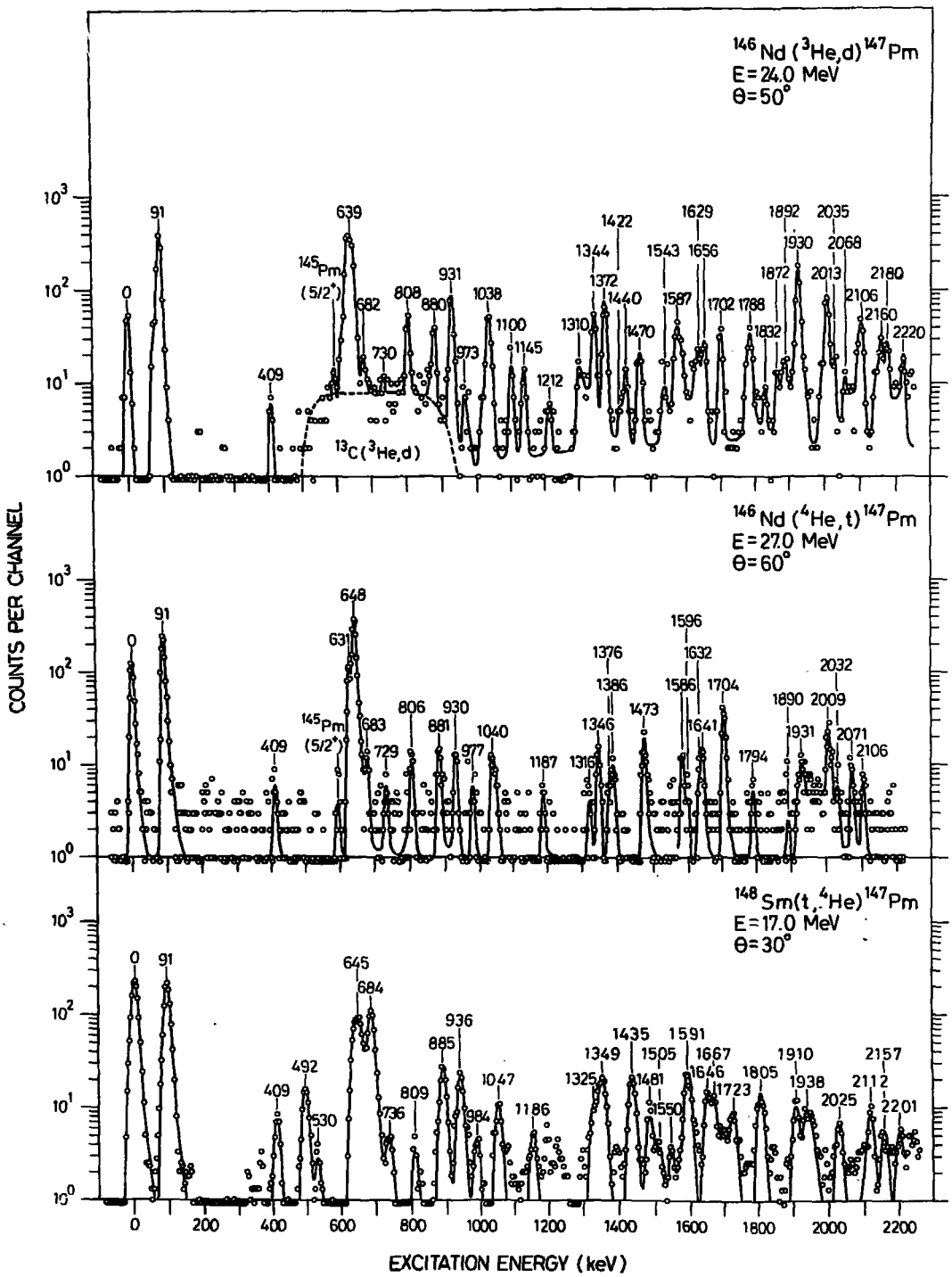


Fig. 1. The $^{146}$Nd($^3$He, $d$)$^{147}$Pm spectrum at $\theta = 50°$, the $^{146}$Nd($\alpha$, $t$)$^{147}$Pm spectrum at $\theta = 60°$ and the $^{148}$Sm($t$, $\alpha$)$^{147}$Pm spectrum at $\theta = 30°$ plotted on a common energy scale. The numbers associated with the peaks are the excitation energies in keV. The channel widths in the stripping reactions were 0.25 mm, and in the ($t$, $\alpha$) reaction ~1.0 mm

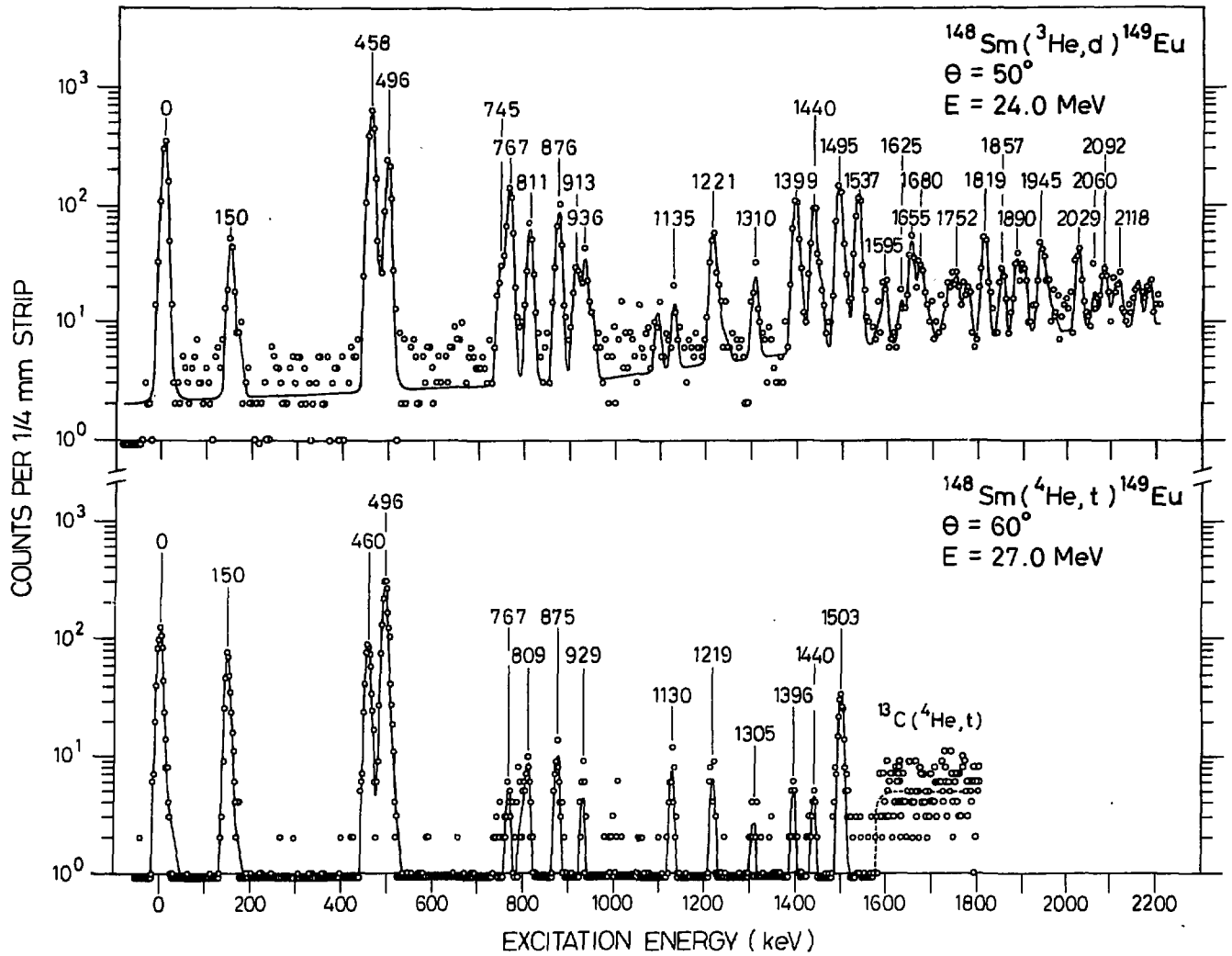


**Fig. 2.** The $^{148}$Sm($^3$He, $d$)$^{149}$Eu spectrum at $\theta = 50°$ and the $^{146}$Sm($\alpha$, $t$)$^{149}$Eu spectrum at $\theta = 60°$ plotted on a common energy scale. The numbers associated with the peaks are the excitation energies in keV

**Table 2.** Levels populated in $^{147}$Pm

| Energies (keV) | | | | Cross-sections (μb/sr) | | | | | | Assignments | | |
|---|---|---|---|---|---|---|---|---|---|---|---|---|
| | | | | ($^3$He, $d$) | | ($\alpha$, $t$) | | ($t$, $\alpha$) | | | | |
| Prev.[a] | ($^3$He, $d$) | ($\alpha$, $t$) | ($t$, $\alpha$) | 25° | 50° | 45° | 60° | 30° | 40° | Prev.[a] | This exp. | Adopted |
| 0 | 0 | 0 | 0 | 36 | 36 | 78 | 72 | 525 | 430 | $7/2^+$ | $l=4$ | $7/2^+$ |
| 91.1 | 91 | 91 | 90 | 302 | 263 | 129 | 142 | 441 | 345 | $5/2^+$ | $l=2$ | $5/2^+$ |
| 408.2 | | | | | | | | | | $9/2^+$ | | $9/2^+$ |
| 410.6 | 409 | 409 | 409 | 7 | 4 | 2.5 | 2.9 | 16 | 16 | $3/2^+$ | ($l=2,3,4$) | $3/2^+$ |
| 489.3 | | | 492 | | | 0.8 | 1.0 | 35 | 30 | $7/2^+$ | | $7/2^+$ |
| 531.1 | | | 530 | | | | | 5.5 | ~7 | $5/2^+$ | | $5/2^+$ |
| 632.8 | | 631 | | | | 55 | 60 | | | $1/2^+$ | $l=0$ | $1/2^+$ |
| 641.3 | 639 | | | 449 | 493 | | | | | $(3/2,5/2)^+$ | | |
| 649.3 | | 648 | 645 | | | 237 | 213 | 308 | 214 | $11/2^-$ | $l=5$ | $11/2^-$ |
| 680.4 | | | | | | | | | | | | |
| 686.1 | 682 | 683 | 684 | 14 | 14 | 1.2 | 6.7 | 221 | 205 | $5/2^+$ | ($l=2,3$) | $5/2^+$ |
| 730.7 | 730 | 729 | 736 | 4 | 9 | – | 2.9 | 8.7 | 14 | $9/2^+$ | ($l=2,0$) | ($l=2$) |
| 807.3 | 808 | 806 | 809 | 29 | 25 | 3.8 | 6.4 | 7.1 | ~7 | $(5/2,7/2)^-$ | $l=2$ | $l=2$ |
| | 880 | 881 | 885 | 30 | 26 | 3.5 | 8.0 | 56 | 51 | | $l=2$ | $l=2$ |
| | 931 | 930 | 936 | 75 | 68 | 2.3 | 7.2 | 46 | 23 | | $l=0$ | $1/2^+$ |
| 970.2 | 973 | 977 | (984) | 14 | 6 | 4.7 | 2.8 | 9.5 | ~7 | $(7/2)^-$ | ($l=3$) | ($7/2^-$) |
| 1,041.2 | 1,038 | 1,040 | 1,047 | ~42 | 44 | 11.2 | 9.9 | 23 | 18 | | $l=2$ | $l=2$ |
| | 1,100 | | | ~19 | 12 | | | | | | $l=0$ | $1/2^+$ |
| | 1,145 | | | ~16 | 11 | | | | | | ($l=2$) | ($l=2$) |
| | | 1,187 | 1,186 | | | 2.0 | 2.1 | 11 | 11 | | | |
| 1,213.9 | 1,212 | | | 10 | 6 | | | | | | | |
| | 1,310 | 1,316 | | 27 | 15 | 1.3 | 1.8 | | | | | |
| | | | 1,325 | | | | | 22 | 43 | | | |
| | 1,344 | 1,346 | 1,349 | 36 | 41 | 7.4 | 7.9 | 47 | | | $l=2$ | $l=2$ |
| 1,382.1 | 1,378 | 1,376 | | 75 | 57 | ~1.0 | 1.9 | | | | $l=0$ | $1/2^+$ |
| | | 1,387 | | | | ~3.0 | 5.0 | | | | | |
| | 1,422 | | | 11 | 4 | | | | | | | |
| 1,434.0 | | | 1,435 | | | | | 43 | 40 | | | |
| | 1,440 | | | 9 | 11 | | | | | | | |
| | 1,476 | 1,473 | 1,481 | 14 | 18 | ~12 | 11 | 17 | 7 | | $l=4(5)$ | ($7/2^+$) |
| | | | 1,505 | | | | | 7 | 14 | | | |
| | 1,543 | | 1,550 | 18 | 11 | | | 7 | 15 | | | |
| | 1,587 | 1,586 | 1,591 | 47 | 47 | | 6.7 | 51 | 43 | | $l=2$ | $l=2$ |
| | | (1,596) | | | | | (1.6) | | | | | |
| 1,627.8 | 1,629 | 1,632 | | 32 | 21 | ~7 | 3.5 | | | | $l=2$ | $l=2$ |
| | | 1,641 | 1,646 | | | | 7.3 | 28 | | | | |
| | 1,656 | | | 31 | 27 | | | | 26 | | ($l=2$) | ($l=2$) |
| | | | 1,667 | | | | | 22 | | | | |
| | 1,702 | 1,704 | | 25 | 21 | ~15 | 22 | | | | $l=5(4)$ | ($11/2^-$) |
| | | | 1,723 | | | | | 19 | 18 | | | |
| | 1,788 | (1,794) | | 36 | 36 | | 2.4 | | | | $l=2$ | $l=2$ |
| | | | 1,805 | | | | | 31 | 29 | | | |
| | 1,832 | | | 8 | 8 | | | | | | | |
| | 1,872 | | | 15 | 12 | | | | | | | |
| | 1,892 | (1,890) | | 14 | 20 | | (0.9) | | | | | |
| | | | 1,910 | | | | | 22 | 16 | | ($l=0$) | ($1/2^+$) |
| | 1,930 | 1,931 | | 146 | 119 | | < 5 | | | | $l=0$ | $1/2^+$ |
| | | | 1,938 | | | | | 19 | 15 | | | |
| | 2,013 | 2,009 | | 75 | 67 | 10 | 17 | | | | $l=2+4.5$ | ($l=2$) |
| | | | 2,025 | | | | | 15 | 14 | | | |
| | 2,035 | (2,032) | | 21 | 10 | | 2.3 | | | | | |
| | 2,068 | 2,071 | | 12 | 13 | 0.9 | 4.8 | | | | ($l=4$) | ($7/2^+$) |
| | 2,106 | 2,106 | 2,112 | 42 | 42 | 1.4 | 3.1 | 17 | 19 | | ($l=2$) | ($l=2$) |
| | 2,160 | | 2,157 | 39 | 25 | | | 11 | 10 | | | |
| | 2,180 | | | 27 | 26 | | | | | | | |
| | | | 2,201 | | | | | 11 | 18 | | | |
| | 2,220 | | | 25 | 21 | | | | | | | |

[a] Data from Ref. 2.

**Table 3.** Levels populated in $^{149}$Eu

| Energies (keV) | | | Cross-sections (μb/sr) | | | | Assignments | | |
|---|---|---|---|---|---|---|---|---|---|
| | | | ($^3$He, $d$) | | ($\alpha$, $t$) | | | | |
| Prev.[a] | ($^3$He, $d$) | ($\alpha$, $t$) | $\theta=25°$ | $\theta=50°$ | $\theta=50°$ | $\theta=60°$ | Prev.[a] | This exp. | Adopted |
| 0 | 0 | 0 | 210 | 217 | 51 | 61 | $5/2^+$ | $l=2$ | $5/2^+$ |
| 149.7 | 150 | 150 | 25 | 33 | 26 | 34 | $7/2^+$ | $l=4,5$ | $7/2^+$ |
| 459.9 | 458 | 460 | 420 | 394 | 38 | 50 | $5/2^+, 7/2^+$ | $l=0$ | $1/2^+$ |
| 496.4 | 496 | 496 | 100 | 157 | 167 | 165 | $11/2^-$ | $l=5$ | $11/2^-$ |
| 748.7 | 745 | | 17 | 19 | | | $7/2^-$ | | $7/2^-$ |
| | 767 | 767 | 97 | 95 | 3 | 3 | | $l=0$ | $1/2^+$ |
| 812.7 | 811 | 809 | 37 | 44 | 3 | 5 | $5/2, 7/2^+$ | $l=2$ | $5/2^+$ |
| 876.0 | 876 | 875 | 51 | 60 | 4 | 5 | $5/2^+$ | $l=2$ | $5/2^+$ |
| 911 | 913 | | 26 | 23 | | | | $(l=2)$ | $(l=2)$ |
| 933.3 | | (929) | | | | 2 | $7/2^+$ | | |
| | 936 | | 26 | 25 | | | | $(l=0)$ | $(1/2^+)$ |
| | 1,135 | 1,130 | | 8 | 3 | 3 | | $l=4,(5)$ | $(7/2^+)$ |
| 1,226 | 1,221 | 1,219 | 35 | 44 | 3 | 3 | $5/2^+$ | $(l=2)$ | $5/2^+$ |
| 1,319 | 1,310 | 1,305 | 19 | 17 | | | $5/2^+$ | $(l=2)$ | $5/2^+$ |
| | 1,399 | 1,396 | 82 | 81 | 1 | 2 | | $l=0$ | $1/2^+$ |
| | 1,440 | 1,440 | 70 | 70 | 3 | 2 | | $l=0$ | $1/2^+$ |
| | 1,495 | | 86 | 107 | | | | $l=2$ | $l=2$ |
| | | 1,503 | | | 15 | 16 | | $l=(4),5$ | $(11/2^-)$ |
| | 1,537 | (1,539) | 100 | 85 | | <1 | | $l=0$ | $1/2^+$ |
| | 1,595 | | 21 | 14 | | | | | |
| | 1,625 | | 15 | 8 | | | | | |
| | 1,655 | | 46 | 33 | | | | | |
| | 1,680 | | 42 | 22 | | | | | |
| | | (1,718) | | | (1) | | | | |
| | 1,752 | | 42 | 22 | | | | | |
| | 1,819 | (1,816) | 48 | 38 | (1) | | | | |
| | 1,857 | | 25 | 19 | | | | | |
| | 1,890 | (1,888) | 40 | 22 | (1) | | | | |
| | 1,945 | | 38 | 52 | | | | | |
| | 2,029 | | 42 | 30 | | | | | |
| | 2,060 | | 48 | 15 | | | | | |
| | 2,092 | | 28 | 25 | | | | | |
| | 2,118 | | 17 | 19 | | | | | |
| | 2,144 | | 15 | | | | | | |
| | 2,168 | | 21 | | | | | | |
| | 2,199 | | 22 | | | | | | |

[a] Data from Refs. 3, 4. Energies from the ($p$, $t$) study in Ref. 3 are quoted as integers and only for levels which were not populated in the $\beta$-decay study of Ref. 4

populated through $l=2$ transitions. Indeed many $l=2$ transitions are identified in the present experiment. For the levels at 91, 880, 1,038, 1,344, 1,587, 1,629 and 1,788 keV the angular distributions firmly suggest $l=2$ assignments, which are supported by cross section ratios. Furthermore the angular distributions also indicate $l=2$ for the levels at 808, 1,145, 1,656 and 2,013 keV. For the latter the cross section ratio is much too high, which might suggest an unresolved high spin state at this energy. Although complete angular distributions could not be obtained, the 682 and 2,106 keV levels have been given $l=2$ assignments based on the cross section ratios alone. Thus altogether it is suggested that 13 levels are fed by $l=2$ transitions. On the basis of the present data it is not possible to distinguish between $3/2^+$ and $5/2^+$ states. In the $\gamma$-decay study [2] these states are not strongly populated and only the 91-keV state can be given a definite $5/2^+$ assignment. Some comments based mainly on systematics and model dependent arguments are postponed to subsection 3.3.

### 3.1.3. States with Higher Spin

The ground state of $^{147}$Pm was previously known to be $7/2^+$ and both the angular distribution and the cross section ratio are consistent with this assign-

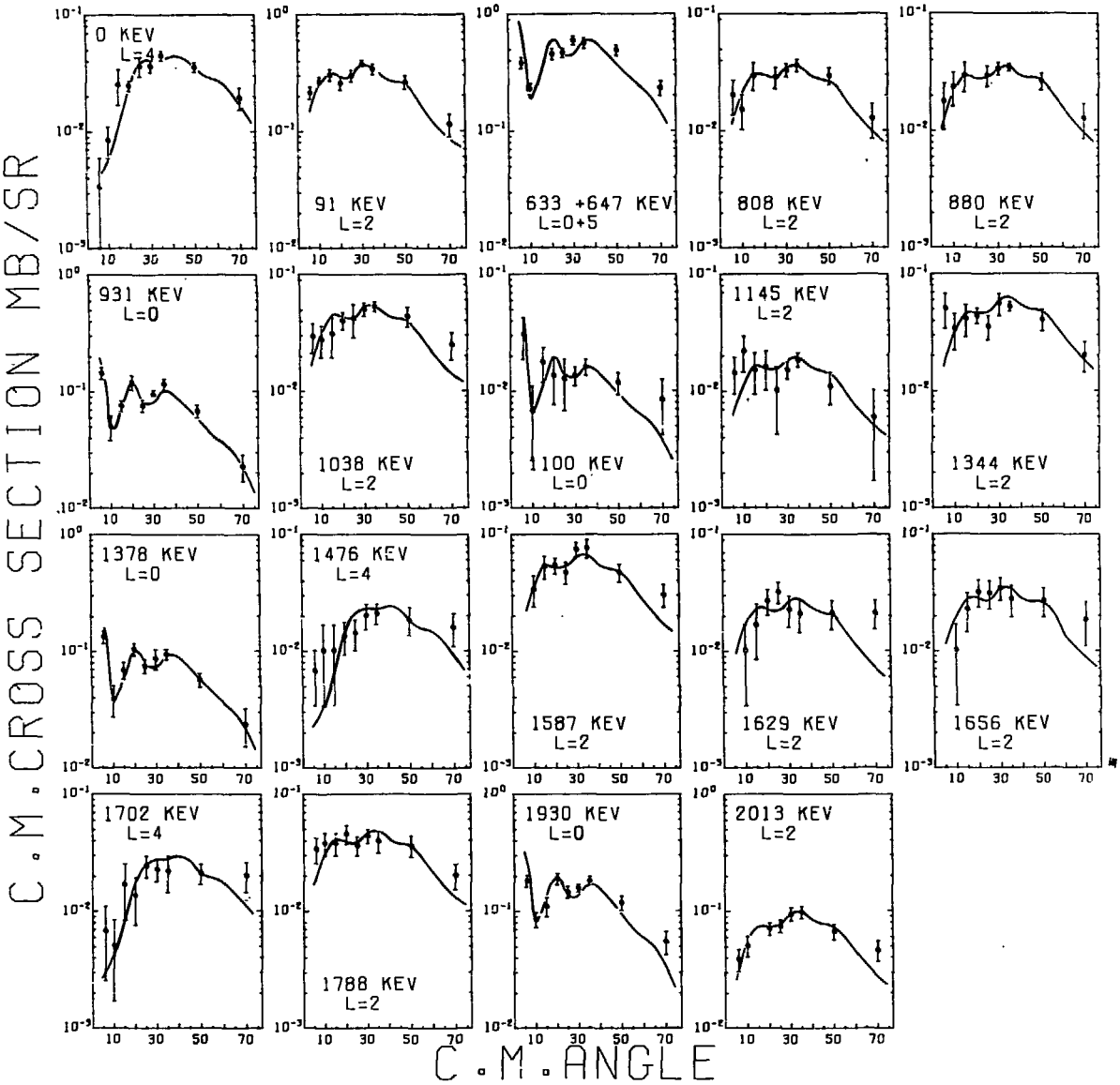


**Fig. 3.** Angular distributions for some of the peaks in the $^{146}$Nd($^3$He, $d$)$^{147}$Pm spectrum. The solid curves result from DWBA calculations and the points represent experimental data

ment. However, the present data cannot conclusively distinguish between $l=4$ and $l=5$ transitions, mainly because the cross section ratios for $l=4$ transitions in many cases [6] are found to be too close to those of the $l=5$ transitions. For the level at 1,476 keV both the angular distribution and the cross section ratio favour an $l=4$ assignment, but on the grounds mentioned above, $l=5$ cannot completely be ruled out. A full angular distribution for the 2,068 keV level could not be obtained and the tentative $l=4$ assignment is based on the cross section ratio alone.

The most strongly populated state in the $(\alpha, t)$ reaction is found at 648 keV. This is identified as being the low lying fragment of the $h_{11/2}$ state [2], which in $^{149}$Eu is found at 496 keV. In the ($^3$He, $d$) $^{147}$Pm reaction the 648 keV level is not well resolved from

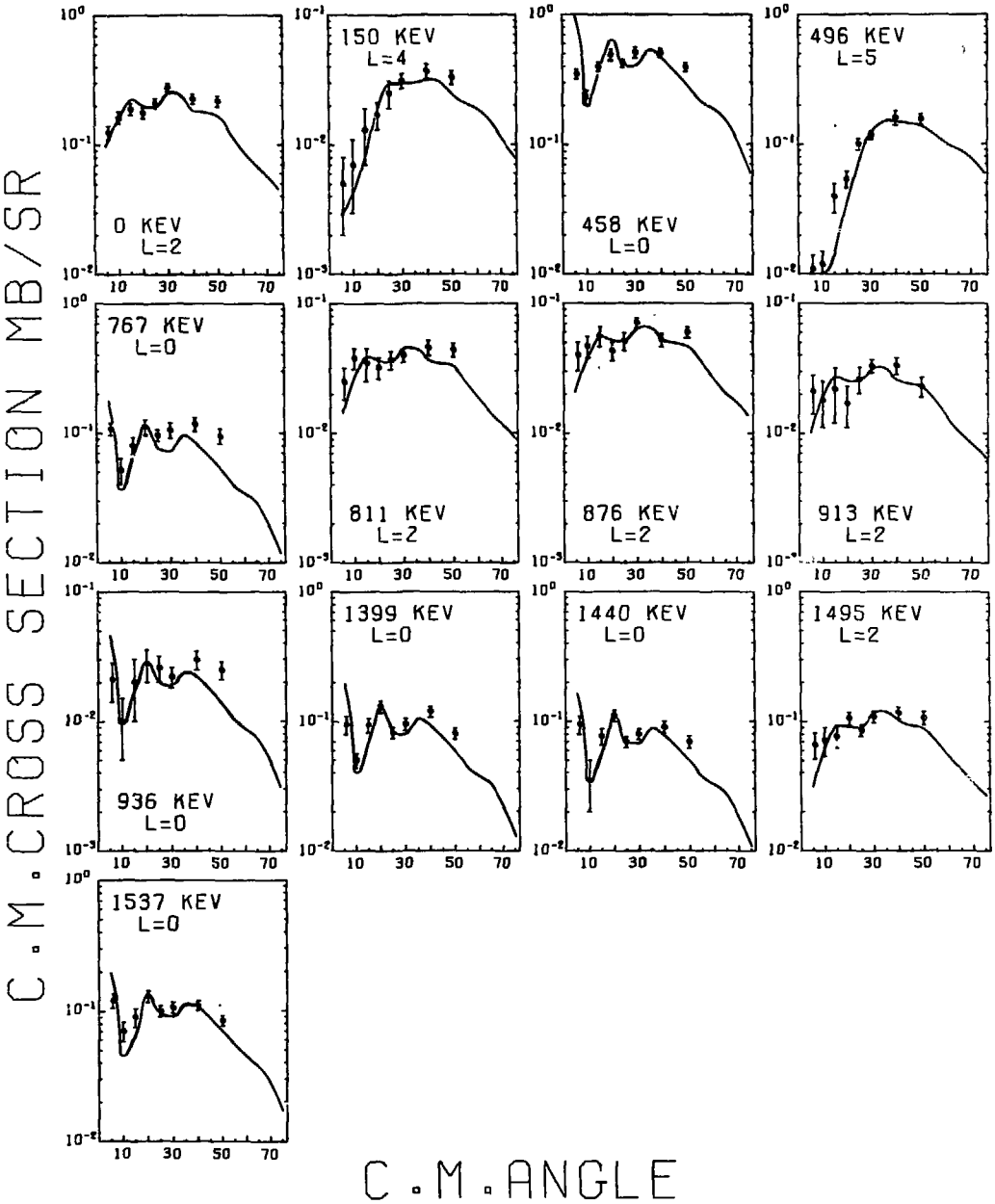


**Fig. 4.** Angular distributions for some of the peaks in the $^{148}$Sm($^{3}$He, $d$)$^{149}$Eu spectrum. The solid curves result from DWBA calculations and the points represent experimental data

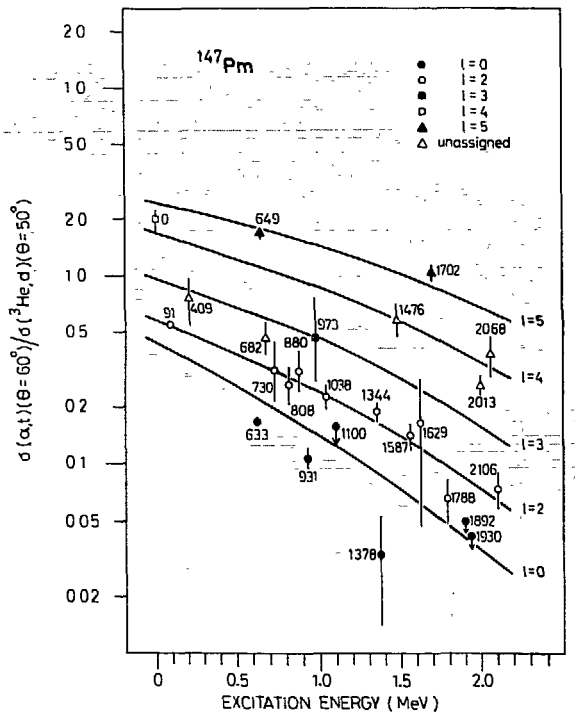


Fig. 5. Ratios of the $(\alpha, t)$ cross sections at $\theta=60°$ to the $(^3He, d)$ cross sections at $\theta=50°$ for $^{147}Pm$. The solid curves result from DWBA calculations, and the data points represent experimental ratios for the levels indicated. Points with arrows indicate upper limits

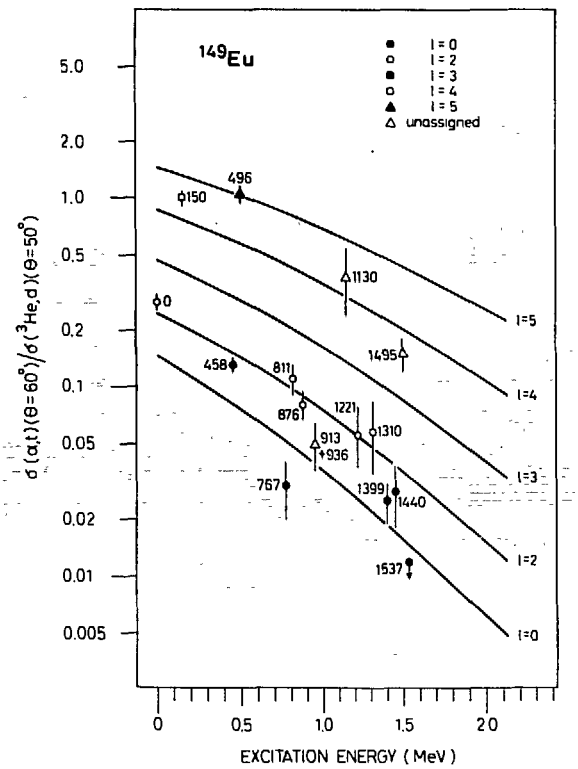


Fig. 6. Ratios of the $(\alpha, t)$ cross sections at $\theta=60°$ to the $(^3He, d)$ cross sections at $\theta=50°$ for $^{149}Eu$. See caption to Fig. 5

the $1/2^+$ state at 631 keV, and reliable angular distributions and cross section ratios cannot be obtained for these two levels independently. The angular distribution for the sum of the two is shown in Fig. 3, and is quite clearly dominated by the $l=0$ component. To obtain the data points labelled 649 and 633 keV (energies from Ref. 2) in the ratio plot (Fig. 5), the strength of the $(^3He, d)$ peak has been divided between the two levels so as to make the $l=5$ point match the DWBA prediction. This also yields a ratio for the $1/2^+$ state which is reasonable. The resulting spectroscopic strengths from this procedure are listed in Table 4, and the DWBA curve shown in Fig. 3 for this doublet contains the appropriate amount of $l=5$ strength.

The angular distribution to the 1,702 keV level suggests an $l$-value of 4 or 5 units, with a small preference for $l=4$ (Fig. 3). However, the strong population of this level in the $(\alpha, t)$ reaction (Fig. 5) favours $l=5$ and tentatively this assignment has been adopted.

From the shell model the only negative parity states expected in this region are fragments of the $h_{11/2}$ state. However, in the $N=88$ study [6] a lowlying $7/2^-$ state, interpreted as a member of a highly distorted "band" based on the $h_{11/2}$ state, was populated in the transfer reactions. In the present study a level at 973 keV exhibits a cross section ratio expected for an $l=3$ transition. This is in agreement with the tentative $7/2^-$ assignment proposed in Ref. 2 for a level at 970.2 keV, and it is tempting to suggest an interpretation for this state in $^{147}Pm$ similar to the one mentioned above for $^{149}Pm$.

### 3.2. *The Nucleus* $^{149}Eu$

#### 3.2.1. States Populated by $l=0$ Transitions

From the angular distributions presented in Fig. 4, the six states at 458, 767, 936, 1,399, 1,440 and 1,537 keV can all readily be assigned as fragments of

**Table 4.** Spectroscopic information for states populated in $^{147}$Pm and $^{149}$Eu

| Shell model state | Energy (keV) | | $(2j+1)S_{ij}^{(a)}$ | $S_{ij}^{(p)}$ | $(2j+1)S_{ij}^{(a)}$ | $\Sigma(2j+1)S_{ij}^{(a)}$ | $\Sigma S_{ij}^{(p)}$ | $\Sigma(2j+1)S_{ij}^{(a)}$ |
|---|---|---|---|---|---|---|---|---|
| | $^{147}$Pm | $^{149}$Eu | ($^3$He, $d$) $^{147}$Pm | ($t$, $\alpha$) $^{147}$Pm | ($^3$He, $d$) $^{149}$Eu | ($^3$He, $d$) $^{147}$Pm | ($t$, $\alpha$) $^{147}$Pm | ($^3$He, $d$) $^{149}$Eu |
| $d_{5/2}$ | 91 | 0 | 2.33 | 1.70 | 1.31 | 2.41 | 2.81 | 2.03 |
| | 530 | 811 | | 0.26 | 0.19 | | | |
| | 682 | 876 | 0.08 | 0.85 | 0.25 | | | |
| | | 1,221 | | | 0.21 | | | |
| | | 1,310 | | | 0.07 | | | |
| $g_{7/2}$ | 0 | 150 | 1.67 | 4.12 | 0.94 | (2.70) | (4.53) | (1.11) |
| | 492 | | | 0.29 | | | | |
| | (1,476) | (1,135) | (0.57) | (0.12) | (0.17) | | | |
| | (2,068) | | (0.56) | | | | | |
| $h_{11/2}$ | 649 | 496 | 8.39 | <2.60[a] | 7.60 | 9.70 | ~1.84 | 8.90 |
| | 1,702 | 1,503 | 1.31 | | 1.30 | | | |
| "$d$" | 409 | | 0.03 | | | | | |
| | 730 | 913 | 0.06 | 0.03 | 0.13 | 1.98 | 0.73 | 0.38 |
| | 808 | | 0.17 | 0.02 | | | | |
| | 880 | | 0.17 | 0.20 | | | | |
| | 1,038 | | 0.23 | 0.08 | | | | |
| | 1,145 | | 0.07 | | | | | |
| | 1,344 | | 0.21 | 0.17 | | | | |
| | 1,587 | | 0.27 | | | | | |
| | 1,629 | | 0.11 | | | | | |
| | 1,656 | | 0.14 | | | | | |
| | 1,788 | | 0.18 | | | | | |
| | 2,013 | 1,495 | 0.34 | | 0.25 | | | |
| $s_{1/2}$ | 633 | 458 | 1.22 | <0.97[a] | 1.01 | 2.00 | ~0.41 | 1.76 |
| | 931 | 767 | 0.26 | 0.11 | 0.23 | | | |
| | 1,100 | 936 | 0.03 | | 0.06 | | | |
| | 1,378 | 1,399 | 0.18 | | 0.16 | | | |
| | 1,892 | 1,440 | 0.03 | | 0.14 | | | |
| | 1,930 | 1,537 | 0.28 | | 0.16 | | | |
| Total observed strength | | | | | | 18.8 | 10.3 | 14.2 |

[a] The numbers are calculated on the basis of the total cross section for the doublett found at 645 keV in the ($\alpha$, $t$) spectrum. Assuming the same relative filling of $h_{11/2}$ and $s_{1/2}$ as seen (Ref. 10) in the ($t$, $\alpha$) $^{149}$Pm reaction, the total cross section divided between the two states gives 1.84 ($h_{11/2}$) and 0.30 ($s_{1/2}$)

the $s_{1/2}$ state. The cross section ratios are consistent with low $l$-transfers for all these states. However the $1/2^+$ state at 458 keV is populated more strongly in the ($\alpha$, $t$) reaction than expected for an $l=0$ transition. One explanation is that there may be an unresolved doublet with the other member having a higher $l$-value.

### 3.2.2. States Populated by $l=2$ Transitions

Reliable angular distributions typical of $l=2$ transitions are obtained in this nucleus only for the five levels at 0, 811, 876, 913 and 1,495 keV. The cross section ratios for the 0, 811 and 876 keV levels confirm these $l=2$ assignments. Due to poor statistics in the ($\alpha$, $t$) spectrum the yields to the 913 and 936 keV levels could not be separated but the ratio for the combined doublet is consistent with the assignment of one $l=2$ and one $l=0$ suggested above. In addition the cross section ratio suggests $l=2$ assignments for the transitions feeding the 1,221 and 1,310 keV levels. The level labelled 1,495 keV in the ratio plot most likely corresponds to a doublet. The ($\alpha$, $t$) peak is located at 1,503 keV, 8 keV higher than the ($^3$He, $d$) peak, and it is much stronger than expected for an $l=2$ transition. This suggests the presence of two closely spaced levels around 1,500 keV, one of which is fed by an $l=2$ transition and the other by $l=4$ or 5.

### 3.2.3. States with Higher Spin

The main component of the $g_{7/2}$ state is found in this nucleus at 150 keV excitation energy. This assignment is supported by the angular distribution (Fig. 4) and

by the cross section ratio (Fig. 6). As was the case in $^{147}$Pm the $(\alpha, t)$ strength is somewhat larger than expected from the DWBA calculations.

The largest peak in the $(\alpha, t)$ spectrum is found at 496 keV and both the cross section ratio and angular distribution suggest an $l=5$ transition to this level, which was previously [4] known to have spin and parity $11/2^-$.

In the $N=88$ isotones a second $l=5$ transition systematically appeared 700–800 keV above the first one as the strongest peak in the high energy part of the spectrum. In $^{147}$Pm, as discussed in subsection 3.1.3, a second $l=5$ transition appears ~1,050 keV above the first one and again as the strongest peak in the high energy part of the spectrum. The strongest peak above 500 keV in the $^{148}$Sm$(\alpha, t)^{149}$Eu spectrum appears at 1,503 keV. This is indeed ~1,000 keV above the first $11/2^-$ state and the 1,503 keV level does contain a high spin component as discussed in the previous subsection. On the basis of these systematics, the most likely assignment for the 1,503 keV level is then $l=5$ plus a component of the $l=2$ transition identified at 1,495 keV in the $(^3\text{He}, d)$ angular distribution. It is now possible to divide the strengths of the peaks at 1,495 keV in $(^3\text{He}, d)$ and at 1,503 keV in $(\alpha, t)$ into one $l=5$ and one $l=2$ component in such a manner that the cross section ratios correspond to the theoretical values for $l=5$ and $l=2$. The spectroscopic strengths presented in Table 4 for these levels were obtained using this procedure. This yields $\sigma(l=2)=78$ and $\sigma(l=5)=29$ μb/sr for the $(^3\text{He}, d)$ reaction, which in terms of spectroscopic strengths correspond to 0.25 and 1.3 respectively.

### 3.3. Spectroscopic Strengths

The differential cross sections for stripping an pick-up reactions on an even-even target are given by

$$d\sigma/d\Omega = S_{lj}^{(s)}(2j+1)\, N^{(s)} \sigma_{lj}^{(s)}(\theta)_{DW} \quad \text{(stripping)} \quad (1)$$

$$d\sigma/d\Omega = S_{lj}^{(p)}\, N^{(p)} \sigma_{lj}^{(p)}(\theta)_{DW} \quad \text{(pick-up)} \quad (2)$$

In the present work $N$ is taken to be 6.0 for the $(^3\text{He}, d)$ reaction and 111.0 for the $(\alpha, t)$ reaction [6]. The normalization constant for the $(t, \alpha)$ reaction is taken to be 44.0 as discussed below. Measures of the spectroscopic strenghts, $(2j+1)S_{lj}^{(s)}$ and $S_{lj}^{(p)}$, can thus be obtained simply by dividing the experimentally observed cross sections by the quantity $N\sigma_{lj}(\theta)_{DW}$. Spectroscopic strengths obtained in this manner are listed in Table 4.

In a shell-model basis one may consider the target nuclei $^{146}_{60}$Nd and $^{148}_{62}$Sm as systems with 10 and 12 protons outside a $Z=50$ closed shell core. Thus the particle states $h_{11/2}$, $d_{3/2}$ and $s_{1/2}$ would be expected to have large spectroscopic factors in the stripping reactions, whereas the $g_{7/2}$ and $d_{5/2}$ states should already be partly filled and give larger cross sections in the pick-up reaction. By summing the strengths $S_{lj}^{(s)}(2j+1)$ from the stripping reactions, one should get the average number of holes in the $Z=50 \rightarrow 82$ shell for the particular target nucleus. Theoretically this number is $32-10=22$ for $^{146}$Nd and $32-12=20$ for $^{148}$Sm.

The levels in $^{147}$Pm and $^{149}$Eu for which $l$-assignments can be given, account for 91 % and 79 % of the observed $(^3\text{He}, d)$ cross section at $\theta=50°$ up to an excitation energy of ~2,200 keV. For these levels the experimental sums of $S_{lj}^{(s)}(2j+1)$ are 18.8 and 14.2 for $^{147}$Pm and $^{149}$Eu respectively. Adjusting these numbers in an approximate manner, to take into account the unassigned peaks, one gets $18.8/0.91=20.7$ and $14.2/0.79=18.0$ which is within 10 % of the expected values, and well within experimental uncertainties.

To further investigate the particle-hole structure of these states, the $(t, \alpha)$ reaction into $^{147}$Pm was performed. However, the normalization constant in the DWUCK calculations is not well known for this reaction (see Ref. 7), and absolute spectroscopic strengths cannot be obtained directly. However a semiempirical value of $N^{(p)}(t, \alpha)$ can be obtained by demanding the total spectroscopic strength in the $^{148}$Sm$(t, \alpha)^{147}$Pm reaction to be equal to the number of protons outside the $Z=50$ closed shell in the $^{148}$Sm target, which is 12. This procedure will be meaningful only if all the fragments of states in the $Z=50$ to 82 shell are contained within the experimentally observed spectrum. This seems to be a reasonable first approximation since in the $(^3\text{He}, d)$ spectra into both $^{147}$Pm and $^{149}$Eu the total strengths agreed well with the number of holes in the targets. In the $(t, \alpha)$ spectrum at 40° the assigned peaks correspond to 87 % of the total cross section to all observed levels below 2,200 keV excitation energy. Thus the total strength of assigned levels in this spectrum ought to be $12 \cdot 0.87 = 10.4$. To obtain this a normalization constant $N(t, \alpha)=44$ has to be used.

This is quite close to the value used in a recent study [7] of the $(t, \alpha)$ reaction into deformed rare earth nuclei. Furthermore from detailed balance it is expected that $N(\alpha, t)=2N(t, \alpha)$, which in the present case is fulfilled within experimental uncertainties.

By summing the experimental strengths $\frac{d\sigma}{d\Omega}(\text{exp.})/N\sigma_{lj}(\theta)_{DW}$ of all fragments of a shell model state "$lj$" one gets the average number of holes (particles) in that orbit and thus one gets a measure of the distribution of the valence protons among the shell model states forming the $Z=50$–82 shell. This

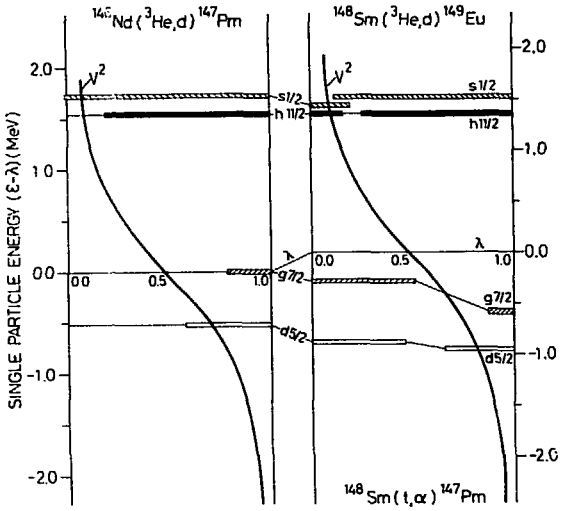


**Fig. 7.** Spectroscopic information from stripping and pick-up reactions into $^{147}$Pm and $^{149}$Eu. The smooth curves represent the fullness factor $V_j^2$ and are plotted as a function of single particle energy. The horizontal bars are summed spectroscopic strengths obtained from Table 5, plotted at single particle energies obtained from the experimentally observed values. See text for discussion

can be compared with the predictions of pairing theory where the emptiness (fullness) of an orbital is denoted by $U_j^2(V_j^2)$, respectively, and thus for the average number of holes (particles) in the state "$lj$" one has to a first approximation

$$U_j^2=\Sigma S_{lj}^{(s)} \quad \text{(holes)} \tag{3}$$

$$V_j^2=\Sigma S_{lj}^{(p)}/2j+1 \quad \text{(particles)} \tag{4}$$

where the summation is over all the fragments of the "$lj$" orbit.

According to pairing theory the fullness factor is

$$V_j^2=1/2(1-(\varepsilon_j-\lambda)/E_j) \tag{5}$$

where $\varepsilon_j$ and $E_j$ are the single particle and quasiparticle energy respectively for the state "$j$", and $\lambda$ is the Fermi energy for the system. The quasiparticle energy is given by

$$E_j=\sqrt{(\varepsilon_j-\lambda)^2+\Delta^2} \tag{6}$$

where $\Delta$ is a measure of the pairing energy and can be estimated from separation energies. An average value $\Delta=1{,}100$ keV has been used in the present calculations.

By assuming that the quasiparticle energy for the groundstate is $\sim\Delta$, an effective value for $E_j$ can be obtained from the excitation energies by

$$E_j=\bar{E}+\Delta \tag{7}$$

where

$$\bar{E}=(\Sigma ES_{lj})/\Sigma S_{lj} \tag{8}$$

is the weighted average excitation energy. Here the sum ranges over all the fragments of a state "$lj$" and $E$ is the experimentally observed excitation energy for each fragment.

Spectroscopic information for states of each "$lj$" configuration populated in $^{147}$Pm and $^{149}$Eu is listed in Table 4 along with excitation energies. As the present experiment is not capable of distinguishing between $d_{3/2}$ and $d_{5/2}$ fragments these are all collected under the label "$d$" unless additional information from previous experiments is available to help determine the spin.

A comparison to pairing theory is given in Fig. 7, where the curved line shows the fullness factor $V_j^2$ as a function of single particle energy calculated from Eq. (5,6). The horizontal bars represent the shell-model states and are plotted at energies $(\varepsilon-\lambda)$ given in Table 5 obtained from the experimental excitation energies by the use of Eq. (6–8). The lengths of the bars represent spectroscopic strengths $\Sigma S_{lj}^{(s)}$ obtained from the $(^3\text{He},d)$ angular distributions, and $\Sigma S_{lj}^{(p)}/2j+1$ obtained from the $(t,\alpha)$ reaction, respectively. These values are also listed in Table 5. Agreement between experiment and theory would thus be obtained if the horizontal bar were just long enough to reach to the $V_j^2$ curve. The agreement for the particle states $s_{1/2}$ and $h_{11/2}$ is quite impressive. Fair agree-

**Table 5.** Energy centroids for $^{147}$Pm and $^{149}$Eu

| | $^{146}$Nd($^3$He,$d$)$^{147}$Pm | | | $^{148}$Sm($t,\alpha$)$^{147}$Pm | | | $^{148}$Sm($^3$He,$d$)$^{149}$Eu | | |
|---|---|---|---|---|---|---|---|---|---|
| | $\bar{E}$ | $\varepsilon-\lambda$ | $\Sigma S_{lj}^{(s)}$ | $\bar{E}$ | $\varepsilon-\lambda$ | $\Sigma S_{lj}^{(p)}/2j+1$ | $\bar{E}$ | $\varepsilon-\lambda$ | $\Sigma S_{lj}^{(s)}$ |
| $d_{5/2}$[a] | 110 | 506 | 0.40 | 310 | 882 | 0.47 | 355 | 952 | 0.34 |
| $g_{7/2}$[a] | 0 | 0 | 0.21 | 32 | 284 | 0.55 | 150 | 593 | 0.12 |
| $h_{11/2}$ | 791 | 1,538 | 0.81 | ~649 | ~1,360 | 0.15 | 643 | 1,352 | 0.74 |
| $s_{1/2}$ | 937 | 1,714 | 1.00 | ~713 | ~1,441 | 0.21 | 776 | 1,520 | 0.88 |

[a] Tentative assignments are not included in these calculations

ment is also observed for the $d_{5/2}$ and $g_{7/2}$ states observed close to the Fermi level. It should be noted that for $g_{7/2}$ only the fragments which are positively known to have spin 7/2 are included while the high spin states given in parenthesis in Table 4 are not. A similar comment holds for the $d_{5/2}$ state, where none of the levels labelled "$d$" in Table 4 is included.

The nucleus $^{148}$Sm has been used as a target for both pick-up and stripping reactions, and thus fullness as well as emptiness factors have been measured for this nucleus. In Fig. 7 the results from the $(t,\alpha)$ reaction are shown under the $V_j^2(^{148}\mathrm{Sm})$-curve. Again it is very encouraging to see the measured value of $(U^2+V^2)$ being very close to unity for $s_{1/2}$ and $h_{11/2}$. For $g_{7/2}$ and $d_{5/2}$ it appears as if some of the strength has not been identified.

The present method of analysis applies to spherical nuclei where the assumption is made that the pairing interaction transforms a number of particles in a shell model state to a state at the corresponding quasiparticle energy and with the appropriate fullness. Fragmentation of this state is then produced by couplings to various core excitations, etc. In a transitional nucleus, however, it is not at all clear if the calculation of the energy centroid represents the single-particle energy of the corresponding spherical shell model state. In the deformed region the pairing factor is taken into account explicitly for each individual Nilsson-orbital, and calculation of the energy centroid as above will obviously not reproduce the spherical single-partical energy. The discussion of how to give pairing a consistent treatment in the transitional region is postponed to a future paper where the general features and the systematic trends of the spectroscopic factors in odd-$Z$ transitional nuclei will be presented.

It is now interesting to compare the main features of the present results with the previous study of the $N=88$ isotones. Having the same number of protons, the Fermilevel ought to be at the same level for different isotopes, and any changes in the filling of the levels would have to be correlated with the neutron-number. In both isotone chains it is seen that the ground state or first excited state contains most of the observed $g_{7/2}$ strength. It seems however that in $^{147}$Pm and especially in $^{149}$Eu, the $g_{7/2}$ state is more filled than in the $N=88$ isotopes. Regarding the "$d$" states, the present experiment cannot distinguish between the $3/2^+$ and $5/2^+$ states, but the total stripping strength for all $l=2$ states corresponds to 2.44 in $^{149}$Eu, while the value increases to 6.5 in $^{151}$Eu. The nature of such a dramatic change is not understood, and it is noted that a similar effect is not observed for the Pm isotopes. For the $h_{11/2}$ state the most dramatic effect is in the Pm isotopes, with 5.3 holes in $^{149}$Pm increasing to 9.7 in $^{147}$Pm. The $s_{1/2}$ state is completely empty in the $N=86$ isotones with 1.99 and 1.76 holes in $^{147}$Pm and $^{149}$Eu respectively, compared to 0.81 and 1.3 in the $N=88$ isotones.

## 4. Summary and Conclusions

Levels in the $N=86$ nuclei $^{147}$Pm and $^{149}$Eu have been studied by proton stripping and pick-up reactions. Previously these nuclei have been studied by radioactive decay and by the $^{151}$Eu$(p,t)^{149}$Eu reaction. The present study confirms the spin assignment to many of the lowlying states in $^{147}$Pm and $^{149}$Eu, and resolves some of the ambiguities in previous works. In addition many fragments of the $s_{1/2}$ orbital have been located for the first time. However, the main motivation for the present study was to probe the nuclear structure of these transitional nuclei by measuring spectroscopic factors. These nuclei have been traditionally regarded as "spherical" and in the present study no well-developed fingerprint patterns of rotational bands have been observed. However, most of the Nilsson states which would be expected in this region, such as the $5/2^+$ [402] and $7/2^+$ [404] orbitals, have their strength concentrated in one $j$-value. Thus only one spin member would be strongly populated and the bands are difficult to identify. Furthermore, Nilsson orbitals originating from the $h_{11/2}$ shell model state would be strongly Coriolis coupled, resulting in a larger spectroscopic factor for the lowest $11/2^-$ level than would be expected for any single orbital by itself. The net result is that it can be difficult to distinguish between spherical states and Coriolis-coupled states of small deformations on the basis of cross sections to the strongly populated levels. To further investigate this a detailed calculation is planned based on the Nilsson model with pairing and Coriolis coupling included, and with a consistent treatment of the Nilsson parameters and the recoil term, a model which recently [9] has shown great success in describing transitional odd neutron nuclei.

The authors are grateful for the opportunity to use the facilities at the Los Alamos Scientific Laboratories and would like to thank E. Flynn and S. Orbeson for assistance with the $(t,\alpha)$ experiments. Financial support for this work was provided by the National Research Council of Canada and in part by Norges Almenvitenskapelige Forskningsråd and is gratefully acknowledged.

## References

1. Fleissner, J.G., Funk, E.G., Venezia, F.P., Mihelich, J.W.: Phys. Rev. C16, 227 (1977)

2. Kortelahti, M., Pakkanen, A., Piiparinen, M., Komppa, T., Komer, R.: Nucl. Phys. A **288**, 365 (1977)
Al-Janabi, T., Hamilton, W.D., Warner, D.D.: J. Phys. G: Nucl. Phys. **3**, 1415 (1977)
3. Taketani, H., Sharma, H.L., Hintz, N.M.: Phys. Rev. C **12**, 108 (1975)
4. Aleksandrov, V.S., Vylov, Ts., Gromova, I.I., Klyuchnikov, A.A., Nogorodov, A.F., Feoktistov, A.I.: Bull. Acad. Sci. USSR Phys. Ser. **39**, No. 3, 9 (1975)
Nakayama, H., Chiba, J., Sekimoto, M., Nakai, K.: Nucl. Phys. A **293**, 137 (1977)
5. Kunz, P.D.: Computer code DWUCK. University of Colorado, unpublished, 1969
6. Straume, O., Løvhøiden, G., Burke, D.G.: Nucl. Phys. A **266**, 390 (1976)
7. Løvhøiden, G., Burke, D.G., Hirning, C.R., Flynn, E.R., Sunier, J.W.: Nucl. Phys. A **303**, 1 (1978)
8. Rekstad, J.: Nucl. Phys. A **247**, 7 (1975)
9. Guttormsen, M., Osnes, E., Rekstad, J., Løvhøiden, G., Straume, O.: Nucl. Phys. A **298**, 122 (1978)
10. Straume, O., Løvhøiden, G., Shahabudin, M.A.M., Burke, D.G., Waddington, J.C.: McMaster Accelerator Laboratory Annual Report 88 (1977)

O. Straume
G. Løvhøiden
Department of Physics
University of Bergen
Allegt. 55
N-5014 Bergen-U
Norway

D.G. Burke
McMaster University
Hamilton, Ontario L8S 4K1
Canada

# P A P E R III

## SINGLE-PROTON STATES IN $^{151}$Pm

I.E.1: 2.G

*Nuclear Physics* A322 (1979) 13–32; © *North-Holland Publishing Co., Amsterdam*


# SINGLE-PROTON STATES IN $^{151}$Pm

O. STRAUME and G. LØVHØIDEN

*University of Bergen, Bergen, Norway*

D. G. BURKE

*Tandem Accelerator Laboratory, McMaster University, Hamilton, Ontario, Canada L8S 4K1* †

and

E. R. FLYNN and J. W. SUNIER

*University of California, Los Alamos Scientific Laboratory, Los Alamos, New Mexico 87545, USA* ††

Received 26 January 1979

**Abstract:** The $^{152}$Sm(t, α)$^{151}$Pm reaction was studied using 17 MeV polarized tritons from the tandem Van de Graaff accelerator at the Los Alamos Scientific Laboratory. The α-particles were analyzed using a Q3D magnetic spectrometer and detected with a helical-cathode position-sensitive counter. The overall resolution was ~ 18 keV FWHM. Measurements of the $^{150}$Nd($^3$He, d)$^{151}$Pm reaction were made using 24 MeV $^3$He beams from the McMaster University tandem accelerator. The deuteron spectra were analyzed with a magnetic spectrograph using photographic emulsions for detectors, yielding a resolution of ~ 13 keV FWHM. By comparing the measured angular distributions of (t, α) and ($^3$He, d) cross sections and (t, α) analyzing powers with DWBA predictions it was possible to assign spins and parities to many levels. The present results confirm earlier assignments of rotational bands based on the low-lying $\frac{5}{2}^+$[413], $\frac{5}{2}^-$[532], $\frac{3}{2}^+$[411] and $\frac{1}{2}^+$[420] orbitals. In addition, states at higher excitation have now been assigned to the $\frac{1}{2}^+$[411] and $\frac{7}{2}^+$[404] orbitals, and members of the $\frac{3}{2}^+$[422], $\frac{5}{2}^+$[402], $\frac{3}{2}^-$[541] and $\frac{7}{2}^-$[523] bands are tentatively proposed. The spectroscopic strengths can be explained reasonably well by the Nilsson model when pairing and Coriolis mixing effects are included.

E NUCLEAR REACTIONS $^{152}$Sm(t, α), $E$ = 17 MeV; measured $\sigma(\theta, E_\alpha)$, $A_y(\theta, E_\alpha)$, $^{150}$Nd($^3$He, d), $E$ = 24 MeV; measured $\sigma(\theta, E_d)$. $^{151}$Pm deduced levels, $J$, $\pi$, $l$, Nilsson assignments. Enriched targets.

## 1. Introduction

The present paper describes a new investigation of the nuclear structure of $^{151}$Pm which has been performed to study the systematics of single-proton states in the deformed rare earth region. The levels in $^{151}$Pm have previously been populated by the ($^3$He, d), (α, t) and (t, α) reactions [1]) and by the β-decay [2]) of $^{151}$Nd. As a result of these previous investigations the low-lying $\frac{5}{2}^+$[413], $\frac{5}{2}^-$[532], $\frac{3}{2}^+$[411]

† Financial support provided by the National Research Council of Canada.
†† Work performed under the auspices of the US Department of Energy.

and $\frac{1}{2}^+[420]$ bands were identified, and tentative assignments for the $\frac{3}{2}^-[541]$ orbital and other levels were suggested, but most of the levels above an excitation energy of ~ 500 keV could not be interpreted. A better understanding of the single particle states in this region becomes of increasing importance as one tries to explain the structure of nuclei near $A \sim 150$ where there is a large change in the deformation.

It has recently been shown that the (t, α) reaction with polarized tritons is a very

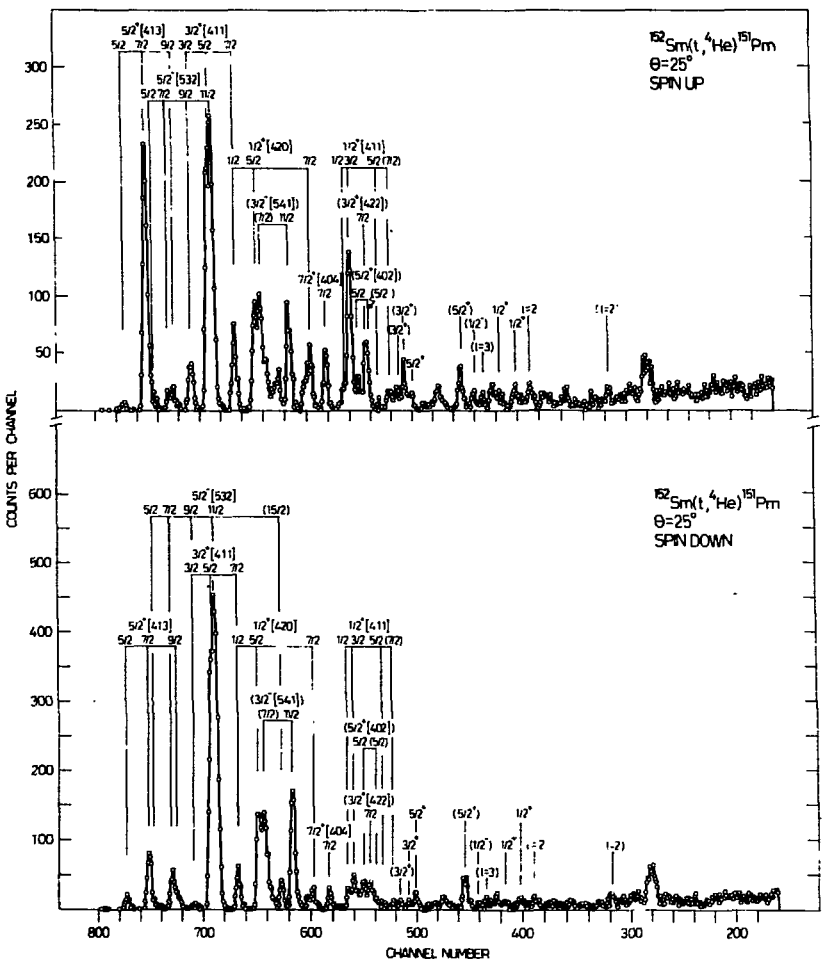


Fig. 1. Spectra from the $^{152}Sm(\vec{t}, \alpha)^{151}Pm$ reaction for projectile spin "up" and "down". The Nilsson assignments shown are discussed in sect. 3. Assignments in parenthesis are considered tentative.

useful spectroscopic tool for studying single-proton states, not only in the closed shell regions, e.g. near $^{208}$Pb[ref. [3])], but also in well-deformed nuclei [4–9]). The present study involves the application of the $(\vec{t}, \alpha)$ reaction to the study of $^{151}$Pm. Additional $^{150}$Nd($^3$He, d)$^{151}$Pm angular distributions have also been measured because in the previous ($^3$He, d) study [1]) several strongly populated levels were left unassigned, and complete angular distributions should help clarify the nature of these levels.

## 2. Experimental procedures and results

Targets for the $^{152}$Sm$(\vec{t}, \alpha)^{151}$Pm reaction were prepared from $Sm_2O_3$, isotopically enriched to 98.29 % in $^{152}$Sm, purchased from the Isotope Sales Division of the Oak Ridge National Laboratory. The oxide was reduced to samarium metal by heating with thorium powder in a vacuum, and the metal was vacuum evaporated onto 30 $\mu$g/cm$^2$ carbon foils. The target thickness for the $(\vec{t}, \alpha)$ experiments was $\sim$ 150 $\mu$g/cm$^2$. The $^{150}$Nd($^3$He, d)$^{151}$Pm experiments were performed with 30 $\mu$g/cm$^2$ targets made in a similar manner from $Nd_2O_3$ which was enriched to 96.13 % in $^{150}$Nd.

The procedures used for the (t, $\alpha$) measurements and for the data analysis are similar to those described in a number of previous studies [3–9]) using the same apparatus. The experiments were performed with beams of 17 MeV tritons having a polarization of 0.80 from the FN tandem Van de Graaff accelerator at the Los Alamos Scientific Laboratory. The $\alpha$-spectra were studied with a Q3D magnetic spectrometer equipped with a position-sensitive helical-cathode detector on the focal plane [10]).

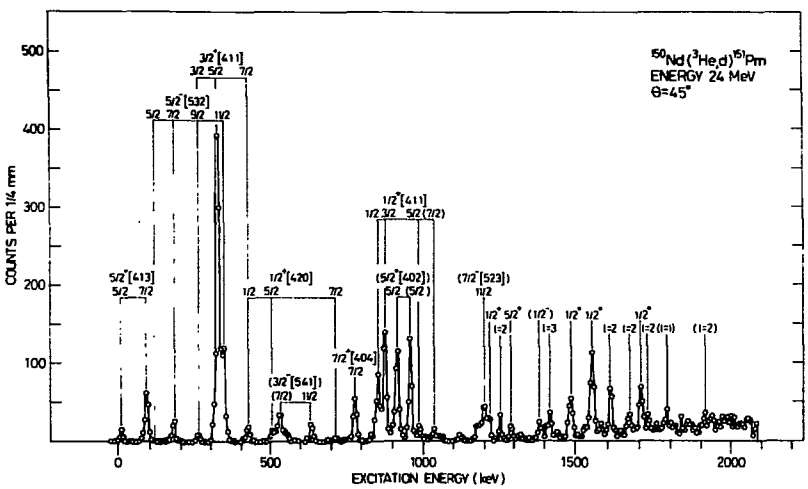


Fig. 2. Spectrum from the $^{150}$Nd($^3$He, d)$^{151}$Pm reaction. See caption to fig. 1.

TABLE

Levels populated

| Energy (keV) | | | Cross section (μb/sr) | | |
|---|---|---|---|---|---|
| prev. [a]) | ($^3$He, d) | (t, α) | (He, d) $\theta = 45°$ | (t, α) $\theta = 25°$ | $A_y$ $\theta = 25°$ |
| 0 | 0 | 0 | 5.1 | 11 | 0.58 (10) |
| 85.1 | 86 | 85 | 27 | 138 | −0.59 (3) |
| 116.8 | (112) | 119 | | 4.3 | −0.42 (16) |
| 175.1 | 176 | 175 | 10.0 | 28 | 0.62 (6) |
| 197.3 | | 199 | | 12 | 0.21 (10) |
| 255.7 | 257 | | 4.1 | | |
| 261.1 | | 260 | | 24 | −0.82 (6) |
| 324.7 | 325 | 323 | 154 | 198 | 0.33 (2) |
| 345 | 345 | 346 | 49 | 301 | 0.37 (2) |
| 426.4 | 426 | 428 | 9.1 | 51 | −0.15 (5) |
| 427.1 | | | | | |
| 507.9 | 508 | 508 | 7.2 | 107 | 0.29 (3) |
| 524.3 | | | | | |
| | 533 | 529 | 18 | 88 | 0.22 (4) |
| 540.3 | | | | | |
| 553 | 554 | 548 | 6.1 | 45 | 0.11 (6) |
| 577.4 | (577) | | | | |
| 597 | | 593 | | 30 | −0.03 (7) |
| 640 | 641 | 642 | 8.6 | 110 | 0.39 (3) |
| 698 | | 700 | | 14 | −0.18 (10) |
| 719 | (718) | 721 | (2) | 32 | −0.40 (6) |
| 746.5 | | | | | |
| 773.6 | | | | | |
| 782 | 778 | 781 | 24 | 29 | −0.38 (6) |
| 809.4 | | 813 | | 1.7 | 0.18 (30) |
| 840.9 | | | | | |
| 851 | 850 | 850 | 35 | 12 | 0.12 (10) |
| 852.9 | | | | | |
| 874.7 | 874 | 876 | 61 | 82 | −0.51 (4) |
| 914.0 | 913 | 914 | 52 | 27 | 0.25 (7) |
| | | 940 | | 40 | −0.25 (6) |
| 960 | 956 | 958 | 47 | 15 | 0.01 (9) |
| 989.8 | 988 | 997 | 8.6 | 6.8 | 0.34 (13) |
| 1038 | 1036 | 1035 | 6.9 | 14 | −0.32 (10) |
| | 1055 | | 3.9 | | |
| 1066.6 | | | | | |
| | | 1078 | | 12 | −0.28 (10) |
| 1098.4 | | 1101 | | 16 | −0.56 (8) |
| | 1125 | | 3.6 | | |
| 1133.2 | | 1134 | | 15 | 0.21 (9) |
| 1182 | 1181 | | 11 | | |
| 1209 | 1200 | | 22 | | |
| 1225 | 1219 | | 13 | | |
| 1246 | | 1244 | | 21 | −0.08 (8) |
| 1260 | 1257 | | 10 | | |
| 1286.2 | | | | | |

l

in $^{151}$Pm

| Assignment | | | Nuclear structure factor | |
|---|---|---|---|---|
| prev. [a]) | $l$-value from ($^3$He, d) | adopted | ($^3$He, d) | (t, α) |
| $\frac{5}{2}^+$ | $l = 2$ | $\frac{5}{2}$ $\frac{5}{2}^+$[413] | 0.031 | 0.030 |
| $\frac{7}{2}^+$ | $l = 4, 5$ | $\frac{7}{2}$ $\frac{5}{2}^+$[413] | 0.56 | 0.75 |
| $\frac{5}{2}^-$ | | $\frac{5}{2}$ $\frac{5}{2}^-$[532] | | 0.007 |
| $\frac{7}{2}^-$ | $l = 3$ | $\frac{7}{2}$ $\frac{5}{2}^-$[532] | 0.018 | 0.063 |
| $\frac{9}{2}^+$ | | $\frac{9}{2}$ $\frac{5}{2}^+$[413] | | 0.054 |
| $\frac{3}{2}^+$ | $l = 2$ | $\frac{3}{2}$ $\frac{3}{2}^+$[411] | 0.026 | |
| $\frac{9}{2}^-$ | | $\frac{9}{2}$ $\frac{5}{2}^-$[532] | | 0.12 |
| $\frac{3}{2}^+$ | $l = 2$ | $\frac{3}{2}$ $\frac{3}{2}^+$[411] | 0.80 | 0.50 |
| $\frac{11}{2}^-$ | $l = 5$ | $\frac{11}{2}$ $\frac{5}{2}^-$[532] | 1.44 | 1.66 |
| $(\frac{1}{2}^+)$ | $l = 0+(l = 4, 5)$ | $\frac{1}{2}$ $\frac{1}{2}^+$[420] | 0.026 ($l = 0$) | 0.11 ($l = 0$) |
| $\frac{7}{2}^+$ | | $\frac{7}{2}$ $\frac{3}{2}^+$[411] | | |
| $(\frac{1}{2})^+$ | $l = 2$ | $\frac{5}{2}^+\frac{1}{2}^+$[420] | 0.033 | 0.20 |
| $(\frac{3}{2})^+$ | | | | |
| | ($l = 3$) | $\frac{7}{2}$ $\frac{3}{2}^-$[541] | 0.14 | 0.17 |
| $\frac{3}{2}^-$ | | | | |
| $(\frac{5}{2}^+)$ | | | | |
| $\frac{5}{2}^-$ | | | | |
| $\frac{11}{2}^-$ | $l = 4, 5$ | $\frac{11}{2}$ $\frac{3}{2}^-$[541] | 0.28 | 0.60 |
| | | $\frac{7}{2}$ $\frac{1}{2}^+$[420] | < 0.04 | 0.16 |
| $\frac{3}{2}^-$ | | | | |
| $(\frac{1}{2}^-)$ | | | | |
| $\frac{11}{2}^-$ | $l = 4, 5$ | $\frac{7}{2}$ $\frac{7}{2}^+$[404] | 0.44 | 0.18 |
| $\frac{1}{2}^+\frac{1}{2}^+$ | | ($\frac{1}{2}$ $\frac{3}{2}^+$[422]) | | |
| $(\frac{1}{2}^+)$ | $l = 0$ | $\frac{1}{2}$ $\frac{1}{2}^+$[411] | 0.07 | 0.026 |
| $\frac{1}{2}$ | | | | |
| $\frac{1}{2}, \frac{3}{2}, \frac{5}{2}, \frac{7}{2}$ | $l = 2$ | $\frac{3}{2}$ $\frac{1}{2}^+$[411] | 0.30 | 0.15 |
| $\frac{5}{2}^+$ | $l = 2$ | $\frac{5}{2}$ $\frac{5}{2}^+$[402] [b]) | 0.25 | 0.046 |
| | | $\frac{7}{2}$ $\frac{3}{2}^+$[422] | | 0.25 |
| | $l = 2$ | $\frac{5}{2}$ $\frac{3}{2}^+$[402] [b]) | 0.20 | 0.03 |
| $\frac{5}{2}, \frac{7}{2}, \frac{9}{2}$ | $l = 2$ | $\frac{5}{2}$ $\frac{1}{2}^+$[411] | 0.035 | 0.071 |
| | | ($\frac{7}{2}$ $\frac{1}{2}^+$[411]) | 0.10 | 0.08 |
| | | ($\frac{1}{2}^+$) | | 0.023 |
| | | ($\frac{3}{2}^+$) | | 0.037 |
| | | $\frac{5}{2}^+$ | | 0.026 |
| | $l = 2$ | $l = 2$ | 0.037 | |
| | $l = 4, 5$ | ($\frac{11}{2}$ $\frac{7}{2}^-$[523]) | 0.57 | |
| | $l = 0$ | $\frac{1}{2}^+$ | 0.024 | |
| | $l = 2$ | $l = 2$ | 0.046 | |

TABLE 1

| Energy (keV) | | | Cross section (μb/sr) | | |
|---|---|---|---|---|---|
| prev. [a]) | ($^3$He, d) | (t, α) | (He, d) $\theta = 45°$ | (t, α) $\theta = 25°$ | $A_y$ $\theta = 25°$ |
| 1297.3 | 1295 | | 9.0 | | |
| | 1328 | | 6.5 (35°) | | |
| 1335 | | 1335 | | 40 | 0.026 (6) |
| 1395 | 1390 | 1388 | 11 | 11 | −0.29 (11) |
| 1424 | 1421 | 1424 | 17 | 9.1 | 0.06 (12) |
| | 1444 | | 6.1 | | |
| 1465 | | 1462 | | 19 | −0.06 (8) |
| 1491 | 1488 | 1494 | 26 | 14 | −0.09 (10) |
| | 1531 | | 7.4 | | |
| 1560 | 1556 | 1553 | 49 | 14 | −0.15 (10) |
| | | 1570 | | 6.9 | −0.11 (14) |
| | 1584 | | 8.8 | | |
| | | 1591 | | 4.6 | 0.00 (17) |
| 1619 | 1616 | 1621 | 27 | 19 | −0.11 (8) |
| 1674 | 1672 | | 16 | | |
| 1713 | 1709 | | 32 | | |
| 1735 | 1733 | | 13 | | |
| | | 1759 | | 12 | −0.09 (11) |
| | 1765 | | 11 | | |
| | 1794 | | 20 | | |
| | 1874 | | 15 | | |
| | 1915 | | 17 | | |
| | | 1932 | | 19 | 0.18 (8) |
| | 1938 | | 19 | | |
| | | 1980 | | 16 | 0.16 (9) |
| | | 2088 | | 38 | 0.11 (6) |
| | | 2115 | | 52 | 0.20 (5) |
| | | 2447 | | 21 | −0.05 (8) |

[a]) Data from refs. [1, 2]).

Spectra recorded with the incident tritons having spin "up" and spin "down" are shown in fig. 1 for the $^{152}$Sm target. The resolution was typically 18 keV (FWHM). Analyzing powers were extracted from the spin "up" and spin "down" intensities in the usual manner [3, 4]). Angular distributions of cross sections and analyzing powers for the various transitions are shown in figs. 4a–4c. The uncertainties in the absolute cross sections are believed to be about ±20%. However the reproducibility of repeated measurements was usually within ±5% and this is regarded as a realistic uncertainty when relative intensities are being considered as in angular distributions. The error bars shown in figs. 4a–4c represent statistical errors only.

The excitation energies of strongly populated levels were adopted from ref. [1]) and energies for the weakly populated levels were obtained by interpolation. The uncertainties on these values should be ≦ 4 keV for levels up to ~ 2.0 MeV.

(continued)

| Assignment | | | Nuclear structure factor | |
|---|---|---|---|---|
| prev. [a]) | $l$-value from ($^3$He, d) | adopted | ($^3$He, d) | (t, α) |
| $\frac{1}{2}^+$ | $l = 2$ | $\frac{1}{2}^+$ | 0.035 | |
| | $(l = 2)$ | $(l = 2)$ | 0.022 | |
| | $(l = 2)$ | $(\frac{3}{2}^+)$ | | 0.078 |
| | $(l = 1)$ | $(\frac{1}{2}^-)$ | 0.017 | 0.012 |
| | $(l = 3)$ | $(l = 3)$ | 0.095 | |
| | $l = 0$ | $\frac{1}{2}^+$ | 0.050 | 0.021 |
| | $l = 0$ | $\frac{1}{2}^+$ | 0.087 | 0.021 |
| | $(l = 2)$ | $(l = 2)$ | 0.051 | |
| | $l = 2$ | $l = 2$ | 0.097 | |
| | $(l = 2)$ | $(l = 2)$ | 0.076 | |
| | $l = 0$ | $\frac{1}{2}^+$ | 0.063 | |
| | $l = 2$ | $l = 2$ | 0.024 | |
| | $(l = 1)$ | $(l = 1)$ | 0.020 | |
| | $(l = 2)$ | $(l = 2)$ | 0.043 | |

[b]) The strength for the $\frac{1}{2}^+$[402] orbital is distributed over at least two states. See text.

Fig. 2 shows a spectrum from the $^{150}$Nd($^3$He, d)$^{151}$Pm reaction. This experiment was performed with a beam of 24 MeV $^3$He from the McMaster University FN tandem Van de Graaff accelerator. An Enge split-pole magnetic spectrograph was used to analyze the triton spectra, and photographic emulsions were used as detectors. The resolution was typically 13 keV (FWHM). Angular distributions of the cross sections are shown in figs. 3a and 3b. Uncertainties are estimated to be $\pm 2$ keV in the excitation energies for strongly populated levels, and 20 % in the absolute cross sections.

In all experiments the intensities of spectra were converted to absolute cross sections through the use of a silicon semi-conductor monitor counter of known solid angle in the target chamber to record elastically scattered beam particles. The elastic scattering cross section at $\theta = 30°$ for 17 MeV tritons on $^{152}$Sm was

taken to be 69 % of the Rutherford value, a result obtained from the DWBA calculations described below.

For the determination of experimental ($^3$He, d) cross sections the elastic scattering cross section at $\theta = 30°$ for 24 MeV $^3$He on $^{150}$Nd was assumed to be 1.05 times the Rutherford value, as predicted by optical-model calculations using the $^3$He parameters of ref. [11]).

The excitation energies for levels populated are listed in table 1 and compared with previously obtained data. Also given in table 1 are the experimental cross sections for the ($^3$He, d) reaction at $\theta = 45°$ and the 17 MeV (t, $\alpha$) reaction at $\theta = 25°$, as well as the ($\vec{t}$, $\alpha$) analyzing powers at $\theta = 25°$. Interpretations listed for the various levels are discussed in the following section.

## 3. Interpretation and discussion

### 3.1. GENERAL PROCEDURES

The Nilsson model is used as a basis for discussing the present results. The cross section for a single-nucleon transfer reaction on an even-even target, leading to a rotational band member of spin $I$ in a deformed residual nucleus, with Coriolis mixing and pairing effects included, is

$$\left(\frac{d\sigma}{d\Omega}\right)_{exp} = 2N|\sum_i (C_{jl})_i a_i P_i|^2 \left(\frac{d\sigma}{d\Omega}\right)_{DW}. \quad (1)$$

For this case the transferred angular momentum, $j$, is equal to $I$. The $(C_{jl})_i$ are expansion coefficients which describe the Nilsson orbitals in terms of spherical shell-model states. The state populated is assumed to consist of a mixture of Nilsson components, each with an amplitude represented by a coefficient $a_i$. The factor $P_i$ takes account of the partial filling of the levels in the target nucleus, due to pairing, and is the fullness factor $V_i$ or the emptiness factor $U_i$ for a pickup or stripping reaction respectively. Single-particle transfer cross sections, $(d\sigma/d\Omega)_{DW}$, can be obtained from DWBA calculations and $N$ is a normalization factor for these calculations.

DWBA calculations for the (t, $\alpha$) reaction were performed with the computer program DWUCK 3 (ref. [12])), using the same optical model parameters and the same value of $N = 23$ that were used in the study of $^{153}$Pm levels [6]). No lower cutoff for the radial integration and no nonlocal parameters were used. Due to ambiguities in the choice of optical-model parameters there are fairly large uncertainties, probably of the order of 30–50 %, in the spectroscopic strengths obtained [6]). DWBA calculations for the ($^3$He, d) reaction were performed with the same optical model parameters and the same value of $N = 6$ as used in the study [11]) of $^{149}$Pm. Experimental values of the nuclear structure factors are obtained by dividing the cross sections by $2N(d\sigma/d\Omega)_{DW}$. These strengths are listed in tables 1 and 2, where they are compared with Nilsson model values and with values predicted when Coriolis mixing is

TABLE 2

Nuclear structure factors for $^{151}$Pm levels

| Level | Energy (keV) | | Nuclear structure factors "pickup" | | | Nuclear structure factor "stripping" | | |
|---|---|---|---|---|---|---|---|---|
| | exp. | calc. | unmixed | mixed | (t, α) exp | unmixed | mixed | ($^3$He, d) exp |
| $\frac{5}{2}\frac{5}{2}^+$[413] | 0 | 0 | 0.02 | 0.02 | 0.03 | 0.02 | 0.01 | 0.03 |
| $\frac{7}{2}$ | 85 | 85 | 0.48 | 0.81 | 0.75 | 0.48 | 0.79 | 0.56 |
| $\frac{9}{2}$ | 199 | 195 | 0.01 | 0.01 | 0.05 | 0.01 | 0.01 | |
| $\frac{3}{2}\frac{3}{2}^+$[411] | 257 [a]) | 257 | 0.004 | 0.004 | | 0.02 | 0.02 | < 0.03 |
| $\frac{5}{2}$ | 325 | 319 | 0.16 | 0.43 | 0.50 | 0.68 | 0.93 | 0.80 |
| $\frac{1}{2}$ | 426 [a]) | 429 | 0.02 | 0.05 | | 0.08 | 0.09 | |
| $\frac{9}{2}$ | | 510 | 0.007 | 0.05 | | 0.03 | 0.05 | |
| $\frac{1}{2}\frac{1}{2}^+$[420] | 428 [a]) | 426 | 0.11 | 0.11 | 0.11 | 0.02 | 0.02 | 0.03 |
| $\frac{3}{2}$ | 524 [b]) | 523 | 0.003 | 0.003 | | 0.001 | 0.003 | |
| $\frac{5}{2}$ | 508 | 507 | 0.53 | 0.27 | 0.20 | 0.09 | 0.002 | 0.03 |
| $\frac{7}{2}$ | 721 | 718 | 0.16 | 0.21 | 0.16 | 0.03 | 0.01 | < 0.04 |
| $\frac{9}{2}$ | | 724 | 0.05 | 0.01 | | 0.009 | 0.003 | |
| $\frac{7}{2}\frac{7}{2}^+$[404] | 778 [a]) | 770 | 0.08 | 0.04 | 0.18 | 0.91 | 0.78 | 0.44 |
| $\frac{9}{2}$ | | 912 | 0.001 | 0.001 | | 0.007 | 0.003 | |
| $\frac{5}{2}\frac{5}{2}^+$[422] | | 767 | 0.06 | 0.04 | | 0.005 | 0.002 | |
| $\frac{5}{2}$ | 841 [b]) | 841 | 0.06 | 0.08 | | 0.005 | 0.01 | |
| $\frac{7}{2}$ | 940 | 940 | 0.78 | 0.40 | 0.25 | 0.07 | 0.11 | |
| $\frac{9}{2}$ | | 1077 | 0.02 | 0.02 | | 0.002 | 0.002 | |
| $\frac{1}{2}\frac{1}{2}^+$[411] | 850 | 850 | 0.01 | 0.01 | 0.03 | 0.12 | 0.13 | 0.07 |
| $\frac{3}{2}$ | 874 | 852 | 0.05 | 0.06 | 0.15 | 0.55 | 0.56 | 0.30 |
| $\frac{5}{2}$ | 988 | 98[illegible] | 0.01 | 0.001 | | 0.14 | 0.12 | 0.03 |
| $\frac{7}{2}$ | 1036 | 997 | 0.008 | 0.16 | (0.08) | 0.10 | 0.02 | (0.10) |
| $\frac{9}{2}$ | | 1225 | | | | 0.006 | 0.003 | |
| $\frac{5}{2}\frac{5}{2}^+$[402] | 913<br>956 | 930 | 0.07 | 0.05 | 0.05<br>0.03 | 0.88 | 0.74 | 0.25<br>0.20 |
| $\frac{7}{2}$ | | 1039 | 0.003 | 0.001 | | 0.04 | 0.007 | |
| $\frac{9}{2}$ | | 1175 | 0.001 | 0.001 | | 0.01 | 0.007 | |
| $\frac{7}{2}\frac{7}{2}^-$[523] | | 782 | 0.001 | 0.004 | | 0.01 | 0.003 | |
| $\frac{9}{2}$ | | 1019 | 0.001 | 0 | | 0.006 | 0.002 | |
| $\frac{11}{2}$ | (1200) | 1239 | 0.08 | 0.15 | | 0.90 | 0.36 | 0.57 |
| $\frac{5}{2}\frac{5}{2}^-$[532] | 117 | 130 | < 0.001 | < 0.001 | 0.007 | < 0.001 | < 0.001 | |
| $\frac{7}{2}$ | 175 | 163 | 0.008 | 0.05 | 0.06 | 0.02 | 0.04 | 0.02 |
| $\frac{9}{2}$ | 261 | 254 | 0.002 | 0.004 | 0.12 | 0.004 | 0.008 | |
| $\frac{11}{2}$ | 345 | 347 | 0.25 | 1.32 | 1.66 | 0.71 | 1.55 | 1.39 |
| $\frac{3}{2}\frac{3}{2}^-$[541] | | 284 | 0.001 | 0.001 | | < 0.001 | < 0.001 | |
| $\frac{5}{2}$ | | 428 | < 0.001 | < 0.001 | | < 0.001 | < 0.001 | |
| $\frac{7}{2}$ | (529) | 522 | 0.05 | 0.04 | 0.17 | 0.01 | < 0.001 | 0.14 |
| $\frac{9}{2}$ | | 728 | 0.003 | < 0.001 | | 0.001 | 0.002 | |
| $\frac{11}{2}$ | (642) | 794 | 0.77 | 0.43 | 0.60 | 0.17 | 0.28 | 0.27 |
| $\frac{1}{2}\frac{1}{2}^-$[550] | | 1400 | < 0.001 | < 0.001 | | < 0.001 | < 0.001 | |
| $\frac{3}{2}$ | | 1136 | 0.003 | 0.003 | | < 0.001 | < 0.001 | |
| $\frac{5}{2}$ | | 1805 | < 0.001 | < 0.001 | | < 0.001 | < 0.001 | |
| $\frac{7}{2}$ | | 1230 | 0.07 | 0.03 | | 0.003 | 0.001 | |
| $\frac{9}{2}$ | | 2380 | < 0.001 | < 0.001 | | < 0.001 | < 0.001 | |
| $\frac{11}{2}$ | | 1584 | 0.88 | 0.08 | | 0.04 | 0.002 | |

[a]) Unresolved doublets.
[b]) Ref. [2]).

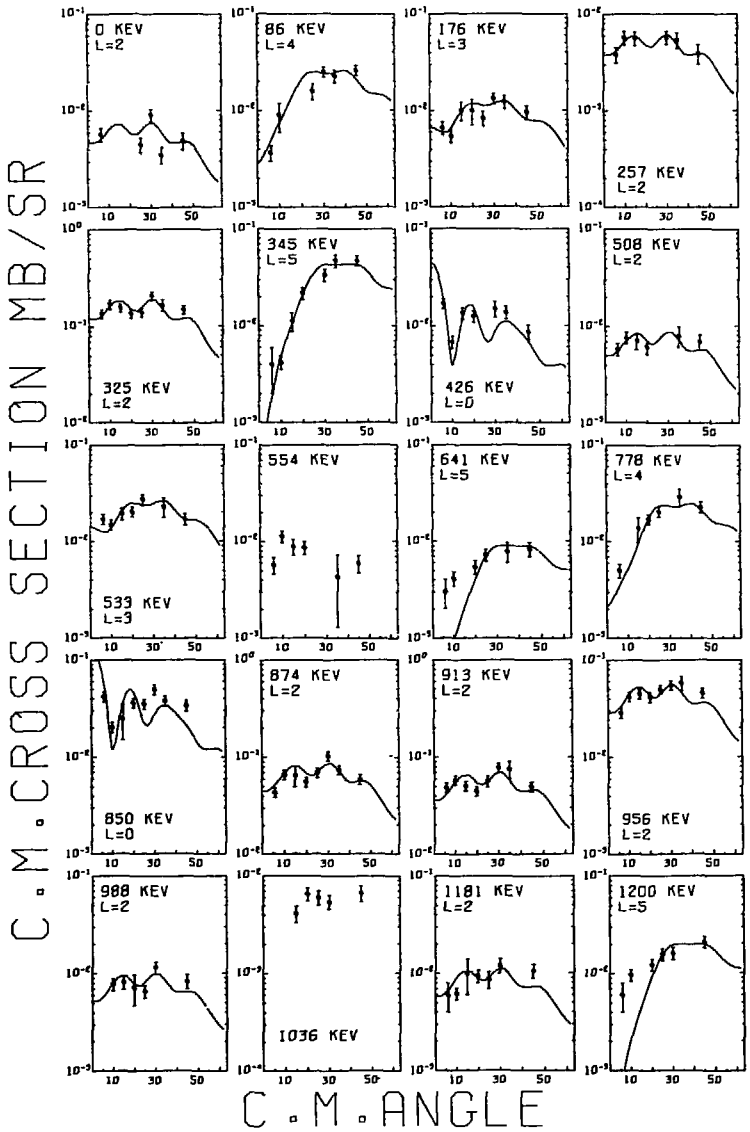
0 KEV
L=2
86 KEV
L=4
176 KEV
L=3
257 KEV
L=2
325 KEV
L=2
345 KEV
L=5
426 KEV
L=0
508 KEV
L=2
533 KEV
L=3
554 KEV
641 KEV
L=5
778 KEV
L=4
850 KEV
L=0
874 KEV
L=2
913 KEV
L=2
956 KEV
L=2
988 KEV
L=2
1036 KEV
1181 KEV
L=2
1200 KEV
L=5
C.M.CROSS SECTION MB/SR
C.M.ANGLE

Fig. 3a.

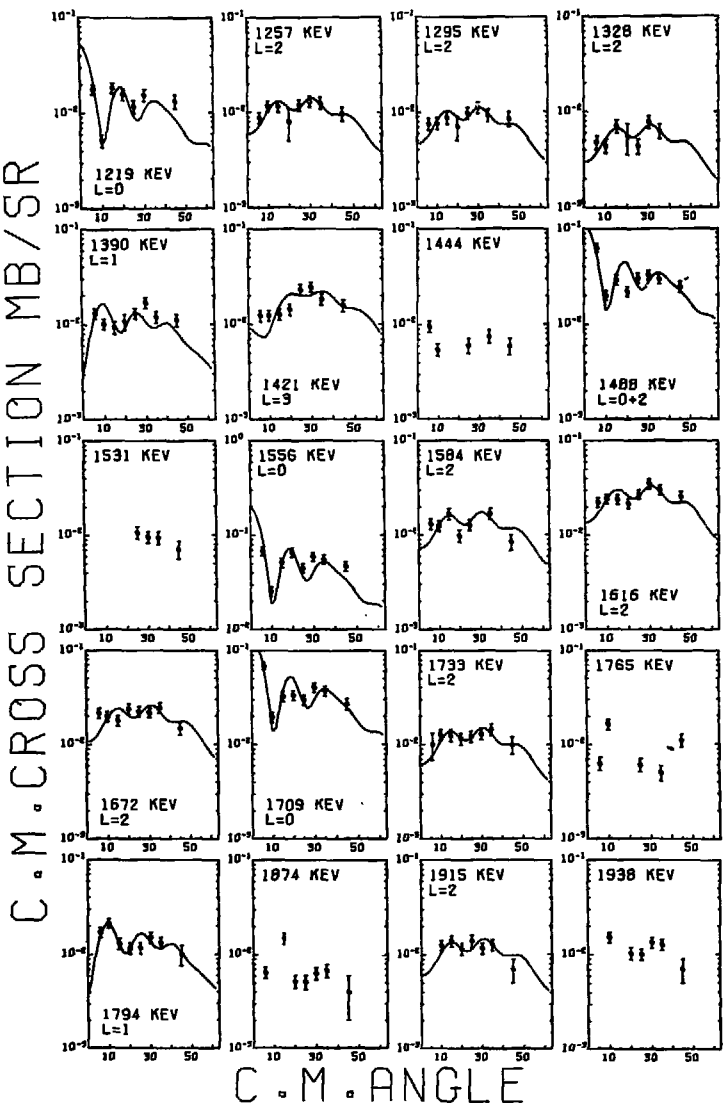


Fig. 3b.

**Fig. 3. Angular distributions for levels in $^{151}$Pm populated in the ($^3$He, d) reaction. The points are experimental data, and the curves are from DWBA calculations for the *l*-values indicated. Error bars shown have been calculated taking into account the statistical standard deviations only.**

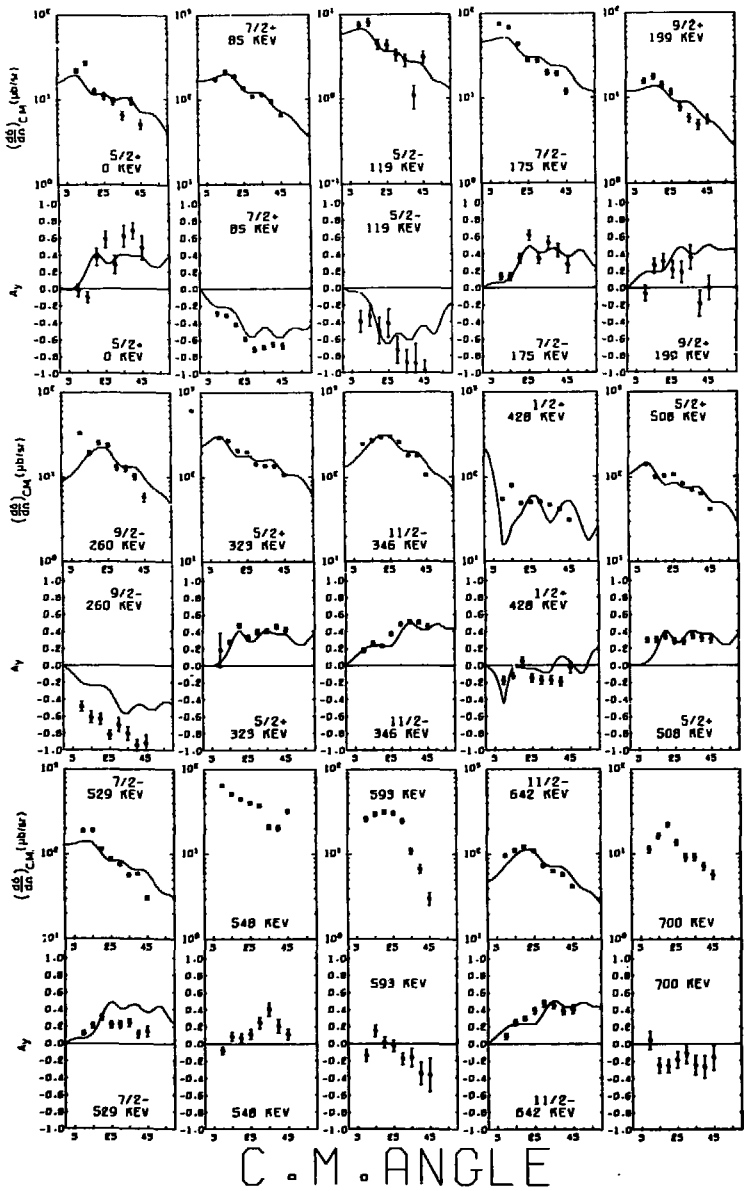
5/2+
0 KEV
7/2+
85 KEV
5/2-
119 KEV
7/2-
175 KEV
9/2+
199 KEV
9/2-
260 KEV
5/2+
323 KEV
11/2-
346 KEV
1/2+
428 KEV
5/2+
508 KEV
7/2-
529 KEV
548 KEV
593 KEV
11/2-
642 KEV
700 KEV
C.M. ANGLE

Fig. 4a.

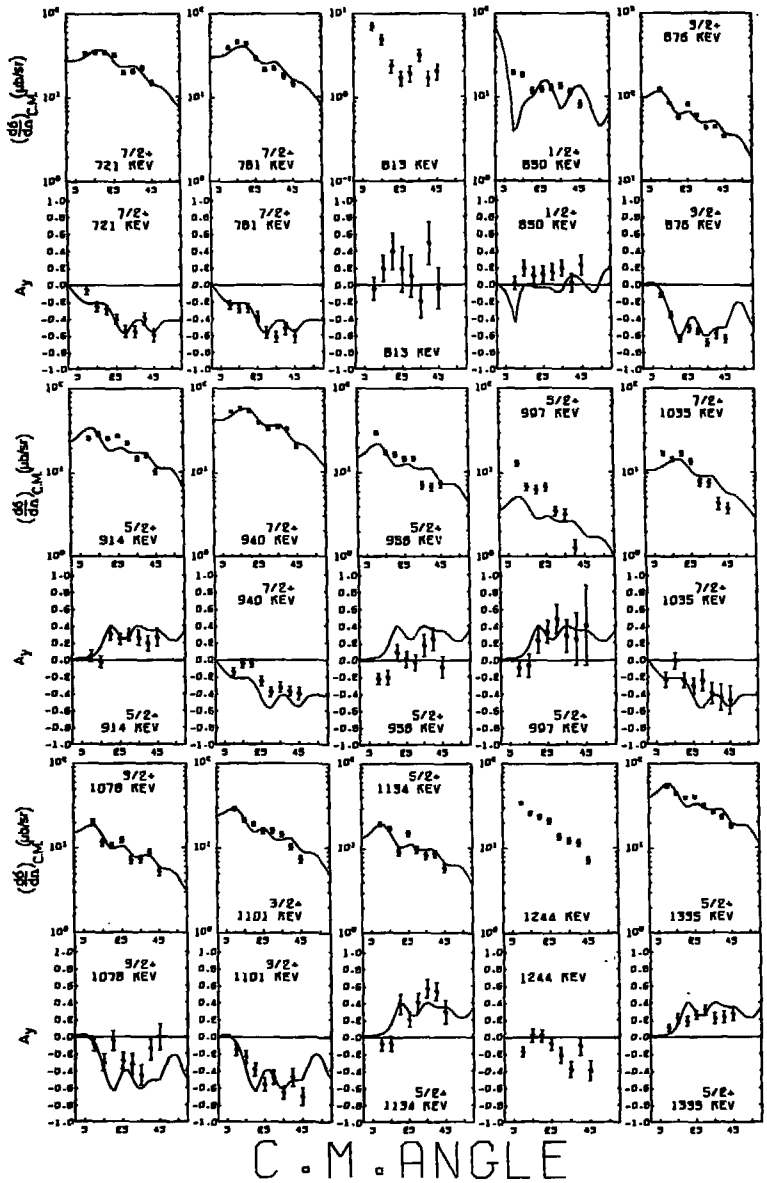
7/2+ 721 KEV
7/2+ 781 KEV
813 KEV
1/2+ 850 KEV
3/2+ 876 KEV
5/2+ 914 KEV
7/2+ 940 KEV
5/2+ 958 KEV
5/2+ 997 KEV
7/2+ 1035 KEV
3/2+ 1078 KEV
3/2+ 1101 KEV
5/2+ 1134 KEV
1244 KEV
5/2+ 1335 KEV
A_y
C.M. ANGLE

Fig. 4b.

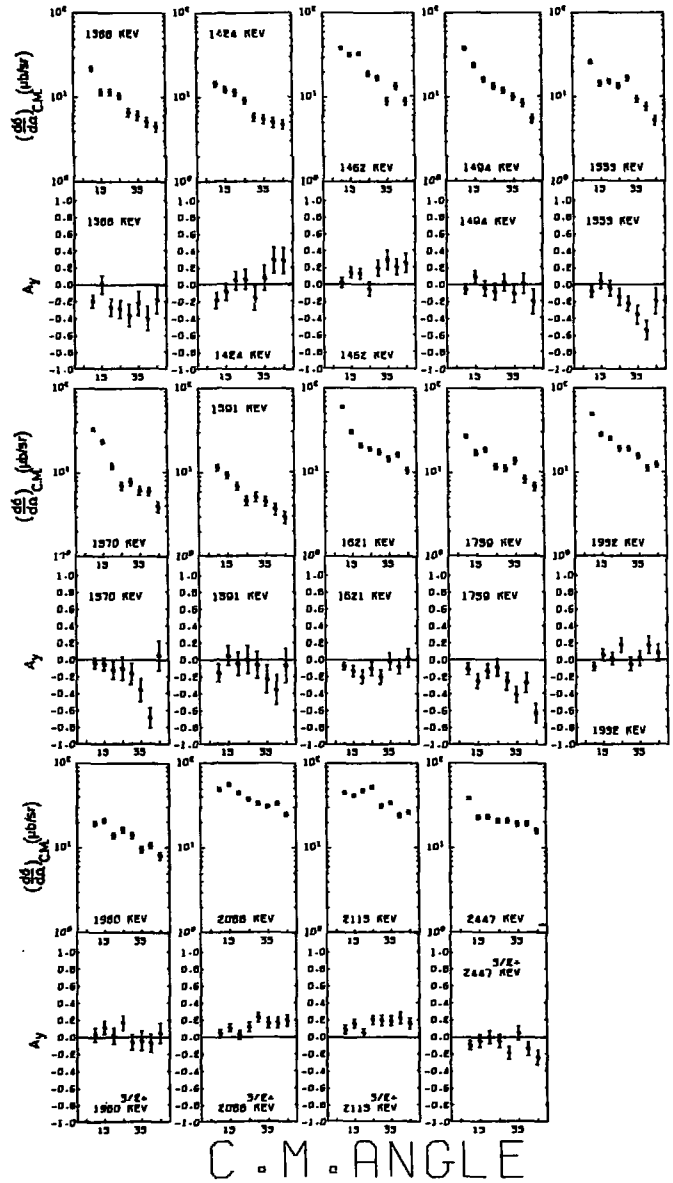


Fig. 4c.

**Fig. 4. Angular distributions of $(\vec{t}, \alpha)$ cross sections and analyzing powers for levels populated in $^{151}$Pm. See caption to fig. 3. The solid curves represent DWBA calculations for the $l^{\pi}$ values given.**

taken into account. As in the previous studies [5–9]) the mixing calculation was intended to show typical effects of the Coriolis interaction only, with little adjustment of possible parameters to obtain the best fit.

With this in mind, most of the input parameters were given values typical of those used in previous studies of other nuclides in this mass region, and these parameters were not varied. The Nilsson calculation was performed with $\kappa = 0.0637$ and $\mu = 0.600$ as recommended by Lamm [13]), and the deformation was assumed to be $\delta = 0.2$. The pairing gap parameter was chosen to be $\Delta = 950$ keV, and the Fermi surfaces in the $^{152}$Sm and $^{150}$Nd targets were assumed to be 200 keV above and 200 keV below the $\frac{5}{2}^+[413]$ orbital, respectively.

In the neighbouring isotope $^{153}$Pm a reasonable description of the experimental data was obtained with a rotational parameter $\hbar^2/2\mathcal{F} = 12$ keV and an attenuation factor 0.75 for the Coriolis matrix elements for both positive and negative parity states. In the present study it was necessary to do more adjustments to these parameters to obtain the same quality in the fit. For the $N = 4$ positive parity states the same attenuation factor of 0.75 was used while the rotational parameters for the various bands had to be varied individually in the region of 12.3 to 16.9 keV. For the negative parity $h_{\frac{11}{2}}$ states a rotational parameter of 19.3 keV had to be used along with an attenuation factor of 0.62.

### 3.2. THE LOW-LYING ROTATIONAL BANDS

The $\frac{5}{2}^+[413]$, $\frac{5}{2}^-[532]$ and $\frac{3}{2}^+[411]$ bands have been assigned in earlier studies [1, 2]), and the present results are consistent with the previous interpretation. These Nilsson orbitals originate from the $g_{\frac{7}{2}}$, $h_{\frac{11}{2}}$ and $d_{\frac{3}{2}}$ shell-model states, respectively, and therefore the three dominant peaks in the low excitation region of the spectra correspond to states with $I^\pi = \frac{7}{2}^+$ (85 keV), $\frac{11}{2}^-$(345 keV) and $\frac{3}{2}^+$(325 keV). The (t, α) angular distributions of cross sections and analyzing powers shown for these strong transitions in fig. 4a are in very good agreement with DWBA predictions. The bandhead of the $\frac{3}{2}^+[411]$ orbital is obscured in the (t, α) reaction by the more strongly populated $\frac{9}{2}\,\frac{5}{2}^-[532]$ level. In the ($^3$He, d) reaction, however, the angular distribution to the 257 keV level exhibits a typical $l = 2$ pattern (compare figs. 3a and 4a).

Fig. 1 shows a tentative assignment for the $\frac{15}{2}$ member of the $\frac{5}{2}^-[532]$ band. Levels with $j > N+\frac{1}{2}$ (where $N$ is the principal oscillator number) should not be populated directly in single-nucleon transfer reactions, but they are frequently observed, probably as a result of multiple processes in the reaction (e.g. ref. [7])). In the present study the level found at ~ 593 keV has the energy expected for the $\frac{15}{2}$ member of the $\frac{5}{2}^-[532]$ band. This alone would not be a strong argument for suggesting this assignment, but in similar (t, α) studies [7, 9]) in the europium isotopes there are peaks with about the same intensities and analyzing powers as these, which occur at energies predicted by the $I(I+1)$ rule for the $\frac{15}{2}$ states. The angular distributions of the 593 keV level (fig. 4a) cannot be reproduced by a simple one step

DWBA calculation. It should also be mentioned that the angular distributions are very similar to those observed for the same suggested levels in previous studies of the europium isotopes [7,9]).

An examination of the results shown in table 2 indicates that the Nilsson model, with pairing and Coriolis effects included, satisfactorily explains the data available for these three bands.

### 3.3. THE $\frac{1}{2}^+[420]$ ORBITAL

On the basis of the earlier ($^3$He, d) and (t, $\alpha$) data it was suggested [1]) that the peak corresponding to the $\frac{7}{2}$ $\frac{3}{2}^+[411]$ level at $\sim$ 426 keV was actually an unresolved doublet. This suggestion was confirmed by decay studies [2]) in which the other member of the doublet was given a tentative $I^\pi = \frac{1}{2}^+$ assignment. Seo [2]) has also proposed that the levels at 426.43, 524.32 and 507.85 keV may be the $I = \frac{1}{2}$, $\frac{3}{2}$ and $\frac{5}{2}$ members, respectively, of the $\frac{1}{2}^+[420]$ band.

The present results provide strong confirmation of this proposed band. The ($^3$He, d) angular distribution (fig. 3) for the $\sim$ 428 keV doublet exhibits a characteristic $l = 0$ shape, indicating that the level which is not resolved from the $\frac{7}{2}$ $\frac{3}{2}^+[411]$ state must have $I^\pi = \frac{1}{2}^+$. The (t, $\alpha$) angular distribution (fig. 4) is seen to have a prominent maximum at $\theta = 15°$, as was observed for the $\frac{1}{2}^+[420]$ bandhead in a number of neighbouring nuclides [6,7,9]). The angular distributions for the 508 keV level indicate $I^\pi = \frac{5}{2}^+$ for this level and the large strength in the pickup reaction provides a strong argument for the $\frac{5}{2}$ $\frac{1}{2}^+[420]$ assignment. Although the (t, $\alpha$) strength observed for the $\frac{5}{2}$ $\frac{1}{2}^+[420]$ level is quite large, it is nevertheless significantly smaller than the value expected for the pure Nilsson state. However, the results of the Coriolis mixing calculation shown in table 2 indicate that this reduction can be attributed to Coriolis mixing, primarily with the lower-lying $\frac{5}{2}$ $\frac{3}{2}^+[411]$ state.

The $I^\pi = \frac{3}{2}^+$ band member [2]) at 524 keV is expected to be very weakly populated in these reactions and was not observed. Small peaks may have been present in the spectra, but would have been obscured by larger peaks due to the 529 keV level. The $I^\pi = \frac{7}{2}^+$ level, observed in the (t, $\alpha$) data at 721 keV, has appropriate excitation energy and strength to be attributed to the $\frac{1}{2}^+[420]$ band also.

The level spacings and relative strengths observed for this band are similar to those found in several neighbouring nuclides [6,7,9]). The excitation energy also fits very well into the systematic trend which has been shown for this orbital in ref. [9]).

### 3.4. THE $\frac{1}{2}^+[411]$ ORBITAL

On the basis of ($\alpha$, t) and ($^3$He, d) cross section ratios it was previously proposed [1]) that the 851 keV level had $l = 0$ character and a tentative $\frac{1}{2}$ $\frac{1}{2}^+[411]$ assignment was suggested. The ($^3$He, d) angular distribution (fig. 3) confirms the $l = 0$ nature of

this level, which is apparently not the same one assigned as $I^\pi = \frac{5}{2}^+$ at 852.92 keV by Seo [2]. The characteristic angular distributions in figs. 3 and 4 indicate an $I^\pi = \frac{3}{2}^+$ assignment for the 876 keV level, which may be the same one that was reported at 874.70 keV by Seo [2]. The $\frac{3}{2}\frac{1}{2}^+[411]$ state is the only one expected to have such a large $\frac{3}{2}^+$ stripping strength in this region. The weakly populated levels at $\sim$ 988 and 1035 keV are candidates for the $\frac{5}{2}^+$ and $\frac{7}{2}^+$ members of this band. It is seen in table 2 that the observed stripping strengths for this band are smaller than the predicted values. This was also pointed out earlier [1]) and attributed to possible mixing with $K = \frac{1}{2}$ gamma vibrational levels based on the $\frac{5}{2}^+[413]$ and $\frac{3}{2}^+[411]$ states. Seo has also noted [2]) that the decay characteristics of the 874.70 keV level may indicate vibrational character. Now that additional rotational members have been assigned it is noted that the decoupling parameter for this band is approximately $a = -0.5$, compared with values of $-0.7$ to $-1.0$ for the "pure" $\frac{1}{2}^+[411]$ state in heavier rare earth nuclei and $a \sim 0$ which is typical of $K = \frac{1}{2}$ gamma vibrations. Thus all the evidence is consistent with the observed band being a mixture of a vibrational and single-particle state, containing a large component ($\geqq$ 50 %) of the $\frac{1}{2}^+[411]$ orbital.

### 3.5. THE $\frac{1}{2}^+[404]$ ORBITAL

The level at 781 keV has an angular distribution suggesting an $l$-value of 4 or 5, and was previously [1]) given a tentative $\frac{11}{2}^-$ assignment. However, the analyzing power (see fig. 4b) clearly shows that this assignment was incorrect, and suggests that this level is rather the band head of the $\frac{7}{2}^+[404]$ Nilsson orbital. This interpretation is also found to conform very nicely with the systematics of the $\frac{7}{2}^+[404]$ orbital in this mass region [14]).

### 3.6. THE $\frac{5}{2}^+[402]$ STRENGTH

Strong $l = 2$ transitions are observed in the stripping reactions for levels at 913 and 956 keV (fig. 3a). Both levels are also populated in the $(\vec{t}, \alpha)$ process, and the 913 level can be given a $\frac{5}{2}^+$ assignment based on the angular distributions (see fig. 4b) in agreement with the previous studies [2]). The situation is not so clear for the 956 keV level, but a $\frac{5}{2}^+$ assignment is favoured. The $\frac{5}{2}^+[402]$ orbital is the only one expected to have a large $I^\pi = \frac{5}{2}^+$ strength in this region of excitation energies above the Fermi surface. It thus appears that the $\frac{5}{2}^+[402]$ strength is fragmented and distributed over at least these two levels. The ($^3$He, d) nuclear structure factors for the 913 and 956 levels add up to 0.45, which is about 60 % of the strength expected for the $\frac{5}{2}\frac{5}{2}^+[402]$ state.

In a recent study [7]) of $^{155}$Eu a similar fragmentation of the $\frac{5}{2}^+[402]$ strength was observed.

### 3.7. THE $\frac{3}{2}^+[422]$ ORBITAL

The level at 940 keV has angular distributions of $(\vec{t}, \alpha)$ cross sections and analyzing powers shown in fig. 4b which indicate $I^\pi = \frac{7}{2}^+$. After the $\frac{5}{2}^+[413]$ band discussed above, the next Nilsson hole state which originates from the $g_{\frac{7}{2}}$ shell is the $\frac{3}{2}^+[422]$ orbital. As the 940 keV level appears to be the lowest one above the $\frac{7}{2}$ $\frac{3}{2}^+[413]$ state which has appreciable $\frac{7}{2}^+$ strength in the $(\vec{t}, \alpha)$ reaction, it is given a tentative $\frac{7}{2}$ $\frac{3}{2}^+[422]$ assignment. Previously [2]), a level was known at 841 keV with a spin assignment of $\frac{3}{2}^+$ or $\frac{5}{2}^+$. This level is situated at an energy predicted by the Coriolis calculation for the $\frac{5}{2}$ member of the band. It is expected to be weakly populated, and has not been observed in the present experiment. In ref. [2]) this level was given a tentative $\frac{3}{2}^+$ assignment. The spectroscopic strength for the proposed $\frac{7}{2}^+$ member is only 60 % of the predicted value (table 2). This is comparable to the situation observed in neighbouring nuclides [6,7]).

### 3.8. THE $\frac{3}{2}^-[541]$ ORBITAL

The strongly populated level at 642 keV has cross sections and analyzing powers characteristic of $I = \frac{11}{2}^-$ (see fig. 4a). After the $\frac{5}{2}[532]$ band the $\frac{3}{2}^-[541]$ orbital is the next one which is expected to have significant $\frac{11}{2}^-$ hole strength. Thus the 642 keV level (as suggested by refs. [1,2]) could be assigned as the $\frac{11}{2}$ $\frac{3}{2}^-[541]$ state although it is severely Coriolis coupled to the other orbitals from the $h_{\frac{11}{2}}$ shell. This assignment is consistent with the ($^3$He, d) angular distribution (see fig. 3a). The $(\vec{t}, \alpha)$ and ($^3$He, d) data for the 529 keV level are consistent with a $\frac{7}{2}^-$ assignment, as can be seen in figs. 3a and 4a, although the strength is larger than expected. However, the features observed in the $(\vec{t}, \alpha)$ data for this band strongly resemble those of the neighbouring $^{153}$Pm isotope [6]).

It was suggested by Seo [2]) that the $\frac{3}{2}$, $\frac{5}{2}$ and $\frac{7}{2}$ members of this band are situated at 540.3, 577.4 and 532.0 keV respectively, consistent with the present interpretation.

### 3.9. OTHER LEVELS

A level at 1200 keV was observed in the ($^3$He, d) and (α, t) reactions [1]) with a population pattern similar to the 641 keV level which has been given a $\frac{11}{2}^-$ assignment. The 1200 keV level has therefore been given a tentative $\frac{11}{2}$ $\frac{7}{2}^-[523]$ assignment since this is the next Nilsson orbital with particle nature to be expected in the spectrum.

Above 1200 keV the levels could not be classified in terms of the Nilsson model, although spins or $l$-values have been inferred in a number of cases from the experimental angular distributions. One may notice that most of the strength is located in $l = 0$ or $l = 2$ transitions (see figs. 1 and 2). A coupling of the γ-vibration to the lower-lying positive parity states would produce several $K = \frac{1}{2}$ bands that could drain spectroscopic strength from the high-lying $s_{\frac{1}{2}}$ state. Similar coupling phenomena were observed in the heavier holmium isotopes [14]).

## 4. Concluding remarks

The new experimental data presented in this work have made it possible to extend the interpretation of $^{151}$Pm levels considerably. The previous [1,2]) assignments of the $\frac{5}{2}^+[413]$, $\frac{5}{2}^-[532]$, $\frac{3}{2}^+[411]$ and $\frac{1}{2}^+[420]$ orbitals have been confirmed, and in addition assignments have been made for the $\frac{1}{2}^+[411]$ and $\frac{7}{2}^+[404]$ orbitals. Tentative assignments have been suggested for several other states.

The availability of the angular distributions in both pick-up and stripping reactions proved very valuable in interpreting the experimental spectra. It is interesting to notice how well the simple Nilsson model accounts for the majority of the observed features in a nucleus so close to the transitional region. A comparison of experimental and calculated energies and nuclear structure factors is shown in table 2. One may notice that the agreement with the experimental data is generally improved when coupling effects are taken into account. Particularly interesting is the result of the coupling between the $\frac{5}{2}^+$ states in the $\frac{3}{2}^+[411]$ and $\frac{1}{2}^+[420]$ bands.

As pointed out in subsects. 3.6 and 3.9 a severe fragmentation of $l = 0$ and $l = 2$ strength is observed for the higher levels. This fragmentation cannot be explained in the simple Nilsson model picture, but may require a model which includes both rotational and vibrational degrees of freedom.

In the neighbouring $^{153}$Pm isotope the $h_{\frac{11}{2}}$ Nilsson orbitals were well described when the Coriolis couplings were taken into account [6]). The $\frac{5}{2}^-[532]$ orbital constituted the ground state band in $^{153}$Pm. In $^{151}$Pm, however, the ground state is found to be $\frac{5}{2}^+[413]$, and the low-lying $\frac{5}{2}^-[532]$ orbital is expected to be a particle state. This is consistent with $^{151}$Pm having a smaller deformation than $^{153}$Pm. In spite of this, the pick-up strength to the $\frac{11}{2}$ member of this band is significantly larger in $^{151}$Pm (1.7) than in $^{153}$Pm (1.1), indicating strong Coriolis couplings to the $\frac{3}{2}^-[541]$ and $\frac{1}{2}^-[550]$ bands in $^{151}$Pm. This is also reflected in the irregular energy spacings in the $\frac{5}{2}^-[532]$ band in $^{151}$Pm. The results of the calculation presented in table 2 give a good description of the low-lying $\frac{5}{2}^-[532]$ band, but fails to account for the experimental energy spacing in the $\frac{3}{2}^-[541]$ band. This is somewhat surprising as this energy spacing is very similar to the one observed in $^{153}$Pm and was well reproduced by a similar coupling calculation there [6]). However, in $^{151}$Pm the $\frac{3}{2}^-[541]$ bandhead is located at about 500 keV excitation, rather close to the $\frac{5}{2}^-[532]$ orbital with which it mixes strongly, while the separation of these two orbitals is $\sim$ 1 MeV in the $^{153}$Pm isotope. Thus the coupling effects may be harder to describe in the calculation performed for $^{151}$Pm.

Seo has assigned [2]) the 773.6 and 746.5 keV levels as the $\frac{1}{2}^-$ and $\frac{3}{2}^-$ members of the $\frac{1}{2}^-[550]$ band. These levels are not expected to be strongly populated in the present study but the $\frac{7}{2}$ and $\frac{11}{2}$ members should have observable strengths. The band is expected to be seriously perturbed by the large decoupling parameter but the $\frac{7}{2}$ and $\frac{11}{2}$ members are predicted to be within $\pm 200$ keV of the bandhead (see table 2). Such levels have not been observed and therefore the assignments of Seo [2]) have

not been supported by the present results. In the Coriolis calculation of table 2 the $\frac{1}{2}^-[550]$ bandhead was arbitrarily located at an excitation energy of 1400 keV, similar to that assumed in the $^{153}$Pm study [6]).

The authors are very grateful to R. Hardekopf and L. Morrison for operating the polarized triton source and to S. Orbesen for assistence with the Q3D spectrometer and helix detector. Y. Peng is also thanked for preparing the targets used in these experiments. The cooperation of the operations personnel at both the Los Alamos and McMaster accelerator laboratories is highly appreciated. The visits and exchanges which made this collaborative effort possible were financed by a research grant from the Scientific Affairs Division of NATO.

## References

1) D. G. Burke and J. C. Waddington, Nucl. Phys. **A193** (1972) 271
2) T. Seo, T. Hayashi and T. Mitamura, J. Phys. Soc. Japan **34** (1973) 1443; T. Seo, Nucl. Phys. **A282** (1977) 302
3) E. R. Flynn, R. A. Hardekopf, J. D. Sherman, J. W. Sunier and J. P. Coffin, Nucl. Phys. **A279** (1977) 394
4) C. R. Hirning, D. G. Burke, E. R. Flynn, J. W. Sunier, P. A. Schmelzbach and R. F. Haglund, Jr., Nucl. Phys. **A287** (1977) 24
5) G. Løvhøiden, D. G. Burke, C. R. Hirning, E. R. Flynn and J. W. Sunier, Nucl. Phys. **A303** (1978) 1
6) D. G. Burke, G. Løvhøiden, E. R. Flynn and J. W. Sunier, Phys. Rev. **C18** (1978) 693
7) D. G. Burke, G.Løvhøiden, O. Straume, E. R. Flynn and J. W. Sunier, Can. J. Phys., in print
8) G. Løvhøiden, D. G. Burke, E. R. Flynn and J. W. Sunier, Nucl. Phys. **A315** (1979) 90
9) D. G. Burke, G. Løvhøiden, E. R. Flynn and J. W. Sunier, Nucl. Phys., accepted for publication
10) S. D. Orbesen, J. D. Sherman and E. R. Flynn, Los Alamos report LA-6271-MS (1975)
11) O. Straume, G. Løvhøiden and D. G. Burke, Nucl. Phys. **A266** (1976) 390
12) P. D. Kunz (1974), computer code DWUCK 4, unpublished
13) I. L. Lamm, Nucl. Phys. **A125** (1969) 504
14) J. D. Panar, O. Straume and D. G. Burke, Can. J. Phys. **55** (1977) 1657

# P A P E R IV

## SINGLE-PROTON STATES IN $^{149}$Pm

# Single-Proton States in $^{149}$Pm

O. Straume and G. Løvhøiden
University of Bergen, Bergen, Norway

D.G. Burke
Tandem Accelerator Laboratory[1]
McMaster University, Hamilton, Ontario, Canada L8S 4K1

E.R. Flynn and J.W. Sunier
University of California, Los Alamos Scientific Laboratory[2]
Los Alamos, New Mexico 87545, U.S.A.

[1]Financial support provided by the National Research Council of Canada

[2]Work performed under the auspices of the U.S. Department of Energy

Abstract

The $^{150}Sm(\vec{t},\alpha)^{149}Pm$ reaction was studied using 17 MeV polarized tritons from the tandem Van de Graaff accelerator at the Los Alamos Scientific Laboratory. The alpha particles were analyzed using a Q3D magnetic spectrometer and detected with a helical-cathode position-sensitive counter. The overall resolution was ~25 keV FWHM. In the present study many of the previous spin assignments have been confirmed, and some ambiguities in earlier studies have been resolved. The important levels at 416 and 751 keV that are strongly populated in the stripping reactions are shown to be $3/2^+$. Also new fragments of the $g_{7/2}$ and $d_{3/2}$ shell model states have been located. The deduced spectroscopic factors are compared to those measured in other promethium isotopes. It was found that the total (t,α) strength of the assigned peaks is stable within 15% for the chain of promethium isotopes ranging from mass number 147 to 153.

## 1. Introduction

A new investigation of the nuclear structure of $^{149}$Pm has been performed to study the systematics of single-proton states in the deformed rare earth region. The levels in $^{149}$Pm have previously been populated by the beta decay of $^{149}$Nd(1), by the ($^{3}$He,d) and (α,t) reactions (2), by the (p,α) and the unpolarized (t,α) reactions (3) and by the (p,nγ) reaction (4). As a result of these investigations several levels have been assigned spin and parity, but for the levels populated in the transfer reactions above an excitation energy of 400 keV only ℓ-values are known. Thus it is not possible to distinguish between fragments from the $d_{3/2}$ and $d_{5/2}$ states. Of particular interest is the 416 keV level which is strongly populated with an ℓ=2 transfer in the ($^{3}$He,d) reaction (2). Also it was noted that the summed ($^{3}$He,d) strength to assigned levels in $^{149}$Pm was somewhat smaller than observed in the heavier isotone $^{151}$Eu (2).

Therefore additional transfer data were needed to resolve some of the questions posed in the previous studies. A better understanding of the single particle states in this region becomes of increasing importance as one tries to explain the structure of nuclei near A=150 where there is a large change in the deformation.

It has recently been shown that the (t,α) reaction with polarized tritons is a very useful spectroscopic tool

for studying single-proton states, not only in the closed shell regions, e.g. near $^{208}$Pb (5), but also in well-deformed and transitional nuclei (6-9). The present investigation involves the application of the $(\vec{t},\alpha)$ reaction to the study of $^{149}$Pm.

## 2. Experimental Procedures and Results

Targets for the $^{150}$Sm$(\vec{t},\alpha)^{149}$Pm reaction were prepared from $Sm_2O_3$, isotopically enriched to 99.9% in $^{150}$Sm, purchased from the Isotope Sales Division of the Oak Ridge National Laboratory. The oxide was reduced to samarium metal by heating with thorium powder in a vacuum, and the metal was vacuum evaporated onto 30μg/cm$^2$ carbon foils. The target thickness for the $(\vec{t},\alpha)$ experiments was 100μg/cm$^2$.

The procedures used for the measurements and for the data analysis are similar to those described in a number of previous $(\vec{t},\alpha)$ studies (5-9) using the same apparatus.

The experiments were performed with beams of 17 MeV tritons having a polarization of 0.80 from the FN tandem Van de Graaff accelerator at the Los Alamos Scientific Laboratory. The alpha spectra were studied with a Q3D magnetic spectrometer equipped with a position-sensitive helical-cathode detector on the focal plane[10].

Spectra recorded with the incident tritons having spin "up" and spin "down" are shown in Fig. 1 for the $^{150}$Sm target. The resolution was typically 25 keV (FWHM).

Analyzing powers were extracted from the spin "up" and spin "down" intensities in the usual manner (5-9). Angular distributions of cross sections and analyzing powers for the various transitions are shown in Figs. 2a,b. The uncertainties in the absolute cross sections are believed to be about 20%. However the reproducibility of repeated measurements was usually within 5% and this is regarded as a realistic uncertainty when relative intensities are being considered in angular distributions. The error bars shown in Figs. 2a,b represent statistical uncertainties only.

The spectrometer was calibrated for the determination of excitation energies by recording spectra from the $^{152}Sm(t,\alpha)^{151}Pm$ reaction, using the known(11,12) level energies of $^{151}Pm$. The excitation energies obtained are listed in Table 1. The uncertainties in these energies should be 5 keV for levels up to 2.0 MeV.

In all experiments the intensities of spectra were converted to absolute cross sections through the use of a silicon semiconductor monitor counter of known solid angle in the target chamber to record elastically scattered beam particles. The elastic scattering cross section at $\theta=30^{o}$ for 17 MeV tritons on $^{150}Sm$ was taken to be 70% of the Rutherford value, a result obtained from the DWBA calculations.

These calculations for the (t,α) reaction were per-

formed with the computer program DWUCK 4 (13), using the same optical model parameters and the same value of N=23 that was used in some of the previous studies (8,9). Due to ambiguities in the choice of optical model parameters there are fairly large uncertainties, probably of the order of 30-50%, in the spectroscopic strengths obtained (8). However, a consistent set of optical model parameters was used so that relative spectroscopic strengths between isotopes are reliable. Experimental values of the spectroscopic factors are obtained by dividing the cross sections by $N\sigma_{DW}$. These strengths are listed in Table 1.

The experimental cross sections for the 17 MeV (t,α) reaction at $\theta=25^{o}$, as well as the $(\vec{t},\alpha)$ analyzing powers at $\theta=25^{o}$ are given in Table 1. Interpretations listed for the various levels are discussed in the following section.

## 3. Interpretation of the Results

The assignment of spins and parities for levels in $^{149}$Pm are discussed in section 3.1. These interpretations are based on previously available data as well as the $(\vec{t},\alpha)$ results from the present study. A discussion of the deduced spectroscopic factors is presented in section 3.2.

### 3.1.1 States Populated by ℓ=0 Transitions

DWBA-calculations for ℓ=0 transfers do not describe the experimental data in the $(\vec{t},\alpha)$ reaction (7-9).

Two levels previously (1) known to have spin and parity $1/2^+$ were populated at 390 and 909 keV in the $(\vec{t},\alpha)$ reactions. The angular distributions of the cross-sections and analyzing powers are displayed in Figs. 2a,b. The analyzing powers are quite structureless for these states, and the cross-section patterns are characterized by having a maximum at $\theta=15^o$. The level populated in the $(\vec{t},\alpha)$ reaction at 646 keV might correspond to the 636 keV level observed in $(^3He,d)$ and a tentative $1/2^+$ assignment proposed.

### 3.1.2 States Populated by $\ell$=2 Transitions

Fragments of the $d_{3/2}$ and $d_{5/2}$ states are expected to be found at low excitation energies, and will both be populated through $\ell$=2 transitions. Indeed many $\ell$=2 transitions are identified in the present experiment. Previously (1) the levels at 114 and 210 keV were known to have spin and parity $5/2^+$ and the level at 188 keV $3/2^+$. The present experiment confirms these spins and furthermore determines uniquely the spin of the levels at 420, 756, 1331, 1392 and 1648 keV to be $3/2^+$. A level at 425.3 keV with spin and parity $(5/2,7/2)^+$ has been reported (1,4), but was not located in the previous $(^3He,d)$ and $(\alpha,t)$ exposures (2). It is possible that the particle group observed at 420 keV in the present experiment contain some strength that should be associated with the 425.3 keV level. Angular distributions of cross sections and analyzing powers are displayed in Figs. 2a,b and the agreement between experiment and theory is indeed quite good. The evidence is not so clear for the states at 881 and 950 keV, but tentative $5/2^+$ assignments are proposed.

### 3.1.3 States with Higher Spin

The ground state of $^{149}$Pm was previously known to be $7/2^+$ and the angular distributions of both cross sections and analyzing powers of the present study are consistent with this assignment. In addition the levels at 360, 462 and 725 keV exhibit the patterns typical for $7/2^+$ and must be fragments of the $g_{7/2}$ shell model state. The level at 240 keV was previously known (2) to be $11/2^-$ which is confirmed by the present study, and in addition, new $11/2^-$ assignment are suggested for the levels at 556 and 795 keV.

In previous $(\vec{t},\alpha)$ studies (9) in this region a state with a characteristic angular distribution with a steep slope and a rather structureless analyzing power has tentatively been assigned as $15/2^-$. In the present study a similar state is found at 513 keV (Fig. 2b). Indeed in a recent $(p,n\gamma)$ study (4) a $(13/2^-, 15/2^-)$ assignment was given to a level at 510 keV. Also in the $(p,\alpha)$ reaction (3) a state at 513 keV was populated with an enhanced cross-section relative to the $(t,\alpha)$ cross-section to the same level. All these observations support a $15/2^-$ assignment to the level at 513 keV. The level at 272 keV was previously known to have spin and parity $7/2^-$. The analyzing powers of the present study confirm this assignment, but the angular distribution of the cross-sections is much steeper than the

DW-curve, also the (p,α) reaction shows a marked enhancement in the cross-section to this level, much similar to that observed for the 513 keV level discussed above. This might indicate that the indirect feeding of these levels can be quite important.

## 3.2 Spectroscopic strengths

The differential cross section for a pick-up reaction on an even-even target is given by

$$\frac{d\sigma}{d\Omega} = S_{\ell j} \, N \sigma_{\ell j}(\theta)_{DW} \qquad (1)$$

Measures of the spectroscopic strengths, $S_{\ell j}$, can thus be obtained simply by dividing the experimentally observed cross sections by the quantity $N\sigma_{\ell j}(\theta)_{DW}$. Spectroscopic strengths obtained in this manner are listed in Table 1.

In a shell-model basis one may consider the target nucleus $^{150}Sm$ as a system with 12 protons outside a Z=50 closed shell core. By summing the strengths $S_{\ell j}$ from the (t,α) reaction, one should get the average number of particles in the Z=50-82 shell for the $^{150}Sm$ target nucleus.

In the present experiment this sum does indeed amount to 12.3 in excellent agreement with the expected value of 12. As was pointed out in ref. 8, however, the values of $\sigma_{\ell j}(\theta)_{DW}$ are quite sensitive to the choice of optical model parameters for the (t,α) reaction. Therefore the extracted spectroscopic strengths will also depend on these parameters and it is rather fortuitous that the present choice of optical model parameters should yield this excellent agreement between calculated and measured spectroscopic strengths.

By summing the experimental strengths $\frac{d\sigma}{d\Omega}$ (exp)/$N\sigma_{\ell j}(\theta)_{DW}$ of all fragments of a shell model state "ℓj" one gets the average number of particles in that orbit and thus one gets a measure of the distribution of the valence protons among the shell model states forming the Z = 50-82 shell. This can be compared with the predictions of pairing theory following the procedure outlined in Ref. 14. This method was in $^{147}$Pm quite successful, especially for the particle states $h_{11/2}$ and $s_{1/2}$. In the present study, however, the filling of the particle states including the $d_{3/2}$ exceeds the expectations of the simple pairing model by more than a factor of two. This result of the present (t,α) study confirmes the findings from the previous ($^3$He,d) experiments (2) where the emptieness of the particle states in $^{149}$Pm was measured to be about a factor of two less than expected from a simple pairing model. Using the new spin assignments of the present work a revised version of the spectroscopic strengths obtained in the ($^3$He,d) reaction (2) has been obtained and is included in Table 1. For numbers given in parentheses the spin-value has not been measured and only the ℓ-value is known.

With the completion of the present study it is now possible to compare the (t,α) strength to fragments of the $h_{11/2}$, $g_{7/2}$, $d_{5/2}$ and $d_{3/2}$ states in promethium nuclei with mass number ranging from A=147 to A=153 (8,9,14). This comparison is shown in Figure 3 where the number associated with each level is the spectroscopic strength extracted as discussed above. It should be noted that the nucleus $^{147}$Pm has only been studied by an incomplete angular distribution of unpolarized (t,α), thus larger uncertainties should be associated with these spectroscopic factors. The numbers in brackets correspond to levels for which the spins have not been measured and only $\ell$-values are known. Finally for the deformed nuclei the Nilsson orbitals assigned to the various levels are also shown. To illustrate the general flow of the spectroscopic strength some levels are connected with dotted lines.

For the strongly populated $g_{7/2}$ hole state it is seen that the major part of its strength is connected to one level in $^{147}$Pm and $^{149}$Pm, and that a dramatic change occurs in going to the deformed nuclei $^{151}$Pm and $^{153}$Pm where the $g_{7/2}$ strength is observed to be distributed over many Nilsson orbitals.

For the $h_{11/2}$ particle state the situation is somewhat different in that the deformed regime seems to penetrate into the $^{149}$Pm nucleus, and only in $^{147}$Pm is the strength gathered into one state. Also the particle nature of this state is well displayed, in the spherical nucleus $^{147}$Pm the $h_{11/2}$ state is far above the fermi surface and is almost empty, while in the deformed case some of the fragments are found to be below the fermi surface and thus give larger spectroscopic factors in the pick-up reaction.

Only with the technique of the polarized (t,α) reaction has it become possible to distinguish fragments of the $d_{5/2}$ state from those of the $d_{3/2}$ state observed in transfer reactions. Examining the top half of Figure 3 it appears that for both $d_{5/2}$ and $d_{3/2}$ some strong coupling effects in $^{147}Pm$ distribute the strengths over many levels. Then in $^{149}Pm$ the $d_{5/2}$ strength is again concentrated in mainly one strong peak, while the $d_{3/2}$ is still split almost evenly into two peaks. Finally in the deformed nuclei the strength is distributed over the Nilsson orbitals, but still some peculiar coupling distributes the strength to the $5/2^+[402]$ orbital over several fragments (9). By summing the pick-up strengths to all known fragments of the four states $d_{3/2}$, $d_{5/2}$, $g_{7/2}$ and $h_{11/2}$ one obtains the numbers: 10.1 ($^{153}Pm$), 9.9 ($^{151}Pm$), 11.9 ($^{149}Pm$), 9.8 ($^{147}Pm$). This shows that although a quite marked redistribution of pick-up strengths occurs passing through this chain of Pm isotopes, the total strength of all assigned peaks remains quite stable with a variation of less than 15%. This is in contrast to the result obtained by Maher et al. (15) where it was reported that for the $^{152}Sm$ $(d,^3He)^{151}Pm$ reaction only 10% of the total strength in the other Pm isotopes was observed.

## 4. Summary and Conclusions

Levels in the N=88 nucleus $^{149}$Pm have been studied by the proton pick-up reaction $(\vec{t},\alpha)$. Previously this nucleus has been studied by radioactive decay and by proton stripping reactions. The present study confirms the spin assignment to many of the low lying states in $^{149}$Pm, and resolves some of the ambiguities in previous works. In particular the levels at 416 keV and 751 keV which were strongly populated by $\ell$=2 transitions in the stripping reactions are shown to have spin and parity $3/2^+$. In addition some new fragments of the $g_{7/2}$ and $d_{3/2}$ orbitals have been located. However, the main motivation for the present study was to probe the nuclear structure of transitional nuclei in the mass 150 region by measuring spectroscopic factors. Although the $^{149}$Pm nucleus could not be described in a spherical scheme, the present study shows no well-developed fingerprint patterns of rotational bands either. However, most of the Nilsson states which would be expected in this region, such as the $5/2^+[402]$ and $7/2^+[404]$ orbitals, have their strength concentrated in one j-value. Thus only one spin member would be strongly populated and the bands are difficult to identify. Furthermore, Nilsson orbitals originating from the $h_{11/2}$ shell model state would be strongly Coriolis coupled, resulting in a larger spectroscopic factor for the lowest $11/2^-$ level than would be expected for any single orbital by itself. The net result is that it can be difficult to distinguish between spherical

states and Coriolis coupled states of small deformations on the basis of cross sections to the strongly populated levels. To further investigate this a detailed calculation is planned based on the Nilsson model with pairing and Coriolis coupling included, and with a consistent treatment of the Nilsson parameters and the recoil term, a model which recently [16] has shown great success in describing transitional odd neutron nuclei.

A comparison of the (t,α) strengths to various fragments of shell model states in promethium isotopes from $^{147}$Pm to $^{153}$Pm has been performed. The total strength of all assigned peaks was found to be stable within 15% throughout this chain of Pm-isotopes.

The authors are indebted to R. Hardekopf and L. Morrison for operating the polarized triton source and to S. Orbesen for assistance with the Q3D spectrometer and helix detector. The co-operation of R. Woods and the operations personnel at Los Alamos was very important for the success of this experiment and is greatly appreciated. Thanks are also due to Y. Peng for preparing the target used in this experiment. Financial support in the form of a research grant from the Nato Scientific Affairs Division is gratefully acknowledged.

## References


1. Seo, T., Hayashi, T.: Nucl. Phys. A159, 494(970) Walters, W.B., private communication.
2. Straume, O., Løvhøiden, G., Burke, D.G.: Nucl. Phys. A266, 390(1976).
3. Shahabuddin, M.A.M., Waddington, J.C., Burke, D.G., Straume, O., Løvhøiden, G.: Nucl. Phys. A307, 239(1978)
4. Pakkanen, A.: private communication.
5. Flynn, E.R., Hardekopf, R.A., Sherman, J.D., Sunier, J.W., and Coffin, J.P.: Nucl. Phys. A279, 394(1977).
6. Hirning, C.R., Burke, D.G., Flynn, E.R., Sunier, J.W., Schmelzbach, P.A. and Haglund, R.F.: Jr. Nucl. Phys. A287, 24(1977).
7. Løvhøiden, G., Burke, D.G., Hirning, C.R., Flynn, E.R. and Sunier, J.W.: Nucl. Phys. A303, 1(1978).
8. Burke, D.G., Løvhøiden, G., Flynn, E.R. and Sunier, J.W.: Phys. Rev. C. 18, 693(1978).
9. Straume, O., Løvhøiden, G., Burke, D.G., Flynn, E.R., Sunier, J.W.: Nucl. Phys. A322, 13 (1979).
10. Orbesen, S.D., Sherman, J.D. and Flynn, E.R.: Los Alamos Report, LA-6271-MS (1975).
11. Burke, D.G. and Waddington, J.C.: Nucl. Phys. A193, 271(1972).
12. Seo, T., Hayashi, T. and Mithamura, T.: J. Phys. Soc. Jap. 34, 1443(1973).
13. Kunz, P.D.: Computer code DWUCK 4, unpublished (1974).

14. Straume, O., Løvhøiden, G. and Burke, D.G.: Z. Phys. A290, 67-80(1979).

15. Maher, J.V., Kamermans, R., Smits, J.W. and Siemssen, R.H.: Annual Report KVI Groningen, p. 28(1976).

16. Guttormsen, M., Osnes, E., Rekstad, J., Løvhøiden, G., Straume, O.: Nucl. Phys. A298, 122 (1978).

Table 1

## Levels populated in $^{149}$Pm

| Excitation energy (keV) | | Cross-section (μb/sr) | Assignment | | Spectroscopic strength | |
|---|---|---|---|---|---|---|
| Prev.[a] | (t,α) | (t,α) (θ=25) | Prev.[a] | (t,α) | (t,α) | ($^3$He,d)[a] |
| 0 | 0 | 325 | $7/2^+$ | $7/2^+$ | 3.2 | 1.8 |
| 114.3 | 114 | 483 | $5/2^+$ | $5/2^+$ | 2.1 | 2.2 |
| 188.6 | 188 | 16 | $3/2^+$ | $3/2^+$ | 0.07 | 0.043 |
| 211.3 | 210 | 9 | $5/2^+$ | $5/2^+$ | 0.05 | 0.084 |
| 240.2 | 240 | 268 | $11/2^-$ | $11/2^-$ | 2.8 | 4.8 |
| 270.1 | 272 | 44 | $7/2^-$ | $7/2^-$ | 0.16 | 0.34 |
| 360.0 | 360 | 32 | | $7/2^+$ | 0.35 | |
| 387.5 | 390 | 66 | $1/2^+$ | $1/2^+$ | 0.27 | 0.32 |
| 415.5 | 420 | 119 | $(3/2,5/2)^+$ | $3/2^+$ | 0.55 | 0.71 |
| 425.3 | | | $(5/2,7/2)^+$ | | | |
| 462.1 | ~462 | 5 | $3/2^-$ | $(7/2^+)$ | 0.05 | |
| 510.0 | 513 | 32 | $(13/2^-,15/2^-)$ | $(15/2^-)$ | | |
| 515.6 | | | $(9/2^-)$ | | | |
| 547.0 | | | $(5/2,7/2)$ | | | |
| 550 | 556 | 37 | $(\ell=5)$ | $(11/2^-)$ | 0.40 | 0.39 |
| 558.1 | | | $(7/2,9/2)$ | | | |
| 636 | ~646 | 8 | $1/2^+$ | $(1/2^+)$ | 0.02 | 0.090 |
| 650.8 | | | | | | |
| 721.4 | 725 | 43 | | $7/2^+$ | 0.43 | |
| 750.7 | 756 | 103 | $\ell=2$ | $3/2^+$ | 0.43 | 0.49 |
| 791.0 | 795 | 48 | $\ell=4,5$ | $11/2^-$ | 0.53 | 1.1 |
| 871 | 881 | 54 | $\ell=2$ | $(5/2^+)$ | 0.19 | 0.39 |
| 906 | 909 | 36 | $1/2^+$ | $1/2^+$ | 0.18 | 0.28 |
| 959 | 950 | 68 | | $(5/2^+)$ | 0.27 | |
| 1034 | | | $\ell=5$ | | | (0.65) |
| 1138 | | | $\ell=2$ | | | (0.4) |
| 1181 | | | $\ell=2$ | | | (0.11) |
| 1327 | 1331 | 35 | | $3/2^+$ | 0.15 | |
| 1394.3 | 1392 | 33 | | $3/2^+$ | 0.13 | |
| 1589 | | | $\ell=4$ | | | (0.32) |
| 1641 | 1648 | 33 | $\ell=2$ | $(3/2^+)$ | 0.14 | 0.38 |
| 1696 | | | $\ell=2$ | | | (0.15) |

a) Data from ref. 1-4. Only levels of interest to the present study are listed.

## Figure Captions

Fig. 1 Spectra from the $^{150}Sm(\vec{t},\alpha)^{149}Pm$ reaction for projectile spin "up" and "down". The numbers associated with the peaks are the excitation energies in keV.

Fig. 2a,b Angular distributions of $(\vec{t},\alpha)$ cross sections and analyzing powers for levels populated in $^{149}Pm$. The solid curves represent DWBA calculations for the $I^{\pi}$ values given. Error bars shown take into account statistical uncertainties only.

Fig. 3 Systematics for the $(t,\alpha)$ strength to the fragments of $d_{3/2}$, $d_{5/2}$, $g_{7/2}$ and $h_{11/2}$ in some promethium isotopes.

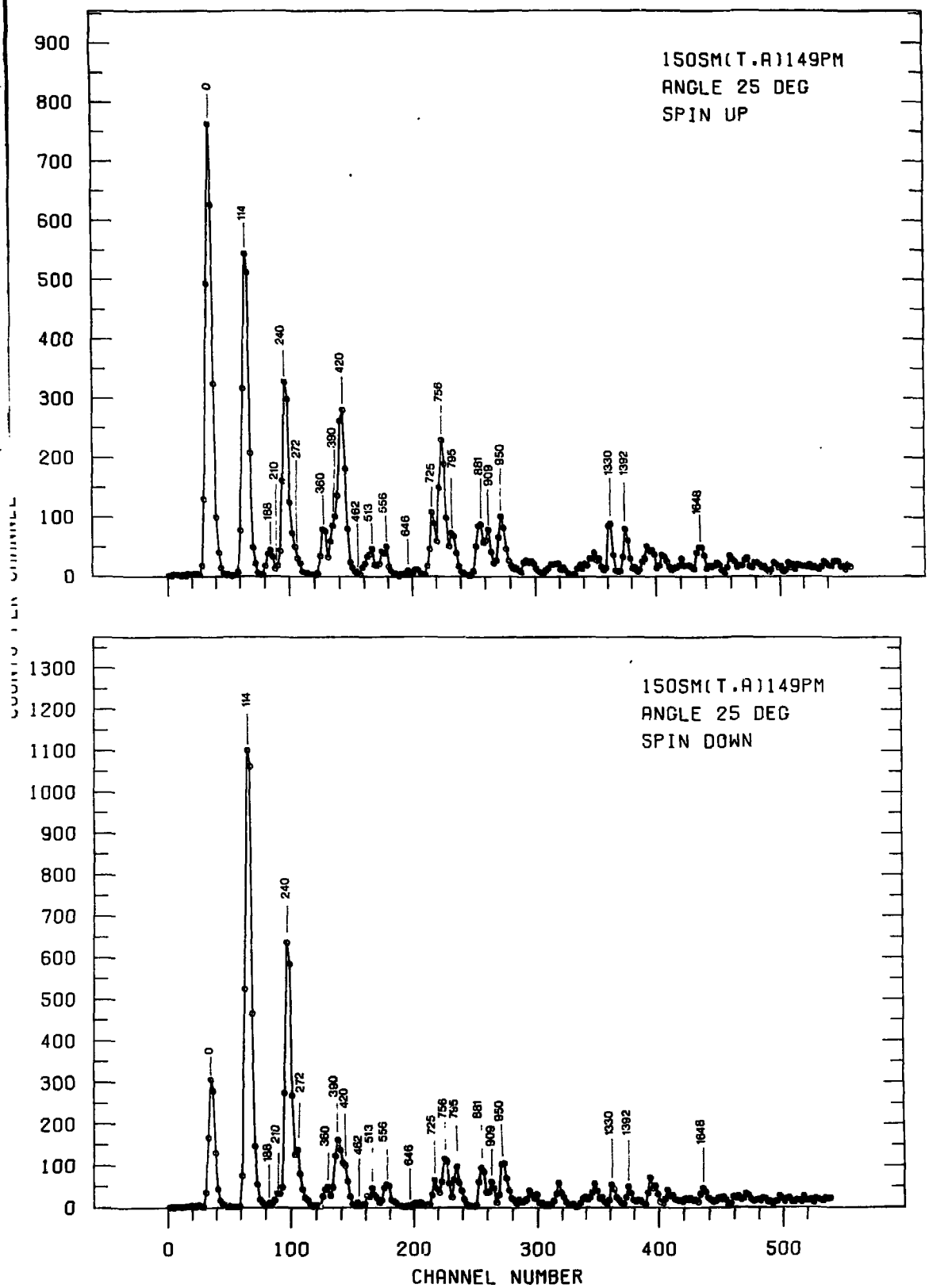
150SM(T,A)149PM
ANGLE 25 DEG
SPIN UP
150SM(T,A)149PM
ANGLE 25 DEG
SPIN DOWN
0
114
188
210
240
272
360
390
420
462
513
556
646
725
756
795
881
909
950
1330
1392
1648
CHANNEL NUMBER

Figure
1

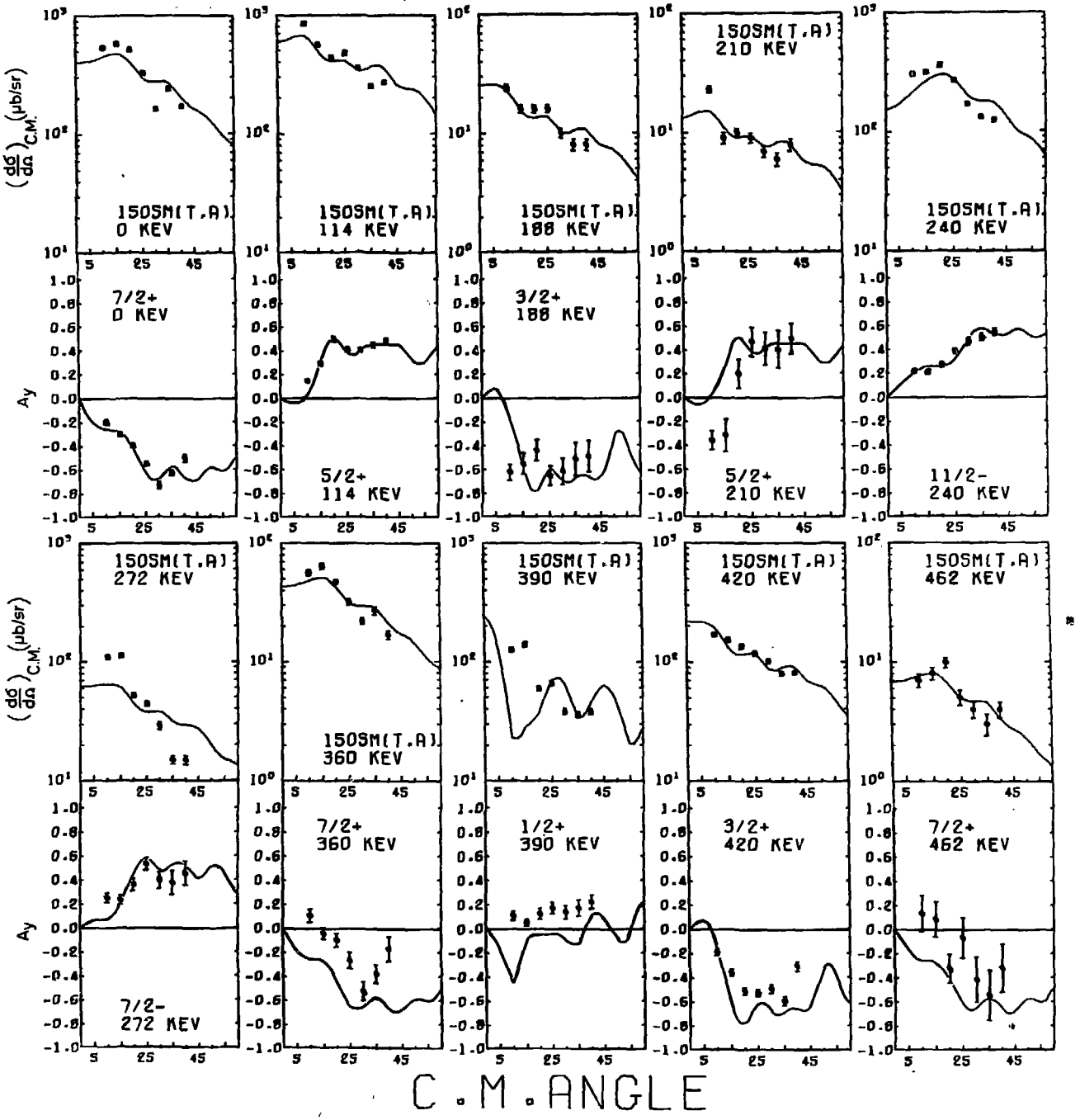
150SM(T,A)
0 KEV
7/2+
0 KEV
150SM(T,A)
114 KEV
5/2+
114 KEV
150SM(T,A)
188 KEV
3/2+
188 KEV
150SM(T,A)
210 KEV
5/2+
210 KEV
150SM(T,A)
240 KEV
11/2-
240 KEV
150SM(T,A)
272 KEV
7/2-
272 KEV
150SM(T,A)
360 KEV
7/2+
360 KEV
150SM(T,A)
390 KEV
1/2+
390 KEV
150SM(T,A)
420 KEV
3/2+
420 KEV
150SM(T,A)
462 KEV
7/2+
462 KEV
Ay
C.M. ANGLE

FIGURE 2A

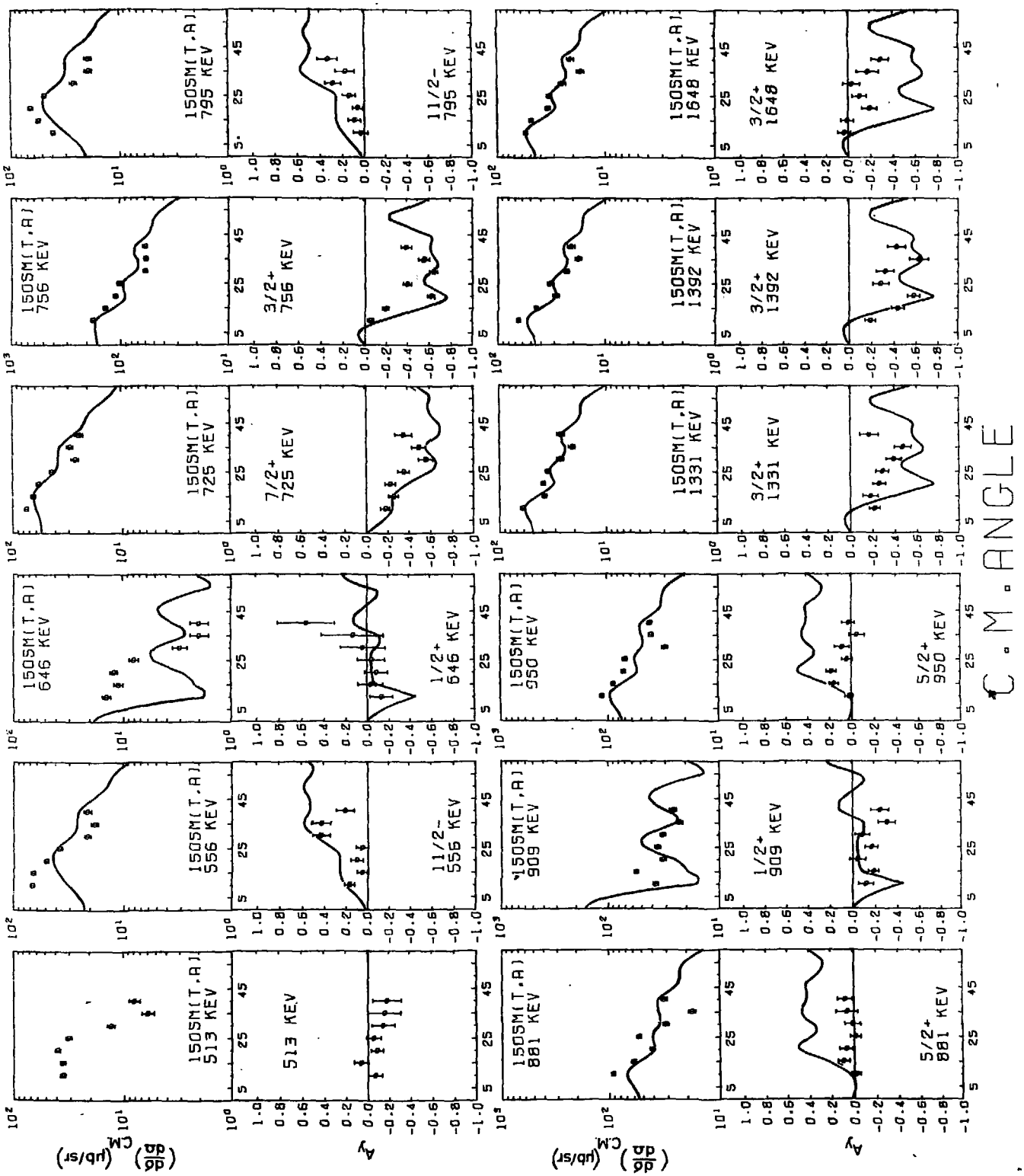
150SM(T,A)
513 KEV
11/2-
555 KEV
1/2+
646 KEV
7/2+
725 KEV
3/2+
756 KEV
11/2-
795 KEV
150SM(T,A)
881 KEV
1/2+
909 KEV
5/2+
950 KEV
3/2+
1331 KEV
3/2+
1392 KEV
3/2+
1648 KEV
5/2+
881 KEV
C.M. ANGLE

FIGURE 2B

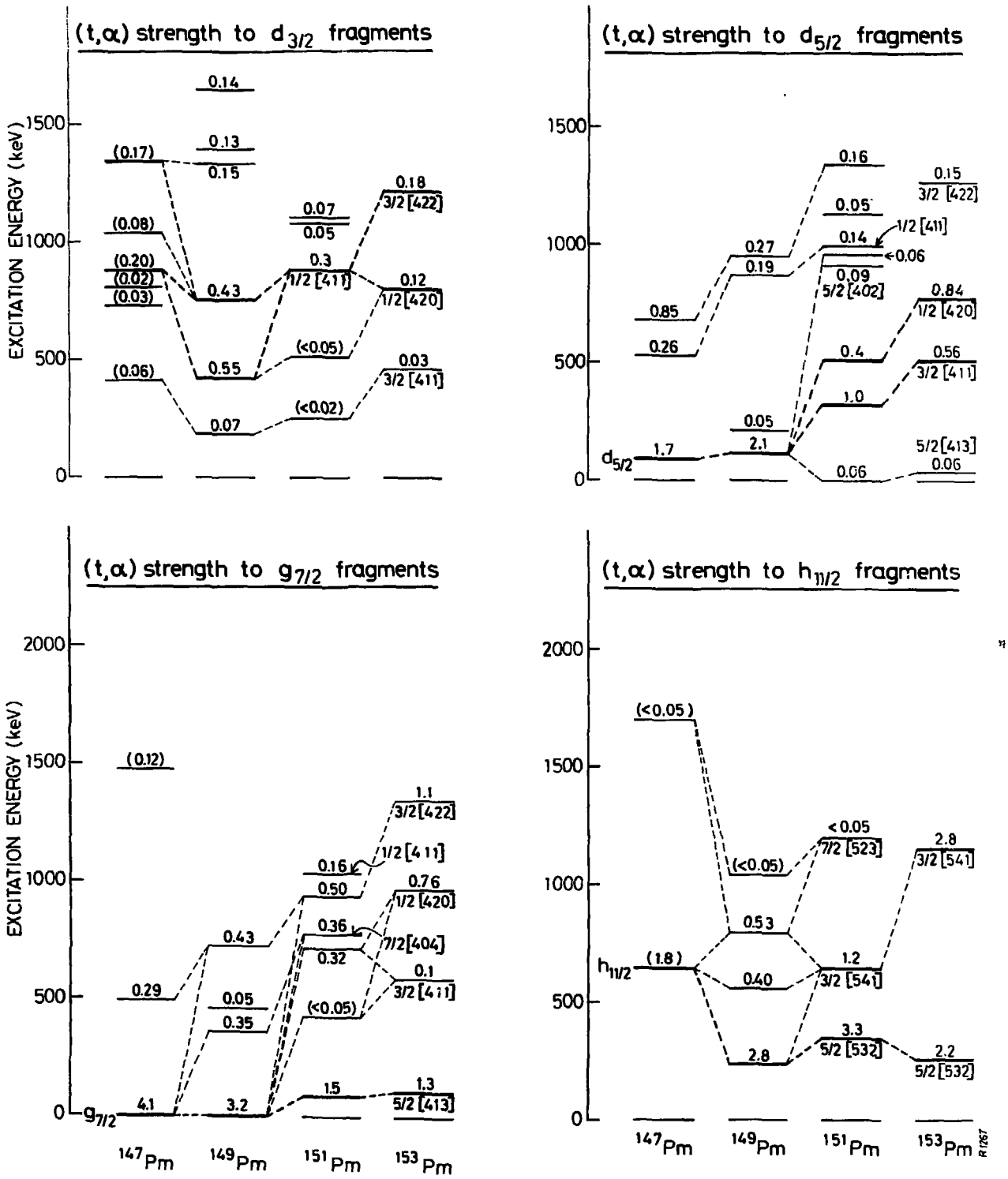
(t,α) strength to d3/2 fragments
(t,α) strength to d5/2 fragments
(t,α) strength to g7/2 fragments
(t,α) strength to h11/2 fragments
EXCITATION ENERGY (keV)
147Pm
149Pm
151Pm
153Pm
3/2 [422]
1/2 [411]
1/2 [420]
3/2 [411]
5/2 [413]
5/2 [402]
7/2 [523]
7/2 [404]
3/2 [541]
5/2 [532]

Figure
3

# P A P E R V

## PROTON STATES IN $^{143}$Pm AND $^{145}$Pm POPULATED IN THE ($^{3}$He,d) REACTION.

# Proton states in $^{143}$Pm and $^{145}$Pm Populated in the ($^{3}$He,d) Reaction.

O. Straume and G. Løvhøiden

University of Bergen, Bergen, Norway

and

D.G. Burke

McMaster University, Hamilton, Ont., Canada L8S 4K1

## Abstract

The ($^{3}$He,d) reaction on targets of $^{142}$Nd, $^{144}$Nd and on a target of natural Nd have been studied, using a beam of 24 MeV $^{3}$He from the McMaster University Tandem Van de Graaff accelerator. The reaction products were analyzed with an Enge type magnetic spectrograph and recorded on photographic emulsions. Information on the $\ell$-values was obtained from the ($^{3}$He,d) angular distributions In the $^{143}$Pm nucleus no fragmentation of the shell model strength was found while in $^{145}$Pm the fragmentation of the $d_{3/2}$ and $s_{1/2}$ states was significant, giving a total of 11 $\ell$=2 and 5 $\ell$=0 transitions. The results are analyzed in terms of the spherical shell model and the agreement with pairing theory is excellent in both cases. A survey of the stripping strength to promethium isotopes with mass numbers ranging from A=143 to A=151, is presented, using normalizations based on the results from the experiments on the target of natural neodymium.

## 1. Introduction.

In order to perform a systematic study of the fragmentation of the stripping strength to odd Z nuclei in the mass A=150 region, a project has been undertaken to investigate the ($^{3}$He,d) reaction on all available targets of even neodymium isotopes. This will yield information from an unbroken chain of isotopes ranging from the spherical case of $^{143}$Pm through the transitional region to the deformed nucleus $^{151}$Pm. Of particular interest is the study of the behavior of the intruder state $h_{11/2}$ as a function of neutron number. A similar study [1] of the $h_{11/2}$ neutron state in this region showed that the deformed characteristics of this state streched far into the transitional region and that the full shell model transfer strength was never obtained. In separate studies [2-4] results have been published for the isotopes $^{151}$Pm, $^{149}$Pm and $^{147}$Pm and the present work concludes this series of experiments with the presentation of the results from the ($^{3}$He,d) reaction into the $^{145}$Pm and $^{143}$Pm isotopes. Previously the $^{143}$Pm nucleus has been studied [5] by both particle transfer reactions and γ-ray work. Recently an extensive in beam γ-ray study of $^{145}$Pm has been published [6,7] but only incomplete data from transfer-reactions existed [6,7] prior to this study. The present series of experiments have all been performed in the same laboratory using the same equipment and under similar conditions in order to reduce the uncertainties in the measured relative cross sections and thereby improving the usefulness of the measured spectroscopic factors. As an additional check on the relative cross sections, separate ($^{3}$He,d) experiments were done with a target of natural neodymium.

In section 2-4, the results obtained from the present experiment are interpreted in the framework of the spherical shell model showing excellent agreement with pairing theory. A comparison of spectroscopic factors for promethium isotopes with mass numbers ranging from A=143 to A=151 are presented in section 5.

## 2. Experimental Details and Results.

The experiments were performed with a beam of 24 MeV $^{3}He$ from the McMaster University Tandem Van de Graaff accelerator giving typical beam currents of 1.5μA. The reaction products were analyzed with an Enge type magnetic spectrograph and detected with Kodak NTB50 nuclear emulsions. The resolution was typically ~18 keV FWHM (full width at half maximum). Targets of $^{142}Nd$ and $^{144}Nd$ were made from samples of $Nd_2O_3$ enriched to 97.55% in $^{142}Nd$ and 97.51% in $^{144}Nd$ respectively, as stated by the supplier, the Stable Isotopes Division of the Oak Ridge National Laboratory. The oxides were reduced with thorium metal and the enriched isotopes were vacuum evaporated onto 30μg/cm$^2$ carbon foils. The resulting target thickness for $^{142}Nd$ was ~110μg/cm$^2$ and for $^{144}Nd$ ~55μg/cm$^2$, as determined by elastic scattering measurements.

Absolute cross sections were determined by comparing the number of tracks in the peaks of the spectra with the numbers of elastically scattered particles detected by a semiconductor

monitor detector placed at $\theta=30^{o}$ in the scattering chamber. The cross-section for elastically scattered $^{3}He$ was determined from the distorted wave Born approximation (DWBA) calculations described below. As a separate check on the normalizations, six short exposures of elastically scattered particles were recorded at different times during the experiments with the spectrograph, on photographic plates. For these the monitor counter was used only to determine the ratio of "exposure-times" for the long and short runs. The absolute cross sections obtained in this manner agreed, within ±6%, with those determined using only the monitor counter and the known solid angles.

The ($^{3}He$,d) reactions were studied at ten angles for the enriched neodymium targets. Figure 1 shows representative spectra for these reactions. In Tables 1-2 are listed cross-sections, energies and assignments for levels populated in the enriched target experiments. Uncertainties in the energy measurements are estimated to be less than 3 keV and the relative cross-sections to large well resolved peaks have probable errors of ~10%. The angular distributions are shown in Figures 2-3 for states populated in $^{143}Pm$ and $^{145}Pm$ respectively. The solid lines represent results from DWBA calculations performed with the computer code DWUCK [8] using the same parameter set as in several previous studies in this region [2-4].

In an effort to obtain reliable relative cross-sections for the different Pm isotopes four exposures on a target of natural neodymium were also obtained. A spectrum at $\theta=65^{o}$ is shown in Figure 4 and resulting cross sections are plotted in Figure 5 where a comparison is presented to previous data obtained using isotopically enriched targets. The absolute normalization of the natural neodymium data has been chosen to fit the results from the $^{144}$Nd($^{3}$He,d) $^{145}$Pm angular distribution. It is gratifying to notice that this normalization also gives a good fit to the data from the other Pm-isotopes where no individual normalization is required other than knowledge of the isotopic composition of natural neodymium which is:
$^{142}$Nd (27.1%), $^{143}$Nd (12.6%), $^{144}$Nd (23.9%), $^{145}$Nd (8.3%), $^{146}$Nd (17.2%), $^{148}$Nd (5.7%) and $^{150}$Nd (5.6%).
With the present check on experimental cross-sections it is possible to obtain spectroscopic factors for levels in the chain of promethium isotopes studied with an experimental relative uncertainty of <10%. A systematic survey of trends in the spectroscopic factors will be presented in sect. 5.

An additional result from the $^{Nat}$Nd ($^{3}$He,d) exposures is an accurate determination of relative Q-values for these reactions. Whereas the measured absolute Q-values have uncertainties of ~30 keV, relative Q-values can be obtained to ±5 keV using the known calibration of the spectrograph. This information is presented in Table 3, and is consistent with previous data [9].

## 3. Interpretation of the $^{143}$Pm and $^{145}$Pm spectra.

The spectrum of $^{143}$Pm is mainly composed of the five peaks previously known [5] to be related to the shell model states: $d_{5/2}$ (0 keV), $g_{7/2}$ (273keV) $h_{11/2}$ (960keV), $s_{1/2}$ (1174 keV) and $d_{3/2}$ (1404). In addition to these, several weakly populated levels at higher excitation energies are observed in the ($^3$He,d) reaction. In particular the level at 1755 keV shows an angular distribution typical of $\ell$=0 transfer and the levels at 1614, 2277, 2331 and 2548 keV show angular distributions resembling that of $\ell$=2 transfer. (Figure 3).

In the $^{145}$Pm nucleus a quite significant fragmentation of the low spin states is observed. The $s_{1/2}$ strength is essentially split into two strongly populated levels at 728 and 1059 keV confirming the preliminary results of ref.6. In addition four weaker $\ell$=0 transitions are found populating the previously unknown levels at 1716, 1753, 1978 and 2112 keV.

Altogether two very strong transitions and seven weaker ones have the shape of an $\ell$=2 angular distribution . The strongest $\ell$=2 transition, feeding the previously known $d_{5/2}$ groundstate, gives a spectroscopic factor comparable to that of the $d_{5/2}$ groundstate in $^{143}$Pm, suggesting that most of the remaining $\ell$=2 strength observed in $^{145}$Pm populates fragments of the $d_{3/2}$ state. The second strongest $\ell$=2 transition is feeding a level at 960 keV. A $5/2^+$ assignment can probably be excluded on the basis of sum rules, and $3/2^+$ is proposed as the spin and parity for this level. It should be noted that in the (p,2n$\gamma$) study [6] a level at 958 keV was populated and given a tentative $5/2^+$ assignment. This would be compatible with the assignment adopted above if two closely spaced levels existed, one at 958 keV observed in (p,2n$\gamma$) and one at 960 keV observed in the transfer reactions.

The spectroscopic factor of the strong $\ell=2$ transition to the 960 keV level is only ~ 45% of that found for the $d_{3/2}$ state in $^{143}$Pm. This indicates a severe fragmentation of the $d_{3/2}$ strength in $^{145}$Pm and suggests on the basis of sum rules that most of the levels at 498, 773, 960, 1226, 1489, 1507, 2008 and 2289 keV, which are populated by $\ell=2$ transitions, can tentatively be given $3/2^+$ assignments. Of these levels only the one at 498 keV has previously [6] been assigned $3/2^+$.

The level at 60 keV was previously known [6] to have spin and parity $7/2^+$ and it is populated with a strength that is consistent with the results from $^{143}$Pm.

One level at 1386 keV shows an angular distribution pattern of $\ell=3$ even though the $f_{7/2}$ shell model state is situated above the Z=82 shell closure. In the (p,2nγ) study [6] a level at 1385 keV has been tentatively assigned $(7/2,9/2)^-$. Similar states populated through $\ell=3$ transitions were found at 973 keV in $^{147}$Pm and at 270 keV in $^{149}$Pm.

The strong $\ell=5$ transition to the 796 keV level carries ~ 80% of the $h_{11/2}$ strength as compared to $^{143}$Pm. The remaining 20% is probably located in a doublet at 1753 keV (see Figure 3). At forward angles this transition is dominated by $\ell=0$, but at back angles the trace of a higher $\ell$-value is clearly seen. Also in the (α,t) reaction this level is populated [6] with an intensity a factor of three larger than would be expected for a pure $1/2^+$ state. Under such conditions it is of course not possible to distinguish between $\ell=4$ and 5, but $\ell=5$ is preferred for the high spin component of this doublet, based on summed spectroscopic factors. A similar fragmentation of the $h_{11/2}$ strength was also observed in $^{147}$Pm.

## 4. Spectroscopic strengths.

For a stripping reaction on an even-even target the spectroscopic factor $S_{lj}$ is related to the experimental cross-section through the formula

$$d\sigma/d\Omega = S_{lj}\ (2j+1)\ N\sigma_{lj}\ (\theta)_{DW}$$

Spectroscopic factors obtained in this manner using a normalization N=6 [2-4] are listed in Table 1 and 2 for states in $^{143}$Pm and $^{145}$Pm respectively. By summing the strengths $S_{lj} \cdot (2j+1)$ one should get the number of holes in the Z=50→82 shell for the Nd target nuclei used in this investigation. Theoretically this number is 32-10=22. The levels in $^{143}$Pm and $^{145}$Pm for which ℓ-assignments can be given, account for 98.4% and 93.6% of the observed ($^{3}$He,d) cross section at $\theta=50^{o}$ up to an excitation energy of ~2.5 MeV. For these levels the experimental sums are 20.1 and 18.8 for $^{143}$Pm and $^{145}$Pm respectively. Adjusting these numbers in an approximate manner to take into account the unassigned peaks one gets 20.1/0.984 = 20.4 and 18.8/0.936 = 20.0. These results are well within experimental uncertainties and show a rather remarkable internal consistency.

By summing the spectroscopic factors $S_{lj}$ for all fragments of a shell model state "lj" one gets a measure the partial filling of that state. According to pairing theory one has to a first approximation $U^2_{lj} \simeq \Sigma S_{lj}$ where $U^2_{lj}$ is the emptiness of the orbital "lj". Following the method outlined in ref. [4] energy centroids and single particle energies are computed and listed in Table 4 along with summed spectroscopic strengths for the shell model states $g_{7/2}$, $d_{5/2}$, $h_{11/2}$, $s_{1/2}$ and $d_{3/2}$ in $^{143}$Pm and $^{145}$Pm. These numbers are based on the information given in

Tables 1 and 2 using an energy gap parameter $\Delta$=1100 keV as in ref.[4]. It should be noticed that the $d_{3/2}$ strength given also contains $\ell$=2 transitions for which the final spin has not been measured directly (see sect. 3).

A comparison to pairing theory is given in Figure 6 where the curved line represents the emptiness factor $U_{lj}^2$ as a function of single particle energy. The horizontal bars represent the shell model states and are plotted at energies ($\varepsilon$-$\lambda$) given in Table 4 obtained from the energy centroids $\bar{E}$, assuming the fermi level $\lambda$ to be at the ground state energy $\varepsilon_0$. The length of the bars represent spectroscopic strengths $\Sigma S_{lj}$ obtained from the ($^3$He,d) angular distributions. Agreement between experiment and theory would thus be obtained if the horizontal bars were just long enough to reach to the $U_{lj}^2$ curve. The agreement is quite satisfactory, and it is gratifying to notice how all the fragments in the $^{145}$Pm spectrum add up to the same general shell model scheme as in $^{143}$Pm. Figure 6 also shows quite clearly the energy gap in the middle of the Z=50 - 82 shell, supporting the idea of a subshell closure at Z=64 after the filling of the $d_{5/2}$ and $g_{7/2}$ orbitals [11].

## 5. Systematics and conclusions.

With the completion of the present experiments it is now possible to display in a systematic manner the trends of the spectroscopic strengths in promethium isotopes ranging in mass number from 143 to 151 as obtained by the ($^3$He,d) reaction. Furthermore the use of a natural neodymium target provides an internal check on experimental cross sections to states in the

various isotopes. Thereby the problems with the absolute normalization in each experiment are bypassed and it is possible to present experimental cross-sections and spectroscopic factors with relative accuracy better than 10%.

At first it is interesting to compare the summed strength to each isotope. This figure represents the number of holes in the neodymium targets and should thus be 22 for all the isotopes provided all the fragments have been identified in the spectra. This yields 20.4 ($^{143}$Pm), 20.0 ($^{145}$Pm), 20.7($^{147}$Pm), 17.7 ($^{149}$Pm) and 13.3 ($^{151}$Pm). In view of the rather dramatic changes in the fragmentation of the shell model states observed in the three lightest isotopes the total strength is remarkably constant. Also the reduction in strength that occurs in going to $^{149}$Pm can be traced to the $h_{11/2}$ orbital which in $^{147}$Pm accounts for a strength of 9.7 while in $^{149}$Pm it is only 7.0. The further reduction in strength observed in going to $^{151}$Pm is brought about by the static deformation of the $^{151}$Pm nucleus which scatters some of the fragments outside the range of our spectra. In this nucleus the reaction data [2] are adequately described in terms of the Nilsson model.

Contrary to what was found for the $h_{11/2}$ neutron hole state in this region, the $h_{11/2}$ proton particle state appears with the full strength expected from the shell model in the three lightest isotopes. In $^{149}$Pm it breaks into a pattern resembling that expected for a lightly deformed, strongly Coriolis coupled nucleus. Indeed the results from a recent (p, 2nγ) study [10] of $^{149}$Pm revealed a strongly perturbed rotational band based on the lowest lying $11/2^-$ state. And in $^{151}$Pm a well behaved rotational band based on the $5/2^-$ [532] Nilsson orbital is established. Thus the anomaly observed for the $h_{11/2}$ strength in odd neutron nuclei in this region is non -existing in odd proton nuclei.

The $^{143}Pm$ and $^{145}Pm$ nuclides have been studied for the first time with high resolution ($^{3}He$,d) angular distributions. Many new levels have been located and several assignments proposed for the first time, especially in $^{145}Pm$ which was poorly known prior to this study and the complementary (p, 2n$\gamma$) study of ref.6. In spite of the rather complex spectrum observed for the $^{145}Pm$ nucleus, energy centroids and summed spectroscopic factors were found to be almost identical to those in the spherical $^{143}Pm$ nucleus.

Acknowledgements:

Financial support in the form of operating grants from the National Sceince and Engineering Research Council of Canada is gratefully acknowledged.

## References


1) G.Løvhøiden, J.R.Lien, S.El-Kazzaz, J.B.Rekstad, C.Ellegaard, J.Bjerregaard, P.Knudsen and P.Kleinheinz, to be published.
J.Rekstad, G.Løvhøiden, J.R.Lien, S.El-Kazzaz, C.Ellegaard, J.Bjerregaard, P.Knudsen and P.Kleinheinz, to be published.

2) O.Straume, G.Løvhøiden, D.G.Burke, E.R.Flynn and J.W.Sunier, Nuc. Phys. A322 (1979) 13.

3) O.Straume, G.Løvhøiden and D.G.Burke, Nucl.Phys. A266 (1976) 390.
O.Straume, G.Løvhøiden, D.G.Burke, E.R.Flynn and J.W.Sunier, to be published (Z.Phys.).

4) O.Straume, G.Løvhøiden and D.G.Burke, Z.Phys. 290 (1979) 67.

5) Nuclear Data Sheets 25 (1978) 603.

6) R.G.Summers-Gill, private communication.
T.Shibata, Y.Nogai, M.Fujiwara, H.Ejiri, Nakanishi and S.Takeda, Nucl.Phys. A257 (1976) 303.
M.Piiparinen, M.Kortelahti, A.Pakkanen, T.Komppa and R.Komu, Research Report No. 6/1977, Dept. of Phys., University of Jyväskylä, Finland.

7) M.Kortelahti, Research Report No. 10/1979, Dept. of Phys., University of Jyväskylä, Finland.

8) P.D.Kunz, Computer code DWUCK, University of Colorado, unpublished, 1969.

9) N.B. Gove and A.H.Wapstra in Nucl.Data Tables 11(1972) 129.

10) M.Kortelahti, A.Pakkanen, M.Piiparinen, E.Hammarén, T.Komppa and R.Komu, Annual Report (1978) 85, Dept. of Physics, University of Jyväskylä, Finland.

11) P.Kleinheinz, S.Lunardi, M.Ogawa and M.R.Maier, Z.Phys. A284 (1978) 351.
P.Kleinheinz, M.Ogawa, R.Broda, P.J.Daly, D.Haenni, H.Beuscher and A.Kleinrahm, Z.Phys. A286 (1978) 27.

Table 1

## Levels populated in $^{143}Pm$

| Energy (keV) Prev.[a] | ($^3$He,d) | Cross section(μb/sr) ($^3$He,d) θ=50 | Assignment Prev.[a] | This exp. | $(2j+1)\,S_{lj}$ |
|---|---|---|---|---|---|
| 0.0 | 0 | 536 | $5/2^+$ | ℓ=2 | 2.99 |
| 272.1 | 273 | 44 | $7/2^+$ | ℓ=4 | 1.01 |
| 959.8 | 960 | 277 | $11/2^-$ | ℓ=5 | 11.1 |
| 1056.5 | 1056 | 18 | $3/2^+$ | ℓ=2 | 0.098 |
| 1173.1 | 1174 | 764 | $1/2^+$ | ℓ=0 | 1.51 |
| 1402.5 | 1404 | 778 | $3/2^+$ | ℓ=2 | 3.15 |
| 1614.1 | 1614 | 13 | (3/2, 5/2) | ℓ=2 | 0.046 |
| | 1755 | 26 | | ℓ=0 | 0.045 |
| 1942.5 | | | $(7/2, 9/2)^-$ | | |
| 1950.8 | 1950 | 23 | $9/2^-$ | | |
| | 2277 | 8 | | ℓ=2 | 0.031 |
| | 2331 | 24 | | ℓ=2 | 0.074 |
| | 2410 | 15 | | | |
| | 2469 | 10 | | | |
| | 2548 | 36 | | ℓ=2 | 0.098 |
| | 2712 | 17 | | | |
| | 2733 | 26 | | | |
| | 2747 | 11 | | | |
| | 2777 | 35 | | | |
| | 2864 | 21 | | | |
| | 2904 | 17 | | | |
| | 2956 | 28 | | | |

Table 1 cont.

Levels populated in $^{143}Pm$

| Energy (keV) Prev.[a] | Energy (keV) ($^3He$,d) | Cross section(μb/sr) ($^3He$,d) θ=50 | Assignment Prev.[a] | Assignment This exp. | $(2j + 1) S_{lj}$ |
|---|---|---|---|---|---|
| 3054 | 3057 | | 10 | | |
| | 3098 | | 32 | | |
| | 3213 | | 28 | | |
| | 3357 | | 26 | | |
| | 3780 | | 31 | | |
| | 3840 | | 31 | | |
| | 3872 | | 42 | | |
| | 3908 | | 34 | | |

a) Ref. 7, Only levels relevant to the present study are listed.

Table 2

## Levels populated in $^{145}Pm$

| Energy (keV) Prev.[a] | Energy (keV) ($^3$He,d) | Cross section(μb/sr) ($^3$He,d) θ=40 | Assignment Prev.[a] | Assignment This exp. | $(2j+1)\,S_{lj}$ |
|---|---|---|---|---|---|
| 0 | 0 | 354 | $5/2^+$ | ℓ=2 | 2.33 |
| 61.2 | 60 | 56 | $7/2^+$ | ℓ=4 | 1.59 |
| 492.5 | 498 | 4 | $3/2^+$ | ℓ=2 | 0.02 |
| 726.5 | 728 | 241 | $1/2^+$ | ℓ=0 | 0.52 |
| | 773 | 30 | | ℓ=2 | 0.15 |
| 794.6 | 796 | 202 | $11/2^-$ | ℓ=5 | 8.77 |
| 958.0 | | | $(5/2^+)$ | | |
| | 960 | 299 | | ℓ=2 | 1.41 |
| 1057.3 | 1059 | 288 | $1/2^+$ | ℓ=0 | 0.56 |
| 1215.2 | | | | | |
| | 1226 | 62 | | ℓ=2 | 0.25 |
| 1233.9 | | | | | |
| | 1260 | 5 | | | |
| 1384.9 | 1386 | 34 | $(7/2,9/2)^-$ | ℓ=3 | 0.19 |
| 1388.5 | | | | | |
| | 1489 | 35 | | (ℓ=2) | (0.16) |
| | 1507 | 60 | | ℓ=2 | 0.23 |
| | 1563 | 21 | | | |
| | 1716 | 12 | | ℓ=0 | 0.030 |
| | 1753 | 46 | | ℓ=0+5 | 0.036(ℓ=0)+1.3(ℓ=5) |
| | 1809 | 11 | | (ℓ=0) | (0.023) |
| | 1849 | 7 | | | |

ble 2

## Levels populated in $^{145}Pm$

| nergy (keV) ev.[a] | Cross section (μb/sr) ($^3$He,d) | | Assignment Prev.[a] | This exp. | (2j + 1) $S_{lj}$ |
|---|---|---|---|---|---|
| | ($^3$He,d) | θ=40 | | | |
| 1978 | 121 | | | ℓ=0 | 0.18 |
| 2008 | 141 | | | ℓ=2 | 0.53 |
| 2112 | 77 | | | ℓ=0 | 0.12 |
| 2168 | 8 | | | | |
| 2190 | 49 | | | (ℓ=2) | (0.18) |
| 2210 | 33 | | | (ℓ=2) | (0.12) |
| 2282 | 82 | | | ℓ=2 | 0.26 |
| 2294 | | | | | |
| 2329 | 24 | | | | |
| 2401 | 11 | | | | |
| 2431 | 16 | | | | |
| 2474 | 21 | | | | |
| 2562 | 18 | | | | |

a) Ref. 6.

Only levels relevant to the present study are listed.

Table 3

Q-values for the ($^{3}$He,d) reaction to some Pm isotopes. Relative uncertainties only are given for this experiment. Absolute uncertainties would be ~30 keV.

| Isotope | $^{151}$Pm | $^{149}$Pm | $^{147}$Pm | $^{145}$Pm | $^{144}$Pm | $^{143}$Pm |
|---|---|---|---|---|---|---|
| This exp. | 1504(5) | 456(5) | -87(5) | -679(5) | -803(5) | -1194(5) |
| Prev.[a] | 1499(11) | 461(4) | -79(3) | -686(7) | -830(40) | -1220(11) |

a) Ref. 9

Table 4

Energy centroids (keV), single particle energies (keV) and summed spectroscopic factors for $^{143}Pm$ and $^{145}Pm$. Included in $d_{3/2}$ are also $\ell=2$ transitions where the final spin is not known.

| | $^{142}Nd(^{3}He,d)^{143}Pm$ | | | $^{144}Nd(^{3}He,d)^{145}Pm$ | | |
|---|---|---|---|---|---|---|
| | $\bar{E}$ | $\varepsilon-\lambda$ | $\Sigma S_{lj}$ | $\bar{E}$ | $\varepsilon-\lambda$ | $\Sigma S_{lj}$ |
| $g_{7/2}$ | 273 | 822 | 0.13 | 60 | 368 | 0.20 |
| $d_{5/2}$ | 0 | 0 | 0.50 | 0 | 0 | 0.39 |
| $h_{11/2}$ | 960 | 1741 | 0.93 | 922 | 1697 | 0.84 |
| $s_{1/2}$ | 1194 | 2013 | 0.78 | 1186 | 2004 | 0.74 |
| $d_{3/2}$ | 1458 | 2309 | 0.88 | 1388 | 2232 | 0.84 |

Figure captions

Fig. 1 The $^{142}Nd(^{3}He,d)^{143}Pm$ spectrum at $\theta=50^{o}$ and the $^{144}Nd\ (^{3}He,d)^{145}Pm$ spectrum at $\theta=40^{o}$.

Fig. 2 Angular distributions from the $^{142}Nd(^{3}He,d)^{143}Pm$ reaction. The solid curves result from DWBA calculations and the points represent experimental data.

Fig. 3 Angular distributions from the $^{144}Nd(^{3}He,d)^{145}Pm$ reaction. The solid curves result from DWBA calculations and the points represent experimental data.

Fig. 4 The $^{Nat}Nd(^{3}He,d)$ spectrum at $\theta=65^{o}$. Levels known from previous experiments are indicated by energy and spin.

Fig. 5 The cross sections to some prominent peaks in the odd Pm spectra obtained using enriched targets (data also from ref. 1 - 3) are plotted (open circles) along with results obtained using a target of natural neodymium. The latter is indicated with filled triangles and is normalized to fit the $^{145}Pm$ data. This same normalization also gives good fit to all the other Pm isotopes and no renormalization of previously obtained cross-sections is called for.

Note that the exposures on the natural neodymium target were recorded at the following angles: $20^{o}$, $30^{o}$, $50^{o}$ and $65^{o}$. In the figure however, the filled triangles are plotted at $18^{o}$, $28^{o}$, $48^{o}$ and $63^{o}$ so as not to obscure the datapoints obtained using enriched targets. The solid curves result from DWBA calculations.

Fig. 6 The summed spectroscopic strenghts for the various shell model states represented by horizontal bars and plotted at the appropriate single particle energies are compared to the pairing prediction represented by the $U^2$ curve.

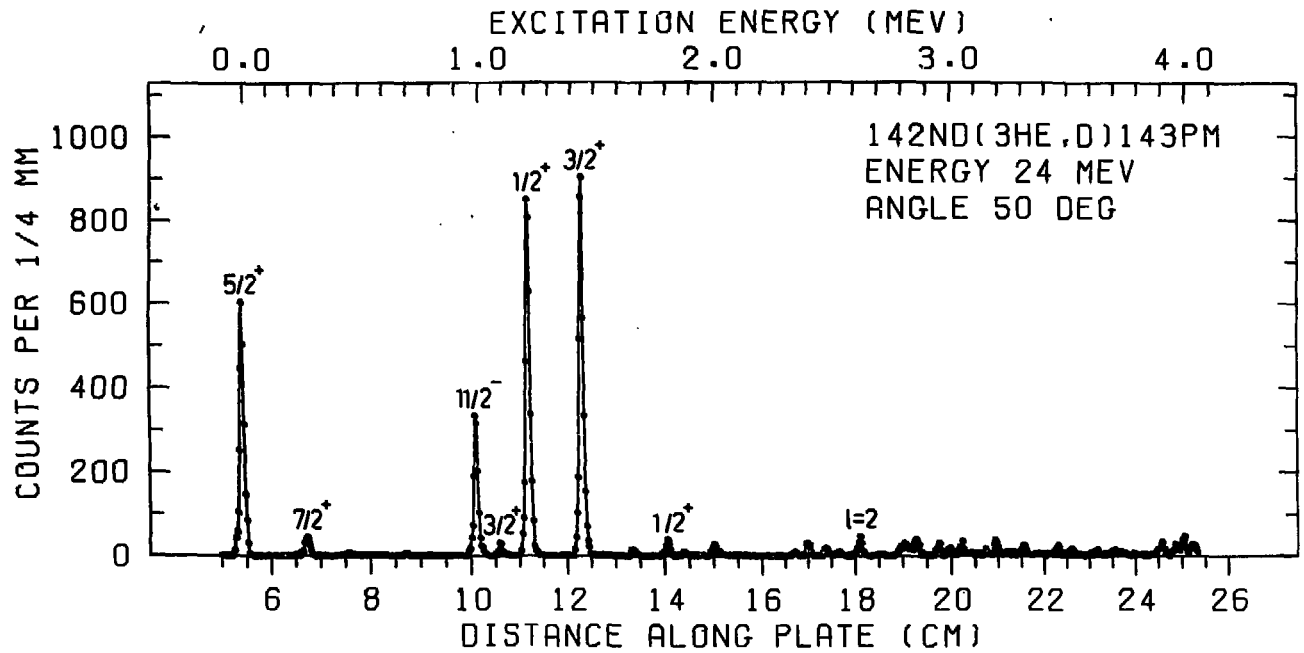
EXCITATION ENERGY (MEV)
0.0
1.0
2.0
3.0
4.0
142ND(3HE,D)143PM
ENERGY 24 MEV
ANGLE 50 DEG
COUNTS PER 1/4 MM
1000
800
600
400
200
0
5/2+
7/2+
11/2-
3/2+
1/2+
3/2+
1/2+
l=2
6
8
10
12
14
16
18
20
22
24
26
DISTANCE ALONG PLATE (CM)

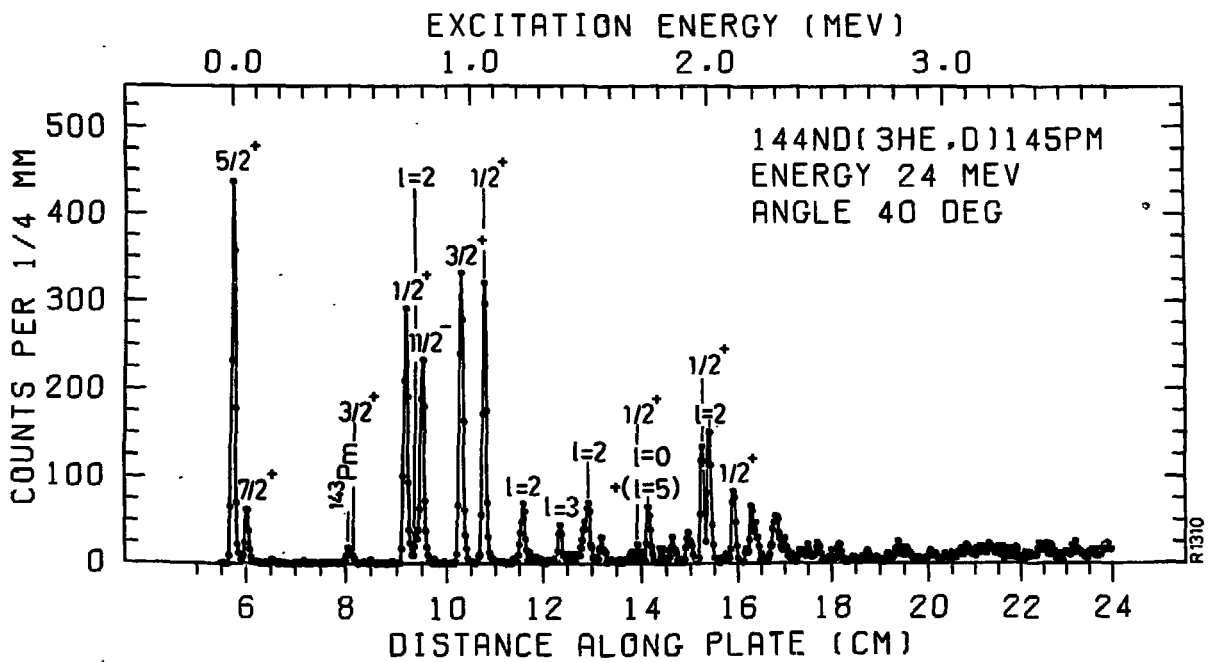
EXCITATION ENERGY (MEV)
0.0
1.0
2.0
3.0
144ND(3HE,D)145PM
ENERGY 24 MEV
ANGLE 40 DEG
COUNTS PER 1/4 MM
500
400
300
200
100
0
5/2+
7/2+
143Pm
3/2+
l=2
1/2+
1/2+
11/2-
3/2+
l=2
l=3
l=2
1/2+
l=0
+(l=5)
1/2+
l=2
1/2+
R1310
6
8
10
12
14
16
18
20
22
24
DISTANCE ALONG PLATE (CM)

FIGURE 1

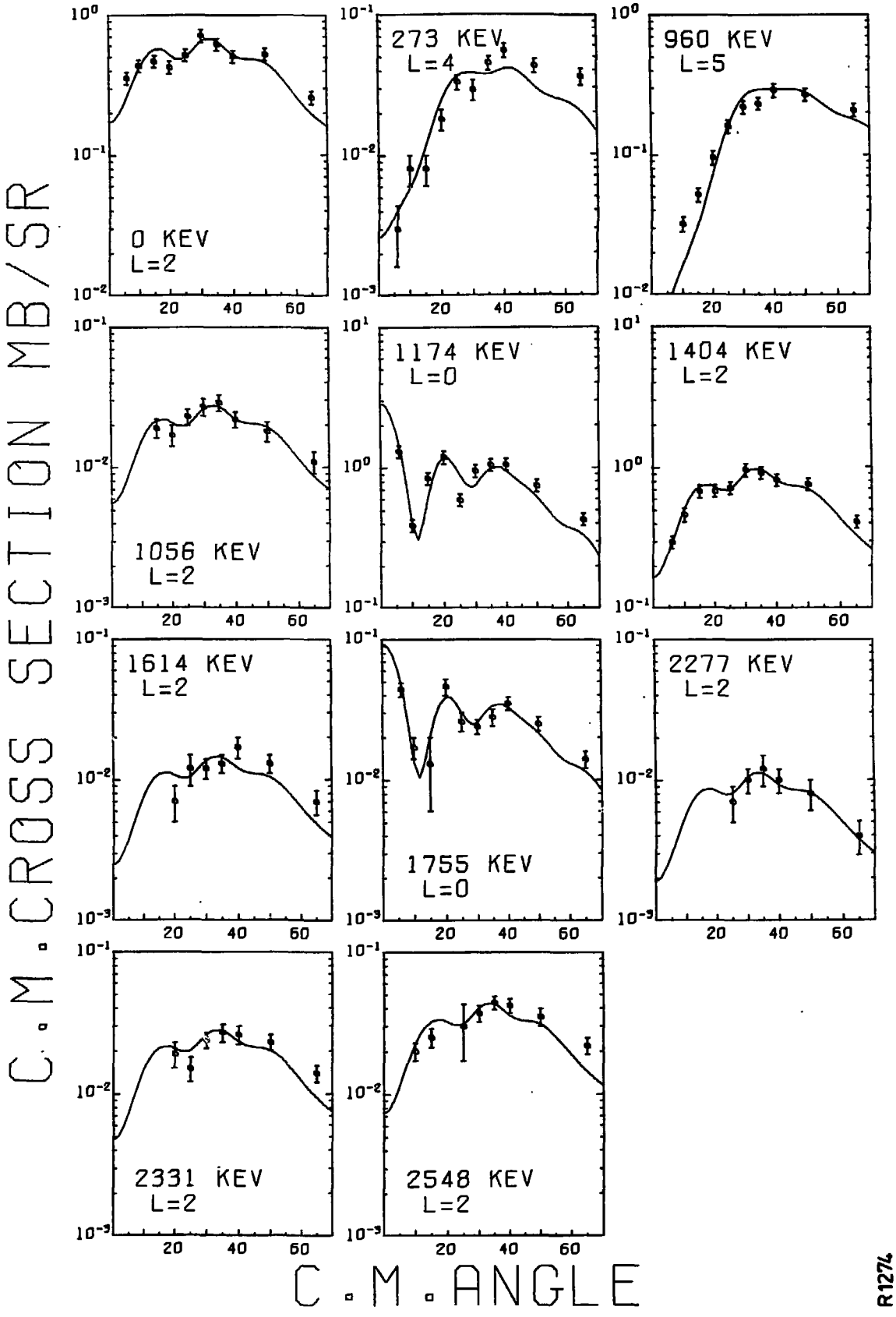
C.M. CROSS SECTION MB/SR
C.M. ANGLE
0 KEV
L=2
273 KEV
L=4
960 KEV
L=5
1056 KEV
L=2
1174 KEV
L=0
1404 KEV
L=2
1614 KEV
L=2
1755 KEV
L=0
2277 KEV
L=2
2331 KEV
L=2
2548 KEV
L=2
R1274

FIGURE 2

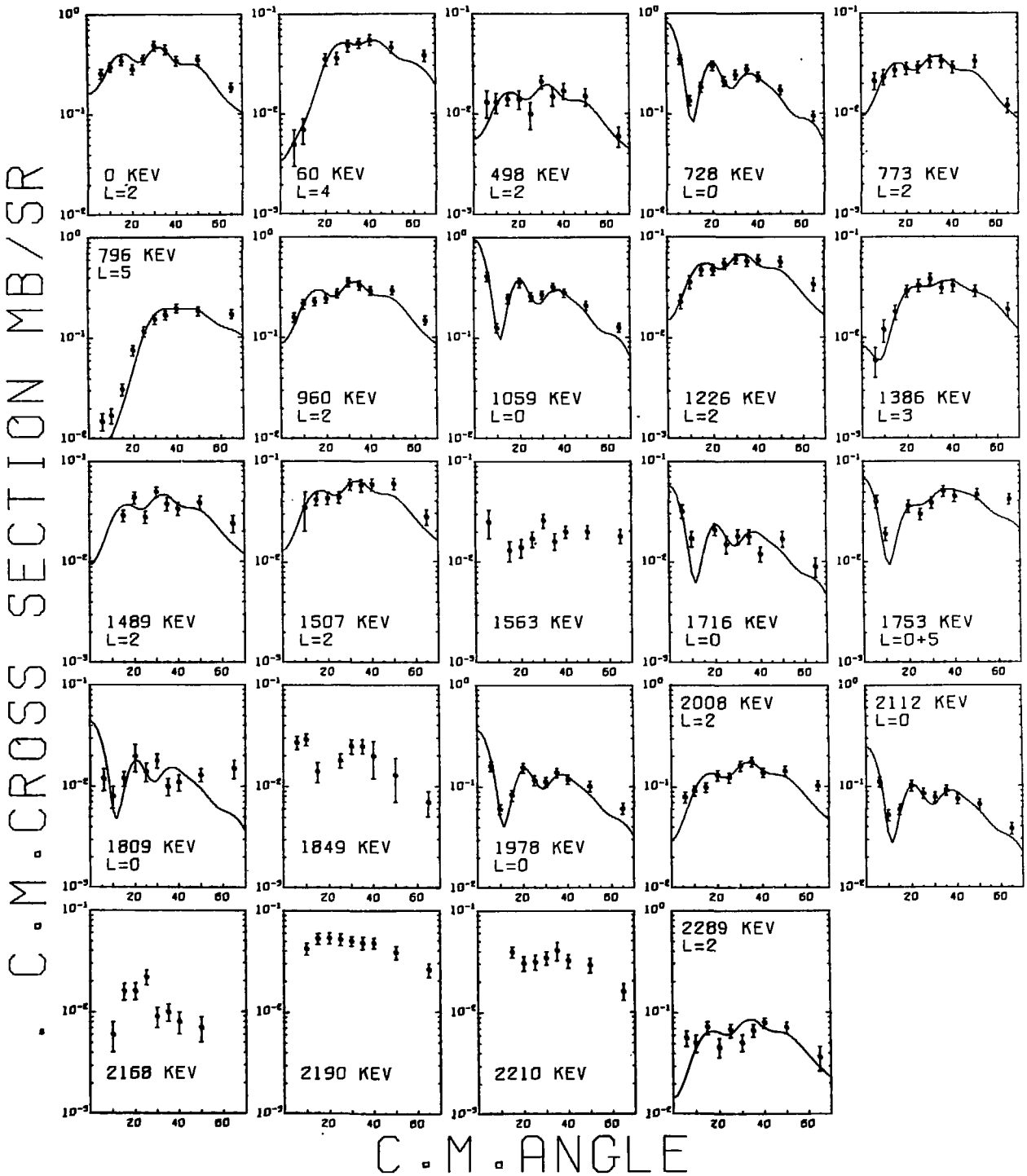
C.M.CROSS SECTION MB/SR
C.M.ANGLE
0 KEV
L=2
60 KEV
L=4
498 KEV
L=2
728 KEV
L=0
773 KEV
L=2
796 KEV
L=5
960 KEV
L=2
1059 KEV
L=0
1226 KEV
L=2
1386 KEV
L=3
1489 KEV
L=2
1507 KEV
L=2
1563 KEV
1716 KEV
L=0
1753 KEV
L=0+5
1809 KEV
L=0
1849 KEV
1978 KEV
L=0
2008 KEV
L=2
2112 KEV
L=0
2168 KEV
2190 KEV
2210 KEV
2289 KEV
L=2
R1273

FIGURE 3

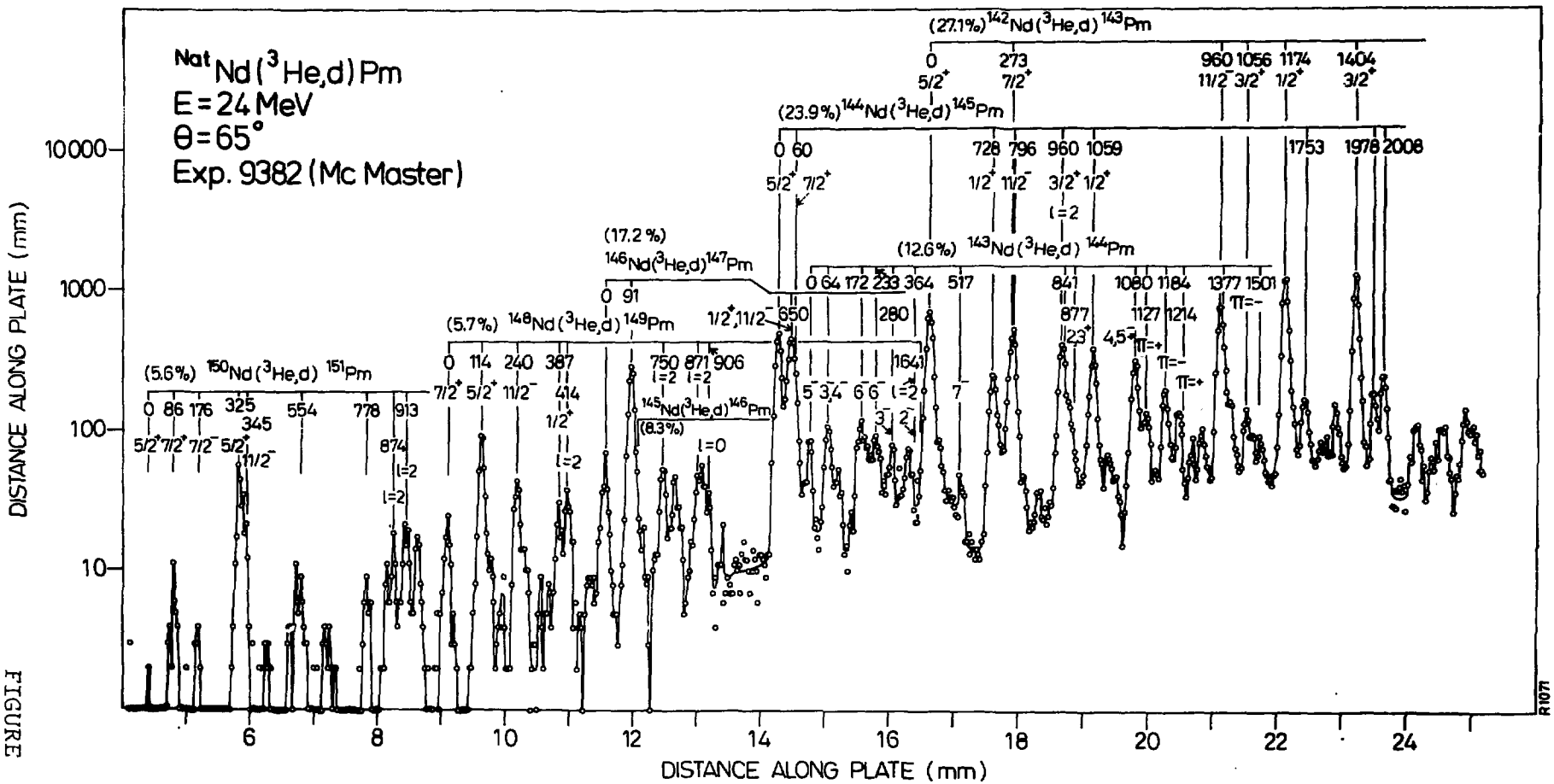
Nat Nd (3He,d) Pm
E = 24 MeV
θ = 65°
Exp. 9382 (Mc Master)
(27.1%) 142Nd (3He,d) 143Pm
(23.9%) 144Nd (3He,d) 145Pm
(17.2 %) 146Nd (3He,d) 147Pm
(12.6%) 143Nd (3He,d) 144Pm
(5.7%) 148Nd (3He,d) 149Pm
(5.6%) 150Nd (3He,d) 151Pm
145Nd (3He,d) 146Pm
(8.3%)
DISTANCE ALONG PLATE (mm)
DISTANCE ALONG PLATE (mm)

FIGURE 4

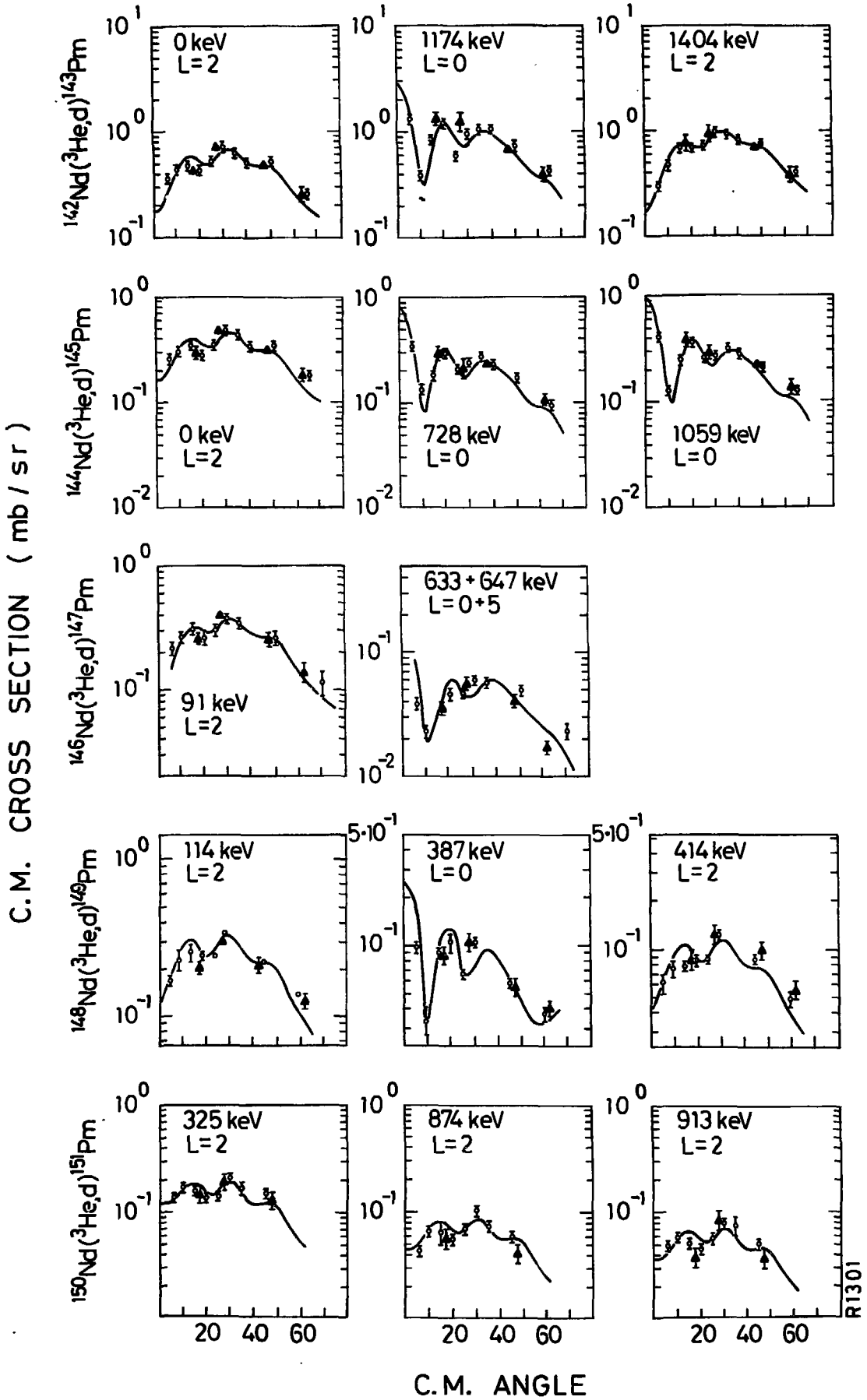
C.M. CROSS SECTION ( mb / sr )
$^{142}$Nd($^{3}$He,d)$^{143}$Pm
0 keV
L=2
1174 keV
L=0
1404 keV
L=2
$^{144}$Nd($^{3}$He,d)$^{145}$Pm
0 keV
L=2
728 keV
L=0
1059 keV
L=0
$^{146}$Nd($^{3}$He,d)$^{147}$Pm
91 keV
L=2
633 + 647 keV
L=0+5
$^{148}$Nd($^{3}$He,d)$^{149}$Pm
114 keV
L=2
387 keV
L=0
414 keV
L=2
$^{150}$Nd($^{3}$He,d)$^{151}$Pm
325 keV
L=2
874 keV
L=2
913 keV
L=2
R1301
C.M. ANGLE

FIGURE 5

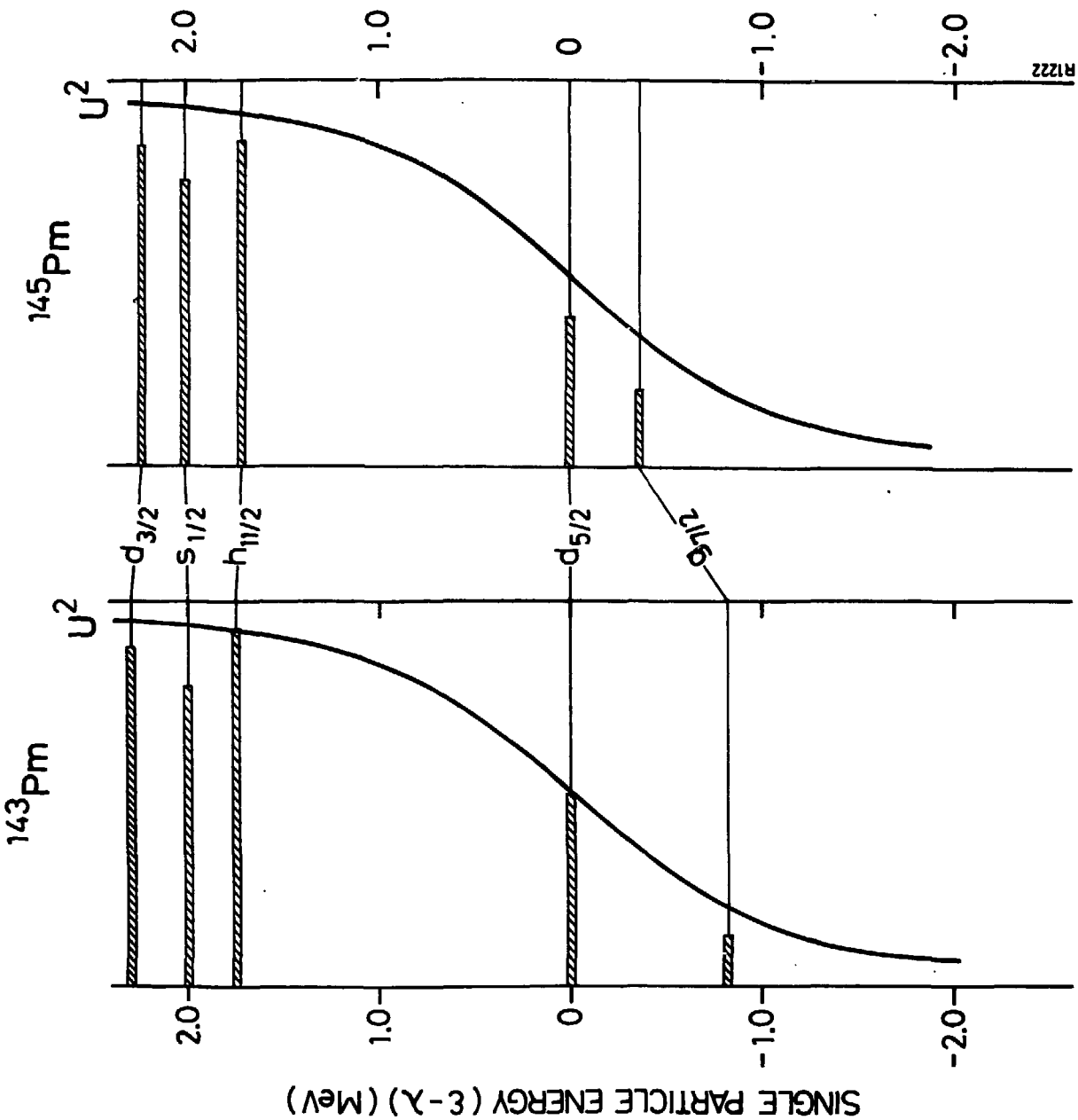
R1222
2.0
1.0
0
-1.0
-2.0
U²
145Pm
143Pm
d3/2
s1/2
h11/2
d5/2
g7/2
SINGLE PARTICLE ENERGY (ε-λ) (MeV)

FIGURE 6